THE ROLE OF HIPPOCAMPAL NEURAL IMMUNE SIGNALING IN STRESS-ENHANCED FEAR LEARNING: IMPLICATIONS FOR POST-TRAUMATIC STRESS DISORDER

Meghan E. Jones

A dissertation submitted to the faculty of the University of North Carolina at Chapel Hill in partial fulfillment of the requirements for the degree of Doctor of Philosophy in the Department of Psychology and Neuroscience.

Chapel Hill
2017

Approved by:

Donald T. Lysle

Regina M. Carelli

Kathryn J. Reissner

Todd E. Thiele

Margaret A. Sheridan

ABSTRACT

MEGHAN E. JONES: The role of hippocampal neural immune signaling in stress-enhanced fear learning: Implications for post-traumatic stress disorder.
(Under the direction of Donald T. Lysle)

Psychopathology and disease states involving depression and anxiety, including post-traumatic stress disorder (PTSD), have been associated with immune dysregulation. Preliminary data from our laboratory has suggested that severe stress induces a time-dependent increase in hippocampal IL-1β immunoreactivity and that centrally blocking IL-1 signaling prevented the development of stress-enhanced fear learning, a rodent PTSD-like phenotype. In parallel, astrocyte-derived cytokines and astroglial signaling have been linked to the development of PTSD-like phenotypes following severe stress. The goal of the current dissertation was to use the stress-enhanced fear learning paradigm to explore the role of neural immune signaling in the development of a PTSD-like phenotype. The experiments described in the current dissertation tested the overarching hypothesis that (1) severe stress induces changes in hippocampal astrocyte-derived IL-1β expression and the morphometric properties of hippocampal astrocytes and (2) that both blocking hippocampal IL-1 signaling and activating hippocampal astroglial G_i signaling prevent the development of SEFL.

Experiments described in Chapter 2 confirm the hypothesis that hippocampal IL-1 signaling is required for the development of SEFL and reveal astrocytes as the predominant cellular source of hippocampal IL-1β. Additional analyses in Chapter 2 revealed that severe stress induces a reduction in ionized calcium-binding adaptor molecule 1 (Iba-1)

immunoreactivity, with no effect on glial fibrillary acidic protein (GFAP) immunoreactivity. Experiments described in Chapter 3 demonstrate that there is no change in hippocampal astrocyte volume, surface area, or colocalization with a synaptic marker, postsynaptic density 95 (PSD95), 48 hours post-stress. However, there was a significant stress-induced reduction in PSD95 immunoreactivity. Finally, experiments described in Chapter 4 show that astroglial G_i activation was sufficient to attenuate SEFL and provide the first direct evidence to support the validity of GFAP-hM4Di in that we detected a CNO-induced reduction in the colocalization between virus-positive cells and cyclic adenosine monophosphate (cAMP), a G_i-dependent second messenger. Collectively, these data suggest that hippocampal astrocytes are critically involved in SEFL and identify two signaling pathways that can be targeted to attenuate the development of a PTSD-like phenotype. This work suggests that neural immune signaling represents a promising target for the development of novel therapeutics to treat PTSD and provides insight to inform future endeavors to better understand the neurobiological mechanisms driving the acquisition and encoding of fear memories.

AKNOWLEDGEMENTS

I would first like to express my most sincere thanks to my advisor, Dr. Donald Lysle. I feel extremely lucky to have been able to complete my graduate work in the Lysle lab not only because of the excellent research environment that Don has created but also because his door was always open, no matter how silly the question. I do not think I could have completed as much working with any other advisor and I hope to know as much and be as great a researcher as Don is some day.

I would like to thank my lab mates, especially Christina Lebonville and Jackie Paniccia, for their help and support both in and out of lab throughout my time in graduate school. I would also like to thank all of the students and faculty of the Behavioral Neuroscience program and Psychology Department, especially my dissertation committee members. I have truly enjoyed the collaborative and supportive environment in our program and I know that it contributes to stronger science all around. I also especially want to thank Dr. Regina Carelli and Dr. Kathryn Reissner who have been important female role models for the ideal excellent researcher to me throughout graduate school.

I would also like to thank my family. Thanks to my siblings for always listening. Thanks to my mom for teaching me how to stand up for myself and be confident, which absolutely applied to different aspects of completing a dissertation. And thanks to my Dad and Jodi for always supporting and encouraging my research and for both financial and emotional support as I've worked on figuring out how to navigate the science world and the real world.

Having two role models in a different field in science has made me a better researcher. Lastly, thanks to my soccer teams, Arrichion Hot Yoga trainers (Marisa, Kelsey, and Steve), and Wednesday friends (Sierra, JR, Kyle, and Aaron) for keeping me sane(ish) throughout my time in lab.

TABLE OF CONTENTS

ACKNOWLEDGEMENTS……...v

LIST OF FIGURES……...……..xii

LIST OF ABBREVIATIONS……...….xiii

Chapter

I. GENERAL INTRODUCTION……1

a. Post-traumatic stress disorder……1

b. Approaches to study PTSD using rodent models…….….3

c. Hippocampal function is important in PTSD and SEFL……...7

d. Role of cytokine signaling in stress response mechanisms……...8

e. Role of astroglial signaling in stress response mechanisms……....11

f. High resolution analysis of the morphometric properties of astrocytes……..13

g. Glial-expressing Designer Receptors Exclusively Activated by Designer Drugs……13

h. Specific Aims……...15

II. EXAMINATION OF STRESS-INDUCED HIPPOCAMPAL IL-1β: EFFECT OF HIPPOCAMPAL IL-1RA ON STRESS-ENHANCED FEAR LEARNING AND IDENTIFICATION OF THE CELLULAR SOURCE[1]……19

[1] This chapter is published as an article in Brain, Behavior, and Immunity. Jones, M. E., C. L. Lebonville, et al. (2017). "Hippocampal interleukin-1 mediates stress-enhanced fear learning: A potential role for astrocyte-derived interleukin-1beta." Brain Behav Immun.

a. Introduction……..19

b. Methods……23

i. Animals……....23

ii. Experiment 2.1: Effect of intra-dorsal hippocampal IL-1RA on the development of SEFL……..24

iii. Surgery…….....24

iv. Stress-enhanced fear learning……..24

v. IL-1 receptor antagonist……...25

vi. Experiment 2.2: Immunofluorescence analysis of severe stress-induced changes in hippocampal GFAP, Iba-1, NeuN, and IL-1β……..…26

vii. Stress exposure…….26

viii. Immunohistochemistry……27

ix. Confocal microscopy, Bitplane Imaris colocalization analysis, and cell counting……..28

x. Statistical analyses……...29

c. Results……..30

i. Experiment 2.1: Intra-dorsal hippocampal IL-RA prevents SEFL……..30

ii. Experiment 2.2a: Stress-induced increase in hippocampal IL-1β is replicated……..32

iii. Experiment 2.2c: Stress-induced hippocampal IL-1β is colocalized primarily with GFAP in both stressed and non-stressed animals…….35

d. Discussion……38

III. EFFECT OF SEVERE STRESS ON THE MORPHOMETRIC PROPERTIES OF HIPPOCAMPAL ASTROCYTES……..42

a. Introduction……..42

b. Methods……46

i. Animals……46

ii. Experiment 3.1 Verification of AAV5-GFAP-HA-hM3Dq-IRES-mCitrine as a membrane-dependent tag……46

iii. Viruses…….46

iv. Surgery and Sacrifice……...46

v. Immunohistochemistry……47

vi. Confocal microscopy and Bitplane Imaris analysis……48

vii. Experiment 3.2: Effect of stress on the morphometric properties of astrocytes……48

viii. Virus…….48

ix. Surgery…….48

x. Stress exposure and sacrifice……...49

xi. Confocal microscopy and Bitplane Imaris analysis…….50

xii. Image Acquisition……....50

xiii. Astrocyte volume, surface area, and colocalization with PSD95……..51

xiv. Quantification of hippocampal PSD95 immunoreactivity……...52

xv. Statistical Analysis……...52

c. Results……..53

i. Experiment 3.1 AAV5-GFAP-HA-hM3Dq-IRES- -mCitrine is expressed in a membrane-dependent manner……...53

ii. Experiment 3.2: Effect of stress on the morphometric properties of astrocytes…….....56

iii. Stress exposure does not alter astrocyte volume, surface area or colocalization with PSD95…….....56

iv. Stress exposure attenuates PSD95 Immunoreactivity……..59

d. Discussion……60

IV. EFFECT OF HIPPOCAMPAL ASTROGLIAL GI SIGNALING ON STRESS-ENHANCED FEAR LEARNING……..63

a. Introduction……..63

b. Methods……....66

i. Animals…….....66

ii. Virus…….67

iii. Surgery…….67

iv. Experiment 4.1: Effect of hippocampal astroglial G_i activation on SEFL…….....67

v. Stress-enhanced fear learning……..67

vi. Drug Administration…….....68

vii. Sacrifice……...69

viii. Immunohistochemistry…….....69

ix. Experiment 4.2: Effect of CNO on colocalization of mCherry-positive cells with cAMP…….....70

x. Sacrifice……...70

xi. Immunohistochemistry……71

xii. Confocal microscopy and Bitplane Imaris colocalization analysis……72

xiii. Image Acquisition…….....72

xiv. Colocalization of mCherry and cAMP……72

xv. Statistical Analysis……...73

c. Results……..74

i. Experiment 4.1: Hippocampal astroglial G_i activation attenuates SEFL……...……74

ii. Experiment 4.2: CNO attenuated colocalization of mCherry-positive cells with cAMP…….76

d. Discussion……77

V. GENERAL DISCUSSION....……81

a. Summary of findings……81

b. Implications of the role of IL-1 signaling in SEFL……..82

c. Implications of the role of astrocytes, and in particular astroglial G_i activation, in SEFL……..84

d. Implications of the effect of severe stress on PSD95……..86

e. Role of additional neural immune signaling pathways in behavioral outcomes of severe stress……88

f. Summary of unanswered questions and future directions…….89

g. Concluding remarks…….92

REFERENCES……93

LIST OF FIGURES

Figure

1.1 Stress enhanced fear learning……..5

1.2 Stressor of the SFEL paradigm enhances general anxiety-like behavior seven days later……..6

1.3 Experiments described in Chapters 2 through 4 address three Specific Aims……..18

2.1 Intra-dorsal hippocampal IL-1RA is sufficient to prevent SEFL……..33

2.2 Severe stress increases hippocampal IL-1β immunoreactivity……..34

2.3 Dorsal hippocampal Iba-1 immunoreactivity, but not GFAP immunoreactivity is attenuated 48 hours after severe stress……36

2.4 IL-1β signal is colocalized with GFAP, and not with Iba-1 or NeuN, in the dorsal hippocampus in stressed and non-stressed animals……38

2.5 IL-1β signal is colocalized with GFAP, and not with Iba-1 or NeuN, in the dorsal hippocampus in stressed and non-stressed animals……39

3.1 GFAP-Lck-GFP is expressed selectively in astrocytes……57

3.2 GFAP-hM3Dq can be used to examine astrocyte morphology……58

3.3 Foot shock does not alter the morphometric properties of astrocytes……...60

3.4 Cells included in morphology analyses were predominantly from CA1 and CA3……61

3.5 Foot shock attenuated PSD95 immunoreactivity……...62

4.1 Experimental timeline for Experiment 4.1……..…72

4.2 Experimental timelines for Experiment 4.2……...75

4.3 Astroglial G_i activation attenuates stress-enhanced fear learning……..79

4.4 CNO attenuates cAMP in GFAP-hM4Di-mCherry-transduced cells……80

LIST OF ABBREVIATIONS

AAV	Adeno-associated virus
ANOVA	Analysis of Variance
AP	Anterior-posterior
ASR	Acoustic Startle Response test
ATP	Adenosine triphosphate
BDNF	Brain-derived neurotrophic factor
CA1	Cornu Ammonis 1
CA3	Cornu Ammonis 3
cAMP	Cyclic adenosine monophosphate
CNO	Clozapine-n-oxide
CNS	Central nervous system
DG	Dentate gyrus
DH	Dorsal Hippocampus
DREADD	Designer receptors exclusively activated by designer drugs
DV	Dorsal-ventral
EPM	Elevated Plus Maze
GDNF	Glial cell-derived neurotrophic factor
GFP	Green fluorescent protein

GFAP	Glial fibrillary acidic protein
GPCR	G protein coupled receptor
Iba-1	Ionized calcium-binding adaptor molecule-1
IL-1β	Interleukin-1β
IL-1RA	Interleukin-1 receptor antagonist
IL-6	Interleukin-6
LTP	Long term potentiation
ML	Medial-lateral
NeuN	Neuronal Nuclear antigen
NIMH	National Institute of Mental Health
PB	Phosphate buffer
PTSD	Post-traumatic stress disorder
PSD95	Postsynaptic density 95
RDoC	Research Domain Criteria Framework
ROI	Region of Interest
SEFL	Stress-enhanced fear learning
TNF-α	Tumor Necrosis Factor- α

Chapter 1

GENERAL INTRODUCTION

Post-Traumatic Stress Disorder

Post-traumatic stress disorder (PTSD) is a complex and devastating mental disorder with a myriad of psychological and physiological consequences (Gill, Saligan et al. 2009; Xia, Zhai et al. 2013). PTSD occurs in 15-20% of people who experience a severe threat to psychological or physical bodily integrity ((Hoskins, Pearce et al. 2015), Diagnostics and Statistical Manual of Mental Disorders, 5th edition). The three hallmark symptoms of the disorder are intrusive memories or re-experiencing of the trauma, avoidance, and hyperarousal (Hoskins, Pearce et al. 2015). These symptoms manifest in many different forms with affected individuals exhibiting constant intrusions of unwanted traumatic memories, dissociation from friends and family, heightened anxiety, hypervigilance –including a hyperreactivity to future stressful events—and significant alterations in mood or cognition. PTSD is also associated with physiological changes, including both neuroimmune and neuroendocrine dysregulation (Gill, Saligan et al. 2009; Xia, Zhai et al. 2013). Furthermore, significant comorbidity between PTSD and substance abuse, depression, and generalized anxiety disorder amplify the emotional and fiscal costs of the disorder on society (Hoskins, Pearce et al. 2015). There are many at-risk populations including active military personnel, emergency responders, cancer patients, victims of natural disasters or accidents, and abused individuals (e.g.,(Bowler, Han et al. 2010; Thomas, Wilk et al. 2010)).

Operations Iraqi Freedom and Enduring Freedom deployed about 2.5 million troops, approximately 13%-20% of which have developed PTSD (Hoge, Castro et al. 2004).

Most treatment options for individuals with PTSD involve cognitive behavioral therapy, re-exposure therapy, and/or the prescription of traditional antidepressants or antianxiety medications (De Jongh, Resick et al. 2016). There are currently no effective pharmacological treatments for PTSD specifically and the ones in current use in this context have small effects with unclear clinical relevance (Hoskins, Pearce et al. 2015). For example, while current pharmaceuticals used may improve mood or general anxiety temporarily, most do not improve symptoms of intrusions or dissociation (Byrne, Krystal et al. 2017). A better understanding of the neurobiological mechanisms driving PTSD is crucial for the development of more targeted pharmaceutical treatments.

Interestingly, clinical studies have suggested that morphine treatment following a combat injury is associated with a significant reduction in PTSD rates among combat veterans (Holbrook, Galarneau et al. 2010; Melcer, Walker et al. 2014). A similar correlation was found in children who experienced a single-incident trauma that required an emergency room visit (Nixon, Nehmy et al. 2010). While a prophylactic pharmaceutical treatment for PTSD would be an extremely important clinical tool, the only way to work towards a better understanding of PTSD and to test the efficacy of and determine the mechanism through which morphine or any pharmacological treatment might act to treat PTSD is to rely on rodent models of the disorder.

Approaches to study Post-Traumatic Stress Disorder using rodent models

Psychiatric disorders, including PTSD, are multi-faceted and involve complex changes to cognition and mood. As such, PTSD can be difficult to thoroughly capture using rodent models. With the introduction of the Research Domain Criteria (RDoC) framework, the National Institute of Mental Health (NIMH) calls for researchers to approach mental health research by studying distinct behavioral constructs within mental disorders on a full continuum of adaptive to maladaptive behavior through multiple levels of analysis. In this way, researchers will uncover specific mechanisms involved in many aspects of a given disorder. The Research Domain Criteria framework defines behavioral constructs and subconstructs within five systems. Our approach to study PTSD is consistent with this organization in that the rodent paradigm used by our laboratory involves threat response constructs within the Negative Valence system defined by the NIMH, as described below.

There are several rodent models of the disorder, all of which focus primarily on the hyperarousal symptom cluster, which involves both acute threat mechanisms (enhanced fear learning) and potential threat mechanisms (enhanced generalized anxiety-like behavior). The Predator Scent Stress (Kozlovsky, Matar et al. 2009; Cohen, Kozlovsky et al. 2012) and Single Prolonged Stress (Yamamoto, Morinobu et al. 2009) models expose rats to a severe stressor, soiled cat litter or a single exposure to a series of three stressors (restraint stress, forced swim, and ether anesthesia), respectively, and test for enhanced anxiety-like behavior in the Elevated Plus Maze (EPM) and Acoustic Startle Response Test (ASR) seven days later. Researchers then categorize rats as extreme, moderate, or low responders with the extreme category (highest generalized anxiety) taken to reflect a PTSD-like phenotype. However, stress-enhanced fear learning (SEFL) models (Rau, DeCola et al. 2005; Blouin, Sillivan et al. 2016)

excellently demonstrate hypervigilance or hyperreactivity to future fear learning, a key component of human PTSD, with impressive experimental control and measurement. The studies in the current dissertation take advantage of the SEFL model.

In our hands, SEFL is based on foot shock-induced contextual fear conditioning. Figure 1.1 shows the basic experimental design for this paradigm in our laboratory. Briefly, animals are exposed a novel context distinct in olfactory, tactile, and auditory cues from the home cage (Context A) where they receive 15 2 mA scrambled foot shocks on a 6 minute variable interval schedule. Control animals are exposed to the context without foot shocks being delivered. One week later, all animals are exposed to a distinctly different context, distinct in olfactory, tactile, and auditory cues from both the home cage and Context A, (Context B) where they receive a single 1 mA scrambled foot shock. Animals who received severe foot shock stress in Context A show significantly enhanced (maladaptive) fear learning to Context B. Critically, prior to the single foot shock in Context B, animals are exposed to Context B without foot shock exposure for a habituation session and to test for generalization of fear between the two contexts. Animals do not show fear to Context B prior to the single shock. Thus, any differences observed between treatment groups reflect altered learning to the subsequent single foot shock. In other words, the severe stressor in Context A changes the way that the animals process the subsequent fear challenge in Context B. This model has been shown to produce pronounced SEFL that is robust and reliable (Rau, DeCola et al. 2005; Szczytkowski-Thomson, Lebonville et al. 2013; Jones, Lebonville et al. 2015).

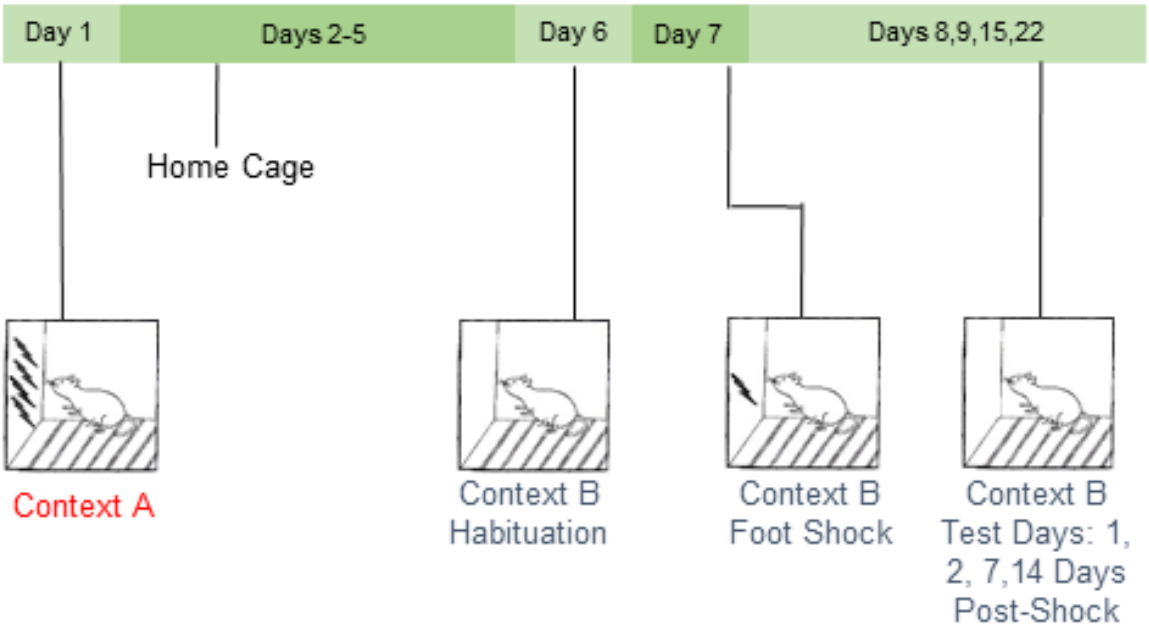

Figure 1.1 Stress-enhanced fear learning. In the SEFL paradigm in our laboratory, rats are exposed to 15 2 mA foot shocks in Context A. Six days later, animals are exposed to Context B without foot shocks to test for generalization of fear between the two contexts. On Day 7, rats are placed back into Context B where they receive a single 1 mA foot shock. Contextual fear learning to Context B is then analyzed. SEFL is used to study how the initial severe stressor in Context A enhances contextual fear learning to the single foot shock in Context B. This phenomenon reflects the hypervigilance or hyperreactivity to future stressors that is a key component of human PTSD.

To further strengthen the use of SEFL as a model through which to study PTSD, we have shown that the severe stressor in SEFL (15 foot shocks in Context A) induces a generalized heightened anxiety-like phenotype in the elevated plus maze seven days post-stress (Figure 1.2), similar to predator scent stress and single prolonged stress. Thus, while behavioral outcomes in the current studies focused exclusively on enhanced fear learning, the severe stressor of the SEFL paradigm is capable of inducing a PTSD like phenotype in rats in two dimensions of the Negative Valence construct within the NIMH Research Domain Criteria framework. Therefore, characterizing stress-induced cellular and molecular changes in the

brain following the severe stressor of SEFL will be important for understanding multiple behavioral outcomes. Converging mechanisms that drive depressive- and anxiety-like phenotypes that are part of the PTSD-like phenotype as a whole will be important in our overall understanding of behavioral outcomes following stress that lead to PTSD.

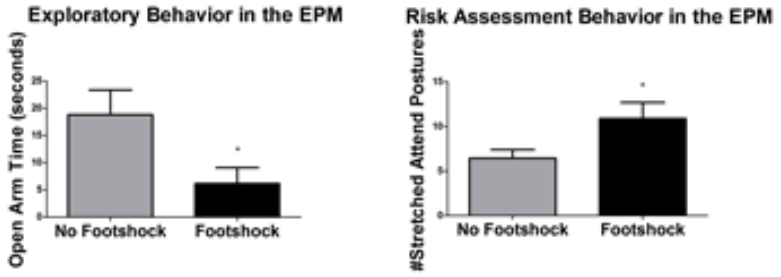

Figure 1.2 Stressor of the SEFL paradigm enhances general anxiety-like behavior seven days later. In order to compare the behavioral consequences of severe foot shock in SEFL to the behavioral consequences of stress in the predator scent stress and single prolonged stress models, rats were exposed to foot shock stress in Context A (15 2 mA scrambled foot shocks over 90 minutes) and then returned to their home cage for six days. Seven days after foot shock stress, animals were tested for anxiety-like behavior in the Elevated Plus Maze. Rats exposed to foot shock stress exhibited less time in the open arms of the maze (left panel) and a greater number of stretched attend postures (right panel, a measure of risk assessment behavior), both of which are reflective of enhanced anxiety in the model. * $p < 0.05$.

Interestingly, using the SEFL model, our laboratory provided the first basic animal research support for the use of morphine as a prophylactic treatment for PTSD. Morphine treatment following exposure to severe foot shock stress attenuated the development of SEFL (Szczytkowski-Thomson, Lebonville et al. 2013). Specifically, acute morphine treatment at 48 hours after, but not immediately after, severe stress attenuated SEFL. This finding provides important rationale to support the value of the studies in the current dissertation because any effect of morphine on pain treatment would be most potent immediately following foot shock.

Thus, these results suggest that morphine treatment exerts its effect on behavioral outcomes following stress through a unique neural mechanism that drives enhanced fear learning.

While it is exciting that the use of morphine has shown promise to clinically prevent or alleviate PTSD, its use clinically in this context is severely limited by its abuse liability. Further, high co-morbidity between opioid abuse specifically and PTSD in a number of settings presents additional problems to its use as treatment (Fareed, Eilender et al. 2013; Dabbs, Watkins et al. 2014). The overarching goal of the current studies stems from an effort to elucidate the mechanisms through which morphine alters stress-enhanced fear learning in order to uncover more targets for the development of a prophylactic pharmaceutical to treat PTSD, without abuse liability.

Hippocampal function is important in PTSD and SEFL

While the experiments described herein focus primarily on the hippocampus, the sole focus on this brain region is well-justified. The hippocampus is known as a structure critical to memory processing, and data from numerous laboratories confirms that hippocampal function is required for contextual fear learning (Phillips and LeDoux 1992; Maren, Anagnostaras et al. 1998; Anagnostaras, Gale et al. 2001; Izquierdo, Furini et al. 2016). In addition, the hippocampus is considered to be an important component of the limbic system, a set of interconnected regions known to be critical in emotional processing (Bubb, Kinnavane et al. 2017). Not surprisingly, data from both human and animal laboratories has implicated the hippocampus in PTSD and PTSD-like phenotypes using rodent models of stress (Woodward, Kaloupek et al. 2006; Kozlovsky, Zohar et al. 2012; Chao, Yaffe et al. 2014; Jones, Lebonville et al. 2015; O'Doherty, Chitty et al. 2015; Rubin, Shvil et al. 2016; Nelson and Tumpap 2017). PTSD patients exhibit reduced hippocampal volume compared to traumatized and non-

traumatized controls (O'Doherty, Chitty et al. 2015) and an interesting recent report suggests that the dentate gyrus volume, specifically, is reduced (Hayes, Hayes et al. 2017). Furthermore, within PTSD populations, hippocampal volume is inversely related to treatment outcomes such that greater hippocampal volume predicts a more favorable treatment response (Rubin, Shvil et al. 2016).

A better understanding of the neurobiological mechanisms driving the acquisition of traumatic or stressful memories is an important step in understanding PTSD. The specific aims described herein make contributions to a greater effort to better understand the hippocampal mechanisms that influence memory acquisition and how such mechanisms might differ between traumatic or stressful vs. normal memories and experiences. How the current findings relate to potential mechanisms that have been hypothesized to be involved in memory acquisition and learning, including alterations in dendritic spine morphology/ synaptic remodeling (Yang, Pan et al. 2009; Lai, Franke et al. 2012; Giachero, Calfa et al. 2015) and secretion of glial-derived neurotrophic factors in the hippocampus (Bekinschtein, Cammarota et al. 2014; Rosas-Vidal, Do-Monte et al. 2014), is discussed throughout Chapters 3 through 5.

Role of cytokine signaling in stress response mechanisms

Psychopathology and disease states involving depression and anxiety have been associated with altered immune function in both human studies and preclinical rodent models (Gill, Saligan et al. 2009; Guo, Liu et al. 2012; Gola, Engler et al. 2013; Passos, Vasconcelos-Moreno et al. 2015; Wang and Young 2016). In parallel, cytokines in the central nervous system have recently emerged as important signaling molecules in the brain that modulate a wide range of behaviors, including stress response (Goshen and Yirmiya 2009; Bull, Freitas et

al. 2014; Hutchinson and Watkins 2014). Recent evidence also suggests that cytokines can directly influence learning and memory processes (Goshen, Kreisel et al. 2007; Goshen and Yirmiya 2009). The experiments described in the current dissertation are based on the conceptually innovative hypothesis that neuroimmunological mechanisms are involved in the development and expression of PTSD.

Interleukin-1β (IL-1β) is a proinflammatory cytokine thought to underlie many of the parallels between the body's response to psychological stress and physical illness. Both conditions lead to a phenotype termed *sickness behavior*, which is characterized in part by enhanced anxiety (Dantzer 2009; Goshen and Yirmiya 2009). More recently, IL-1β has been shown to be critical to fear learning and memory related phenomena (Goshen, Kreisel et al. 2007). Interestingly, several groups have also reported upregulated circulating peripheral cytokines, including IL-1β, in PTSD patients (Gill, Saligan et al. 2009; Guo, Liu et al. 2012; Gola, Engler et al. 2013; Lindqvist, Wolkowitz et al. 2014; Passos, Vasconcelos-Moreno et al. 2015; Wang and Young 2016), even suggesting cytokine expression as a biomarker for affected individuals following trauma (Cohen, Meir et al. 2011).

Recently, we examined the time course of IL-1β immunoreactivity and mRNA expression in the brain over the 72 hours following exposure to the severe stressor within the SEFL paradigm. Published data from our laboratory demonstrates that the severe stressor of SEFL, that is capable of inducing a PTSD-like phenotype (enhanced fear learning), induces a time-dependent increase in IL-1β immunoreactivity and mRNA expression specifically in the dorsal hippocampus, with no effect of foot shock on IL-1β expression in the basolateral amygdala or the perirhinal cortex (Jones, Lebonville et al. 2015). The effect emerges at 6 hours post-stress and persists through 72 hours post-stress. Of note, we also quantified IL-1β

immunoreactivity by hippocampal subregion, and the dentage gyrus exhibited the most dense IL-1β expression by far (relative to cornu ammonis (CA)1 and CA3). A subsequent experiment showed that centrally blocking IL-1 signaling through an intracerebroventricular (ICV) infusion of IL-1 receptor antagonist (IL-1RA) at 24 and 48 hours after Context A exposure prevented the development of SEFL (Jones, Lebonville et al. 2015). These data strongly suggest that IL-1 is causally related to SEFL in the hippocampus. Furthermore, the extremely dense IL-1β signal observed in the dentate gyrus is interesting given the recent report that the dentate gyrus, specifically, may be altered in human populations diagnosed with PTSD as well (Hayes, Hayes et al. 2017). Follow up studies found that the same systemic morphine treatment that prevented the development of SEFL (Szczytkowski-Thomson, Lebonville et al. 2013) also attenuated hippocampal stress-induced IL-1β (Jones, Lebonville et al. 2015). Collectively, our published work provides strong evidence that morphine exerts an anti-inflammatory effect on the hippocampus that has direct implications in fear learning behavior.

Given that the stress-induced increase in IL-1β was specific to the dorsal hippocampus, the first goal of the current dissertation was to directly test whether hippocampal IL-1 signaling is involved in the development of SEFL. Subsequently, our attention shifted to understanding the cellular signaling dynamics of stress-induced IL-1β in this region. IL-1β can be expressed by astrocytes, microglia, and neurons and IL-1 activation can lead to distinct signaling pathways in each cell type (Srinivasan, Yen et al. 2004). Understanding the complex cellular signaling dynamics of stress-induced hippocampal IL-1 is critical to the development of pharmacological agents that can attenuate maladaptive inflammatory signaling in the CNS that contributes to PTSD without interfering with peripheral immune defense (O'Neill 2006). As

an important first step to this endeavor, the second goal of the current dissertation was to identify the cellular source of hippocampal stress-induced IL-1β.

Role of astroglial signaling in stress response mechanisms

While cytokines can be expressed by multiple cell types in the brain, astrocyte-derived cytokines, including IL-1β, have been increasingly implicated in stress response mechanisms (Goshen and Yirmiya 2009) (Sugama, Takenouchi et al. 2011). Data presented in Chapter 2 of the current dissertation provides even further support for this hypothesis in that that hippocampal astrocytes are the cellular source of stress-induced IL-1β, which we have shown to be causally related to the development of SEFL (See Figures 1.4 and 1.5). Traditionally viewed merely as neuronal "glue", glial cells are now known to be critically involved in a diverse array of functions in development and disease of the central nervous system (CNS), however, the heterogeneity of glia remains underappreciated (Barres 2008). We argue that astrocyte function, especially in the context of severe stress, merits further scientific study.

Astrocytes are process-bearing cells that make direct contact with synapses (Blanco-Suarez, Caldwell et al. 2016). A "tripartite" synapse consists of a pre-synaptic cell, a post-synaptic cell, and an astrocyte that envelops the synapse. Converging evidence confirms that in this context, astrocytes engage in bidirectional communication with neurons through the release of gliotransmitters, such as ATP, d-serine, and/or glutamate, such that astrocytes can directly regulate synaptic transmission (Bernardinelli, Randall et al. 2014; Blanco-Suarez, Caldwell et al. 2016).

While there are several reports of stress-induced changes in astrocyte reactivity and morphology, there are inconsistencies regarding changes in astrocytes throughout the brain in

depressive and anxiety-like phenotypes that are observed in PTSD. Glial fibrillary acidic protein (GFAP) expression, a cytoskeletal protein selectively expressed by astrocytes and commonly employed as a marker of astrocyte activation or reactivity, has been reported to be altered in several brain regions, including the hippocampus, following a variety of different stress protocols (Colombo and Farina 2016) (Tynan, Beynon et al. 2013; Xia, Zhai et al. 2013; Choi, Ahn et al. 2016; Saur, Baptista et al. 2016). Impaired astrocyte glutamate transport, decreased release of astrocyte-derived neurotrophic factors, and altered astrocyte density have also been observed in the context of preclinical models of depression (Niciu, Henter et al. 2014). Furthermore, effective antidepressants, which are sometimes used to alleviate PTSD symptoms, have been associated with gliotrophic effects (Czeh, Muller-Keuker et al. 2007; Banasr, Chowdhury et al. 2010; Niciu, Henter et al. 2014). Given the significant role of the hippocampus in PTSD described above, it is important to note a recent report by Iwata and colleagues showed that the protective effect of imipramine in a model of learned helplessness was blocked by fluorocitrate, a reversible astrocyte inhibitor, directly into the hippocampus (Iwata, Shirayama et al. 2011). Similarly, Zhang and colleagues demonstrated that gastrodin, a compound shown to protect against depressive-like phenotypes, acts by enhancing astrocyte-derived brain-derived neurotrophic factor (BDNF) (Zhang, Peng et al. 2014).

In summary, evidence from multiple rodent paradigms of stress-induced depressive or anxiety-like behavior, as is seen in PTSD, suggests that astrocyte function may be important in the behavioral consequences of stress. Another overarching goal of the current dissertation was to gain a better understanding of hippocampal astrocyte function in the context of SEFL. To accomplish this, we took advantage of two novel innovations that have recently become available to study astrocytes with impressive precision and specificity. These new technologies

allow researchers to thoroughly describe the morphometric properties of astrocytes and to directly manipulate astroglial G protein coupled receptor (GPCR) signaling *in vivo*.

High resolution analysis of the morphometric properties of astrocytes

Dr. Kathryn Reissner and colleagues have optimized a method to isolate and quantify astrocyte volume and synaptic contacts throughout a 3-dimensional reconstruction of an individual cell (Scofield, Li et al. 2016). With their method, an adeno-associated virus serotype 5 (AAV) is used to express Green Fluorescent Protein (GFP) in a membrane-dependent manner under a GFAP promoter such that entire astrocyte, including the most distal perisynaptic processes can be visualized and quantified. Double label fluorescence immunohistochemistry can be used to quantify the colocalization of GFP with synaptic markers, such as synapsin or postsynaptic density 95, within an individual cell. As such, high resolution confocal microscopy and Bitplane Imaris analysis can produce thorough measures of the volume, surface area, and synaptic colocalization of individual astrocytes. This technology has been employed in one peer-reviewed article thus far and is known to produce results that are robust and reliable (Scofield, Li et al. 2016). The goal of Chapter 3 of the current dissertation was to employ this technology to analyze how the severe stressor the SEFL paradigm alters the morphometric properties of hippocampal astrocytes.

Glial-expressing Designer Receptors Exclusively Activated by Designer Drugs

Designer Receptors Exclusively Activated by Designer Drugs (DREADDs) are synthetically engineered muscarinic receptors that have lost their affinity for acetylcholine but can be activated by Clozapine-n-oxide (CNO), which crosses the blood brain barrier when injected peripherally (Zhu and Roth 2014; Roth 2016). AAVs can be used to express

DREADDs coupled to G_i, G_q, or G_s under a variety of different promotors in a brain region-specific manner. While it is important to note that CNO may have non-specific physiological effects that need to be controlled for (Roth 2016), this technology allows researchers to non-invasively manipulate GPCR signaling in the brain in a cell-specific and region-specific manner. Glial-expressing DREADD constructs have now been developed such that astrocyte GPCR signaling can also be manipulated. The studies described herein take advantage of this technology to examine the role of astroglial GPCR signaling in the context of SEFL. The goal of Chapter 4 of the current dissertation was to test whether activation of hippocampal astroglial G_i signaling is sufficient to attenuate SEFL.

Specific Aims

As reviewed above, PTSD is a debilitating condition that imposes severe fiscal and emotional costs on society. A better understanding of the neurobiological mechanisms driving PTSD is crucial to the development of more targeted treatments. Rodent paradigms that examine behavioral responses to severe stress can be used to elucidate mechanisms involved in PTSD-like behaviors. The goal of the current dissertation was to examine hippocampal neural immune signaling as a potentially important mechanism involved in stress-enhanced fear learning, a PTSD-like phenotype. To accomplish goal, the three specific aims described below examined stress-induced changes at the cellular level in the hippocampus following severe stress and tested the involvement of two specific signaling pathways in the development of SEFL.

Cytokines in the central nervous system have recently emerged as important signaling molecules in the brain that modulate a range of behaviors, including stress response (Goshen and Yirmiya 2009; Bull, Freitas et al. 2014; Hutchinson and Watkins 2014). We have previously published strong preliminary data to suggest that hippocampal interleukin-1 signaling may be critical to the development of SEFL (Jones, Lebonville et al. 2015). Further, while the cellular source of stress-induced IL-1β remains unclear, astrocyte signaling, including astrocyte-derived cytokine signaling, has also been hypothesized to be important in behavioral responses to stress in rodent models of PTSD (Ben Menachem-Zidon, Avital et al. 2011; Xia, Zhai et al. 2013; Levkovitz, Fenchel et al. 2015). The experiments described below and in Chapters 2 through 4 tested the overarching hypothesis that (1) severe stress induces changes in hippocampal astrocyte-derived IL-1β expression and the morphometric properties

of astrocytes and (2) that both blocking hippocampal IL-1 signaling and activating hippocampal astroglial G_i signaling prevent the development of SEFL (Figure 1.3).

Specific Aim 1 tested the hypothesis that blocking IL-1 signaling in the dorsal hippocampus prevents SEFL and isolated the specific cellular source of hippocampal stress-induced IL-1β. Strong preliminary data suggest that blocking IL-1 signaling directly in the dorsal hippocampus is sufficient to prevent the development of SEFL. However, the cellular source of hippocampal stress-induced IL-1 remains unknown. The experiments in this aim contribute to our understanding of the role of central IL-1 in SEFL in that we (1) directly tested whether dorsal hippocampal IL-RA is sufficient to attenuate SEFL and (2) identified the cellular source of stress-induced IL-1. Furthermore, analyses in this aim contribute to our knowledge of stress-induced changes of two common markers for astrocytes and microglia, glial fibrillary acidic protein (GFAP) and ionized calcium-binding adaptor molecule -1 (Iba-1). Specific Aim 1 is described in Chapter 2.

Specific Aim 2 tested the hypothesis that astrocyte volume and synaptic contacts are altered and postsynaptic density 95 immunoreactivity is decreased following severe stress. Preliminary data suggest that astrocytes are one cellular source of stress-induced IL-1β (Sugama, Fujita et al. 2007) and astrocyte-dependent signaling has shown promise to prevent PTSD (Ben Menachem-Zidon, Avital et al. 2011; Xia, Zhai et al. 2013). This aim advances our understanding of how the morphology of astrocytes may be affected by severe stress exposure. We used novel technology to isolate and quantify astrocyte surface area, volume, and synaptic contact through 3-Dimensional reconstructions of individual hippocampal astrocytes (Scofield, Li et al. 2016). In analyzing hippocampal astrocyte synaptic contacts, we also tested the hypothesis that stress attenuates PSD95 immunoreactivity. Implications of a

potential stress-induced reduction in postsynaptic density 95 (PSD95) are discussed. Specific Aim 2 is described in Chapter 3.

Specific Aim 3 tested the hypothesis that astroglial G_i activation attenuates SEFL expression. Data from Chapter 2 provides strong evidence that astrocyte-derived IL-1β can influence SEFL and GPCR signaling has been shown to regulate IL-1β expression (Ye 2001). This aim makes a significant contribution to our understanding of glial-expressing DREADDs and our understanding of the role of astrocyte signaling in SEFL. In this aim, we tested the hypothesis that hippocampal astroglial G_i signaling is sufficient prevent SEFL. In addition, we measured colocalization of the GFAP-hM4Di-positive cells with cAMP, a G_i-dependent second messenger, in an effort to validate the function of this DREADD. Specific Aim 3 is described in Chapter 4.

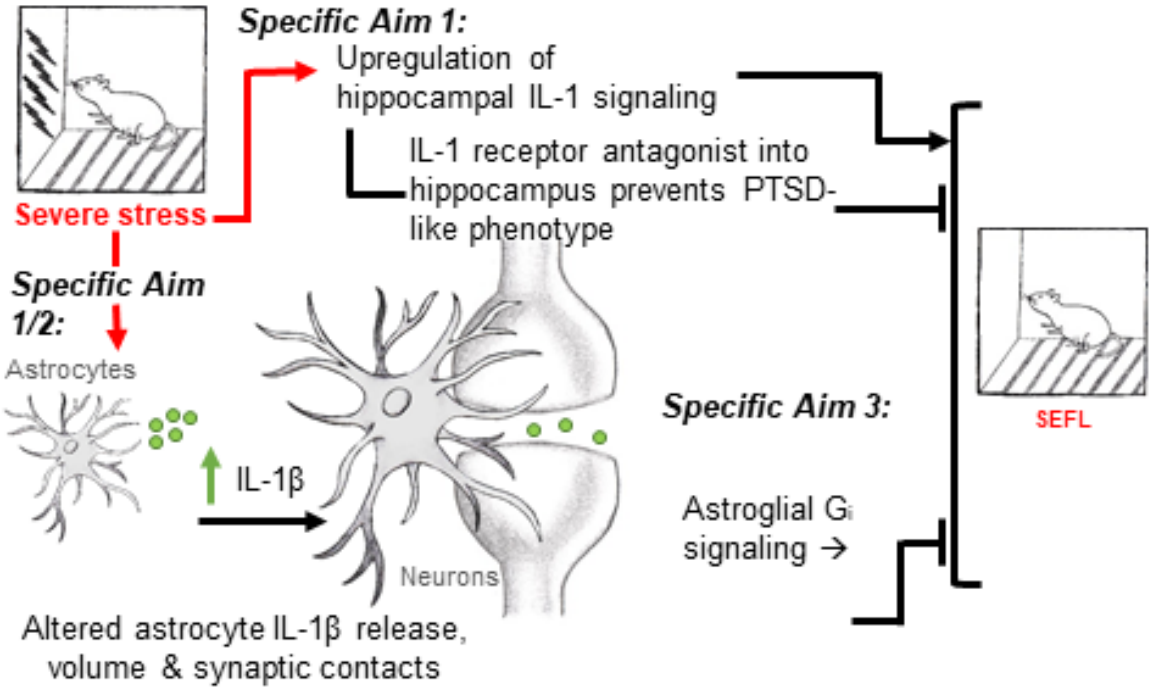

Figure 1.3 Experiments described in Chapters 2 through 4 address three Specific Aims. The goal of specific Aim 1 was to test whether dorsal hippocampal IL-1 signaling is required for SEFL and to identify the cellular source of stress-induced IL-1β. The goal of Specific Aim 2 was to provide a thorough analysis of the stress-induced changes in the morphometric properties of astrocytes 48 hours after the severe stressor of the SEFL paradigm. (A supplemental goal of Specific Aim 2 was to test whether stress attenuates hippocampal PSD95. This was done in the process of measuring astrocyte synaptic contacts.) The goal of Specific Aim 3 was to test whether hippocampal astroglial G_i signaling is sufficient to attenuate SEFL.

Chapter 2

EXAMINATION OF STRESS-INDUCED HIPPOCAMPAL IL-1β: EFFECT OF HIPPOCAMPAL IL-1RA ON STRESS-ENHANCED FEAR LEARNING AND IDENTIFICATION OF THE CELLULAR SOURCE[2]

Introduction

Converging evidence from both human and animal studies has suggested that psychiatric disorders involving depression and anxiety, including post-traumatic stress disorder (PTSD), involve substantial immune system dysregulation (Silverman, Macdougall et al. 2007; Gill, Saligan et al. 2009; Koo and Duman 2009; Stepanichev, Dygalo et al. 2014; Jones, Lebonville et al. 2015). As mentioned previously, several published studies have reported that PTSD is associated with elevated peripheral cytokines, including interleukin-1β (IL-β), tumor necrosis factor-α (TNF-α), and interleukin-6 (IL-6) (Gill, Saligan et al. 2009; Guo, Liu et al. 2012; Gola, Engler et al. 2013; Passos, Vasconcelos-Moreno et al. 2015; Wang and Young 2016). Cohen and colleagues have even suggested IL-1 as a potential biomarker for susceptibility to PTSD (Cohen, Meir et al. 2011). Central IL-1 signaling is consistently shown to be upregulated by a variety of different stress protocols in rodents and to be critically involved in stress response mechanisms that drive behavioral outcomes (Avital, Goshen et al. 2003; Goshen and Yirmiya 2009). For example, peripheral administration of IL-1β has been shown to lead to enhanced anxiety-like behavior in the elevated plus maze (EPM) (Swiergiel

[2] This chapter is published as an article in Brain, Behavior, and Immunity. Jones, M. E., C. L. Lebonville, et al. (2017). "Hippocampal interleukin-1 mediates stress-enhanced fear learning: A potential role for astrocyte-derived interleukin-1beta." Brain Behav Immun.

and Dunn 2007), and blocking IL-1 signaling centrally prevents stress-induced reductions in social interaction (Arakawa, Blandino et al. 2009). As mentioned in Chapter 1, we recently published the finding that stress-enhanced fear learning (SEFL), a preclinical animal model of PTSD developed by Rau and colleagues (Rau, DeCola et al. 2005), requires central IL-1 signaling. Our data demonstrated that the severe stressor of the SEFL paradigm (15 foot shocks) induces an increase in IL-1β in the dorsal hippocampus (DH) 24-48 hours after the stressor. Furthermore, blocking IL-1 signaling in the brain through an intracerebroventricular infusion of IL-1 receptor antagonist (IL-1RA) prevents the development of enhanced fear learning (Jones, Lebonville et al. 2015). Together these data suggest that central IL-1RA may be acting specifically in the hippocampus. Accordingly, the first goal of the current chapter was to test whether hippocampal IL-1 signaling 24-48 hours after severe stress is necessary for the expression of SEFL.

The second goal of the current chapter was to isolate and quantify colocalization of stress-induced IL-1β with cell-specific markers glial fibrillary acidic protein (GFAP), ionized-calcium binding adaptor molecule-1 (Iba-1), and neuronal nuclear antigen (NeuN) in order to isolate the cellular source of stress-induced hippocampal IL-1β. IL-1β can be expressed by many cell types in the brain, including microglia, astrocytes, and neurons (Yabuuchi, Minami et al. 1994; Guasch, Blanco et al. 2007; Ringwood and Li 2008; Flannery and Bowie 2010; Zhang, Sun et al. 2010; Huang, Smith et al. 2011). A critical component to better understanding the mechanism through which hippocampal IL-1 might influence behavioral outcomes following stress is to identify which cell type(s) produce(s) it in response to stress. While there is evidence of IL-1 expression in neurons (Kwon, Seo et al. 2008; Zhang, Sun et al. 2010; Huang, Smith et al. 2011), there is only one report to our knowledge of an

effect of stress on neuron-derived IL-1β. Kwon and colleagues reported an increase in IL-1β colocalized with neuronal nuclei following four days of restraint stress (Kwon, Seo et al. 2008). In contrast, there are several published studies to support the potential for microglia-derived or astrocyte-derived IL-1β, as described below.

Microglia are brain macrophage cells that play important roles in the healthy brain, both maintaining the cellular environment and protecting against injury or immune challenge (Perry, Hume et al. 1985; Minghetti, Ajmone-Cat et al. 2005; Block, Zecca et al. 2007; Calcia, Bonsall et al. 2016; Mendiola and Cardona 2017). A substantial population of microglia are present in the hippocampus (Lawson, Perry et al. 1990), and IL-1β is just one of the proinflammatory mediators released by activated microglia (Perry, Hume et al. 1985; Minghetti, Ajmone-Cat et al. 2005; Block, Zecca et al. 2007; Mendiola and Cardona 2017). While microglial activation and release of proinflammatory cytokines are well-established in the context of neurodegenerative diseases, there are inconsistencies regarding the timing, brain region–specificity, and direction of the effect of psychological stressors on microglia. Two independent groups reported no change in microglial gene expression in the hippocampus immediately following exposure to foot shock (Blandino, Barnum et al. 2009; Brzozowska, Smith et al. 2017). However, Sugama and colleagues reported that microglial activation was increased one to six hours following a two hour exposure to restraint stress in the thalamus, hypothalamus, and hippocampus (Sugama, Fujita et al. 2007). Interestingly, in the same report, hypothalamic microglial activation was only associated with an increase in IL-1β mRNA and immunoreactivity when induced by lipopolysaccharide (LPS), but not when induced by restraint stress. Consistent with an increase in microglial activation and proliferation in response to stress, Frank et al. reported that major histocompatibility complex II

immunoreactivity (MHC II, predominantly expressed by microglia) was increased in the hippocampus 24 hours after inescapable tail shock (Frank, Baratta et al. 2007), but they observed no change in either GFAP or Iba-1 immunoreactivity in the same tissue.

The final candidate for a potential source of stress-induced IL-1β is astrocytes. As mentioned in Chapter 1, though traditionally viewed merely as neuronal "glue", astrocytes are now known to be critically involved in a diverse array of functions in development and disease (Barres 2008). Converging evidence from several laboratories using a variety of different severe stress procedures suggests that both GFAP expression and astrocyte process length are altered over time in the brain following stress (Tynan, Beynon et al. 2013; Xia, Zhai et al. 2013; Choi, Ahn et al. 2016; Saur, Baptista et al. 2016). Choi and colleagues observed an increase in the length and number of astrocyte processes but a decrease in GFAP in the DH one hour, but not 24 hours, after exposure to foot shock fear conditioning (Choi, Ahn et al. 2016). In contrast, others have observed decreases in the number of astrocyte processes either following chronic restraint stress (Tynan, Beynon et al. 2013) or 24-48 hours after foot shock exposure (Saur, Baptista et al. 2016). Of particular relevance here, Sugama and colleagues found that IL-1β expression was increased specifically in astrocytes, and not microglia, following cold stress (Sugama, Takenouchi et al. 2011).

Importantly, much of the previous literature regarding gene expression and morphology of both astrocytes and microglia focuses on early time points post-stress. Given that we have previously reported that the IL-1-dependent mechanism that attenuates the development at SEFL is specific to the later time points following stress, 24-48 hours (Szczytkowski-Thomson, Lebonville et al. 2013; Jones, Lebonville et al. 2015), here we focus on changes in the DH at 48 hours after foot shock stress. Specifically, Experiment 2.1 tested

whether IL-1 signaling in the DH is critical to the development of a PTSD-like phenotype in SEFL. Experiment 2.2 examined stress-induced changes in astrocytes and microglia in the DH and identified the cellular source of stress-induced IL-1β in this region. Analyses from Experiment 2.2a replicated our previous finding of stress-induced IL-1β in the dorsal hippocampus. Analyses from Experiment 2.2b quantified GFAP and Iba-1 immunoreactivity to examine stress-induced changes in astrocytes and microglia, respectively. Finally, analyses in Experiment 2.2c used Bitplane Imaris software in combination with confocal microscopy to visualize the colocalization of IL-1β with GFAP, Iba-1, and NeuN following foot shock to isolate and quantify astrocyte-derived, microglia-derived, and neuron-derived IL-1β, respectively. Collectively, these experiments tested the hypotheses that IL-1 signaling in the DH is critical for the development of SEFL and that astrocytes are the predominant cellular source of hippocampal IL-1β following stress in this context.

Methods

Animals

Male Sprague Dawley rats (225-250 g, Charles River Laboratories, Raleigh, NC) were housed individually under a reversed 12 hour light-dark cycle. They were given ad libitum access to food and water and were handled regularly throughout all experiments. All procedures were conducted in accordance with and approval by the UNC Institutional Animal Care and Use Committee.

Experiment 2.1: Effect of intra-dorsal hippocampal IL-1RA on the development of SEFL

Surgery

Animals were anesthetized with a 1.0 mg/kg intraperitoneal injection of 9:1 (vol:vol) ketamine hydrochloride (100mg/ml) mixed with xylazine (100 mg/ml). Guide cannulae (26 Gauge, Plastics One, Roanoke, VA) were directed bilaterally at the DH (AP -3.4 mm, ML ± 3.1 mm, DV -2.2 mm, 15 degrees, relative to bregma). Animals were given one week for postoperative recovery prior to the start of any experimental procedures. Upon completion of the experiment, correct cannula placement was verified and any animals with incorrect placement were dropped from the analysis.

Stress-enhanced fear learning

All animals (N = 36, n = 9) were assigned to a Context A treatment (Foot Shock in Context A or No Foot Shock in Context A) and a drug treatment (IL-1RA or vehicle) and exposed to the SEFL paradigm (Figure 2.1), as has been previously described (Szczytkowski-Thomson, Lebonville et al. 2013; Jones, Lebonville et al. 2015). Briefly, on Day 1, animals were exposed to Context A (BRS/LVE, Laurel, MD; 26.7 cm × 24.8 cm × 30.7 cm) which was housed in a separate room with distinct textile, olfactory, and auditory characteristics from the home cage. Animals assigned to the Foot Shock in Context A condition received 15 2 mA scrambled foot shocks over 90 minutes on a 6 minute variable interval schedule while control animals were exposed to the context for the same amount of time without foot shocks being delivered. Six days later, animals were exposed to Context B, a standard rodent chamber housed in a wooden sound attenuating cubicle (Med Associates, St. Albans, VT, 20.5 cm x 23.5 cm x 30.7 cm), which was again housed in a separate room from Context A and the home

cage. Context B was also associated with distinct textile, olfactory, and auditory characteristics from both Context A and the home cage. In addition, behavior in Context B was recorded using a video recording system (Sony Video Camera Model HDR-CX150). Similar to Rau and colleagues (Rau, DeCola et al. 2005), animals were exposed to Context B for 30 minutes without foot shocks being delivered to allow for habituation to the new context. On Day 8, animals were placed back into Context B where all animals received a single 1 mA scrambled foot shock, 3 minutes, 12 seconds after being placed into the context. Behavior during the three minutes prior to the single shock was recorded and analyzed to test for generalization of fear between the two contexts (these data are presented as 'baseline'). On Days 9, 10, 15 and 22 (Test Days 1, 2, 7 and 14), animals were placed in Context B for 8 minutes, 32 seconds and behavior was recorded.

Ethovision XT video tracking software (Noldus Information Technology Inc.) was used to analyze freezing behavior, a measure of learned fear defined as a lack of all movement except that required for breathing. Specifically, the activity analysis feature (Activity Threshold = 10) was used to calculate the percent of time each animal was inactive during each contextual fear test and at baseline. No animals in any group demonstrated significant freezing behavior to Context B prior to the single foot shock, suggesting that there was no generalization of fear between contexts (Results 2.1). Thus, any differences observed between treatment groups presented here reflect altered learning to the single foot shock in Context B.

IL-1 receptor antagonist

IL-1RA (GenScript, Piscataway, NJ) was reconstituted in sterile saline (2.5 µg/µl). Twenty-four hours prior to Context A exposure, animals were given a sham microinfusion to allow for habituation to microinfusion procedures. Twenty-four and 48 hours after removal

from Context A, on Days 2 and 3, animals were microinfused with 1.25 µg of IL-1RA or sterile saline vehicle per hemisphere at a rate of 0.25 µl/min. Injectors had a 1mm projection and were left in place for 1 minute after the infusion to allow for diffusion. These time points were based on our earlier published findings that morphine administration and intracerebroventricular IL-1RA prevent the development of SEFL when administered 48 hours after Context A (Szczytkowski-Thomson, Lebonville et al. 2013; Jones, Lebonville et al. 2015).

Experiment 2.2: Immunofluorescence analysis of severe stress-induced changes in hippocampal GFAP, Iba-1, NeuN, and IL-1β

Stress exposure

Animals (N = 16, n = 8) were randomly assigned to either a Foot Shock (in Context A) or No Foot Shock (in Context A) treatment and exposed to only the initial severe stressor of the SEFL paradigm described in Experiment 2.1. As such, animals assigned to receive foot shocks were exposed to 15 2 mA scrambled foot shocks in Context A as described above, an environment distinct from the home cage, while control animals were exposed to the same context without foot shocks being delivered. Forty-eight hours after removal from Context A, animals were deeply anesthetized with 9:1 (vol:vol) ketamine hydrochloride (100 mg/ml) mixed with xylazine (100 mg/ml) and transcardially perfused with cold phosphate buffer (PB; pH = 7.4) for three minutes at a rate of 15 mls/minute followed by 4% paraformaldehyde in 0.1M PB for seven minutes at a rate of 15 mls/minute. Brains were extracted, post-fixed in paraformaldehyde for 4-6 hours and placed in 30% sucrose with 0.1% sodium azide at 4°C for cryoprotection. Brains were sectioned into 40 µm sections on a freezing microtome.

Immunohistochemistry

For colocalization analyses, tissue was stained with three primary antibodies. All primary antibodies were verified by no primary control stains in which tissue was only exposed to secondary antibodies to ensure specificity of each signal in the triple label. Tissue was first washed three times for 10 minutes in 0.1M phosphate buffer (PB, pH = 7.4). For tissue stained with anti-Iba-1 antibody, tissue was incubated in endogenous biotin and streptavidin blocks (Vector Laboratories, Burlingame, CA, USA) for 30 minutes each at room temperature, according to the manufacturer's instructions. All tissue was incubated in 5% Normal Goat Serum (NGS) and 0.5% TritonX100 in 0.1 M PB for 3 hours at room temperature. Tissue was incubated in primary antibody, 5% NGS, and 0.5% TritonX100 in 0.1M PB overnight at 4°C, washed three times for 10 minutes in 0.1M PB, and incubated in secondary antibody, 5% NGS, and 0.5% TritonX100 in 0.1M PB for 60-120 minutes at room temperature. Each antibody was applied individually and thus the entire triple stain procedure occurred over three subsequent nights. The following primary antibodies were used: rabbit anti-IL-1β (1:500, Abcam, Cambridge, MA, Cat # Ab9722), mouse anti-GFAP (1:1000, ThermoFisher Scientific, Waltham, MA, Cat # MS-1376P), mouse anti-NeuN-Alexa 568 (1:1000, Abcam Cambridge, MA, Cat # Ab207282), and rabbit anti-Iba-1-biotinylated (1:500, Wako, Richmond, VA, Cat # 016-26461). To visualize IL-1β and GFAP, goat anti-rabbit Alexa Fluor 488 (1:1000, ThermoFisher Scientific, Waltham, MA, Cat #A11008) and goat anti-mouse Dylight 405 (1:1000, ThermoFisher Scientific, Waltham, MA, Cat # 35501BID) were used. Goat anti-rabbit Alexa Fluor 488 was applied for 60 minutes and goat anti-mouse Dylight 405 was applied for 120 minutes. To visualize Iba1, a streptavidin-conjugated Alexa Fluor 568 antibody (1:1000, ThermoFisher Scientific, Waltham, MA, Cat #S11226) was used and was applied for

60 minutes. Sections were mounted onto SuperFrost Plus slides (Fisher Scientific, Pittsburgh, PA) using Vectashield hard set mounting medium (Vector Laboratories, Burlingame, CA). Tissue from poor perfusions that yielded high nonspecific background which interfered with thresholding and colocalization calculations was dropped from the analysis, and any such decision was made blind to treatment group.

Confocal microscopy, Bitplane Imaris colocalization analysis, and cell counting

All image acquisition and analysis was completed by an experimenter blind to treatment group. Tissue was imaged using a Zeiss LSM800 confocal microscope with laser lines that excite at 405 nm, 488 nm, and 561 nm. Images were acquired using a 63X oil immersion lens. Z stacks of the dentate gyrus of the dorsal hippocampus (AP -3.12 mm through -3.84 mm from bregma) were acquired using a frame average of 4, 1024 by 1024 frame size, 12 bit image resolution, and 0.8 µm step size. We focused our analysis on the dentate gyrus based on our previous finding that IL-1β expression is most dense in this subregion of the DH (Jones, Lebonville et al. 2015).

Z stacks were deconvolved using Bitplane AutoQuant X3 (10 iterations, (Lee, Wee et al. 2014)) and exported to Bitplane Imaris software (Zurich, Switzerland). For background correction of each channel individually, absolute intensity thresholds were manually set. In the colocalization module, voxels above the threshold in both channels were included as colocalized voxels. A two-dimensional scatter plot was used to visually inspect the accuracy of colocalization thresholds. The colocalization between IL-1β and GFAP, IL-1β and Iba-1, and IL-1β and NeuN was calculated. The following values were recorded: % volume above the absolute intensity threshold selected for each channel, % IL-1β colocalized with Iba1, GFAP, and NeuN, respectively, and the Pearson's correlation coefficient for each pair of

signals. In addition to Imaris volume and colocalization analyses, the number of GFAP-positive and Iba-1-positive cells in the dentate gyrus was counted in images acquired at 10X by an experimenter blind to treatment group.

Statistical analyses

For Experiment 2.1, a one way ANOVA with treatment group as the between subjects factor was used to analyze baseline freezing data during the three minutes prior to the foot shock during Context B conditioning in order to ensure there were no group differences in freezing to Context B prior to the single shock. A 2 x 2 x 4 repeated measures ANOVA with Context A treatment and drug treatment as between subject factors and test day as a within subjects factor was used to analyze freezing behavior across test days 1, 2, 7 and 14. For Experiment 2.2, unpaired, two-tailed student's t tests were used to test whether Foot Shock treatment altered GFAP or Iba-1 immunoreactivity and an unpaired one-tailed student's t test was used to test whether Foot Shock treatment altered IL-1β immunoreactivity. For colocalization data, the percent of IL-1β colocalized with each signal and the Pearson's correlation coefficient for each pair of signals were subjected to a 2 x 3 ANOVA with Foot Shock treatment and cell type specific signal analyzed as factors. Significant interactions were examined using Tukey's post-hoc comparisons. Specifically, for Experiment 2.1 planned comparisons included: Foot shock in Context A/ Vehicle vs. Foot shock in Context A/ IL-1RA and No Foot shock in Context A/ Vehicle vs. Foot shock in Context A/ Vehicle. For colocalization data, planned comparisons included GFAP/IL-1β colocalization parameters vs. Iba-1/IL-1β colocalization parameters and GFAP/IL-1β colocalization parameters vs. NeuN/IL-1β colocalization parameters.

Results

Experiment 2.1: Intra-dorsal hippocampal IL-RA prevents SEFL

Figure 2.1 shows freezing behavior across all four test days. There was no effect of Context A treatment on baseline freezing in Context B prior to the single shock, $F(3, 24) = 2.674$, $p > 0.05$, confirming that there was no generalization of fear between the two contexts. A 2 x 2 x 4 ANOVA revealed a significant main effect of Context A treatment, $F(1, 23) = 5.159$, $p = 0.033$, and a significant main effect of drug treatment, $F(1, 23) = 9.354$, $p = 0.006$. In addition, there was a significant main effect of test day, $F(1, 23) = 23.344$, $p < 0.001$, indicating that contextual fear diminished across test days. Importantly, there was a significant Context A treatment by drug treatment interaction, $F(1, 23) = 4.394$, $p = 0.047$. Tukey's post hoc comparisons revealed a significant stress-enhanced fear learning effect within vehicle-treated groups in that foot shock in Context A significantly enhanced freezing to Context B, $p = 0.038$. Critically, IL-1RA treatment prevented stress-enhanced fear learning within groups that received foot shock in Context A. Rats that received foot shock in Context A followed by IL-1RA exhibited significantly less freezing than rats that received foot shock in Context A followed by vehicle, $p = 0.001$. Further, rats that received foot shock in Context A followed by IL-1RA exhibited a comparable amount of freezing behavior (no statistically significant difference), to both control groups of rats that received no foot shock in Context A, $p > 0.05$.

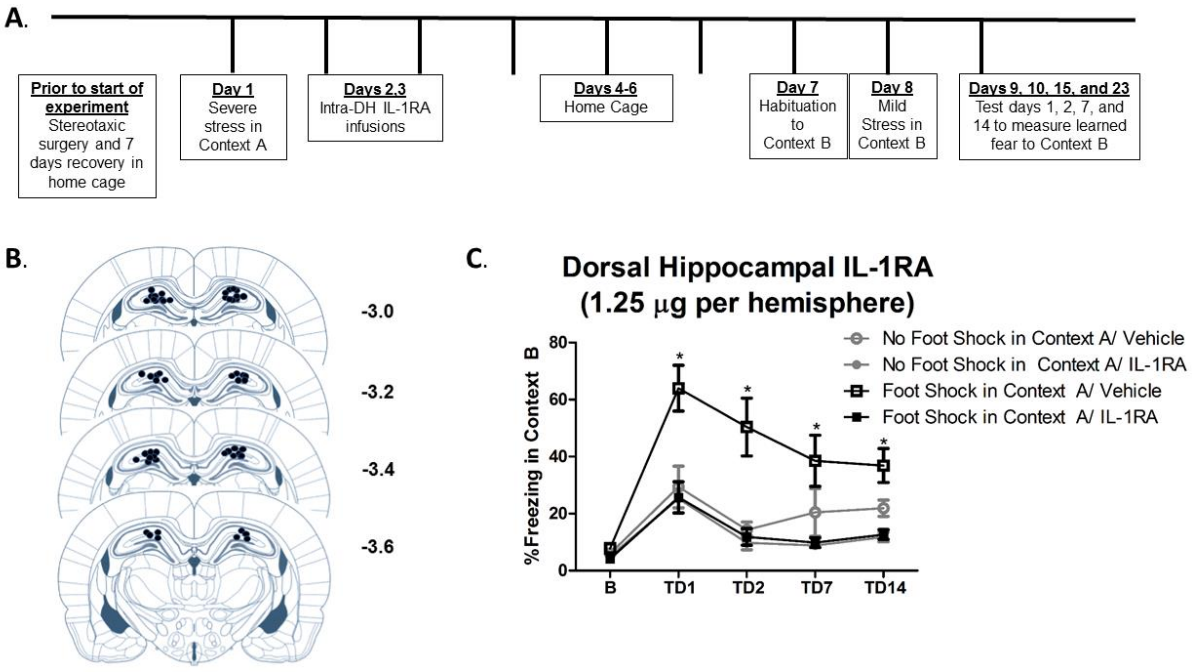

Figure 2.1 Intra-dorsal hippocampal IL-1RA is sufficient to prevent SEFL. (A) Schematic shows Experiment 2.1 timeline of surgical procedures, intra-DH microinfusions, and severe stress exposure and contextual fear learning in the SEFL paradigm. (B) Paxinos and Watson (2007) schematics of the rat brain show approximate cannulae placement. Coordinates -3.0 through -3.6 from Bregma are shown. Each circle represents where damage from the cannula tract was observed for all animals included in the analysis. (C) DH-IL-1RA significantly attenuated SEFL. There were no differences between groups in freezing to Context B prior to the single shock. Stress-enhanced fear learning was observed within vehicle-treated groups in that rats that received foot shock in Context A followed by vehicle exhibited significantly more fear learning to Context B than rats that received no foot shock in Context A followed by vehicle. Critically, animals that received foot shock in Context A followed by IL-1RA exhibited significantly less freezing than animals that received foot shock in Context A followed by vehicle. Thus, IL-1RA prevented the expression of SEFL. * Foot Shock in Context A/ Vehicle vs. Foot Shock in Context A/ IL-1RA, $p < 0.05$.

Experiment 2.2a: Stress-induced increase in hippocampal IL-1β is replicated

We previously reported that the severe stressor of the SEFL paradigm induces an increase in hippocampal IL-1β immunoreactivity and mRNA that emerges at 6 hours and persists through 72 hours following stress exposure (Jones, Lebonville et al. 2015). Here, this effect is replicated in that exposure to the severe stressor of SEFL significantly enhanced hippocampal IL-1β immunoreactivity 48 hours later, t (10) = 2.083, $p = 0.0319$ (Figure 2.2).

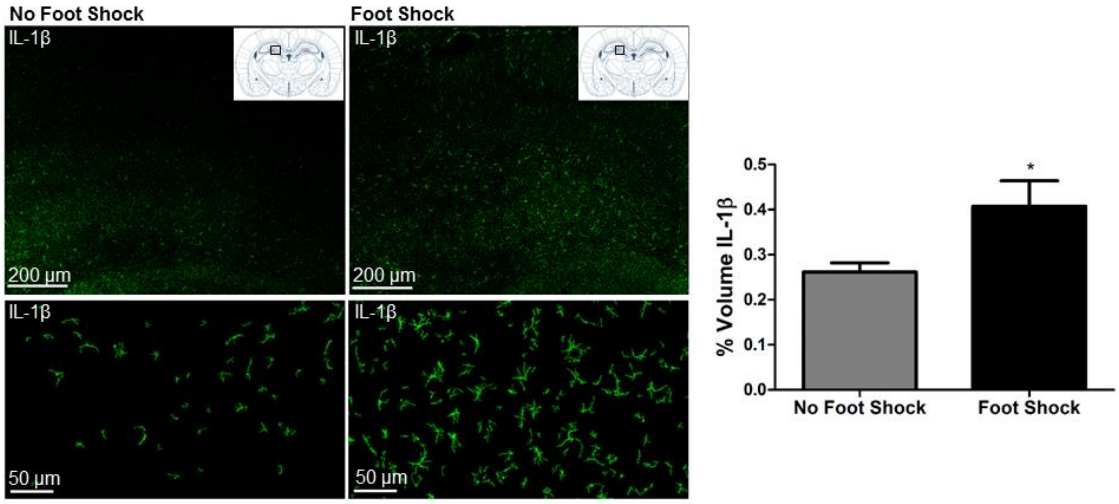

Figure 2.2 Severe stress increases hippocampal IL-1β immunoreactivity. The stress-induced increase in hippocampal IL-1β that we previously reported is replicated here. Representative images of IL-1β immunoreactivity in the dentate gyrus of the DH acquired at 10X are shown from stressed (Foot Shock in context A) and non-stressed (No Foot Shock in Context A) rats. Top panel shows a tiled 10X image, while bottom panel shows a single 10X image. For the bottom panel, Bitplane Imaris was used for background subtraction to better visualize individual cells presented. Paxinos and Watson (2007) schematic shows the approximate region of the DH where images were acquired, AP -3.36 from bregma. Quantification of IL-1β immunoreactivity revealed that exposure to severe stress (15 foot shocks) significantly increased IL-1β immunoreactivity in the DH 48 hours post-stress. * $p < 0.05$.

Experiment 2.2b: Severe stress attenuates Iba-1, but not GFAP, in the dorsal hippocampus

Exposure to severe stress did not alter hippocampal GFAP immunoreactivity. There was no effect of Context A treatment on Imaris quantification, $t(9) = 1.295$, $p > 0.05$, or the number of GFAP-positive cells, $t(11) = 0.9563$, $p > 0.05$. However, exposure to severe stress significantly reduced hippocampal Iba-1 immunoreactivity. Exposure to Foot Shock in Context A attenuated both Imaris quantification of Iba-1 immunoreactivity, $t(9) = 2.497$, $p = 0.0340$, and the number of Iba-1-positive cells, $t(10) = 2.375$, $p = 0.0389$. Figure 2.3 shows representative images and quantification of hippocampal GFAP and Iba-1, respectively.

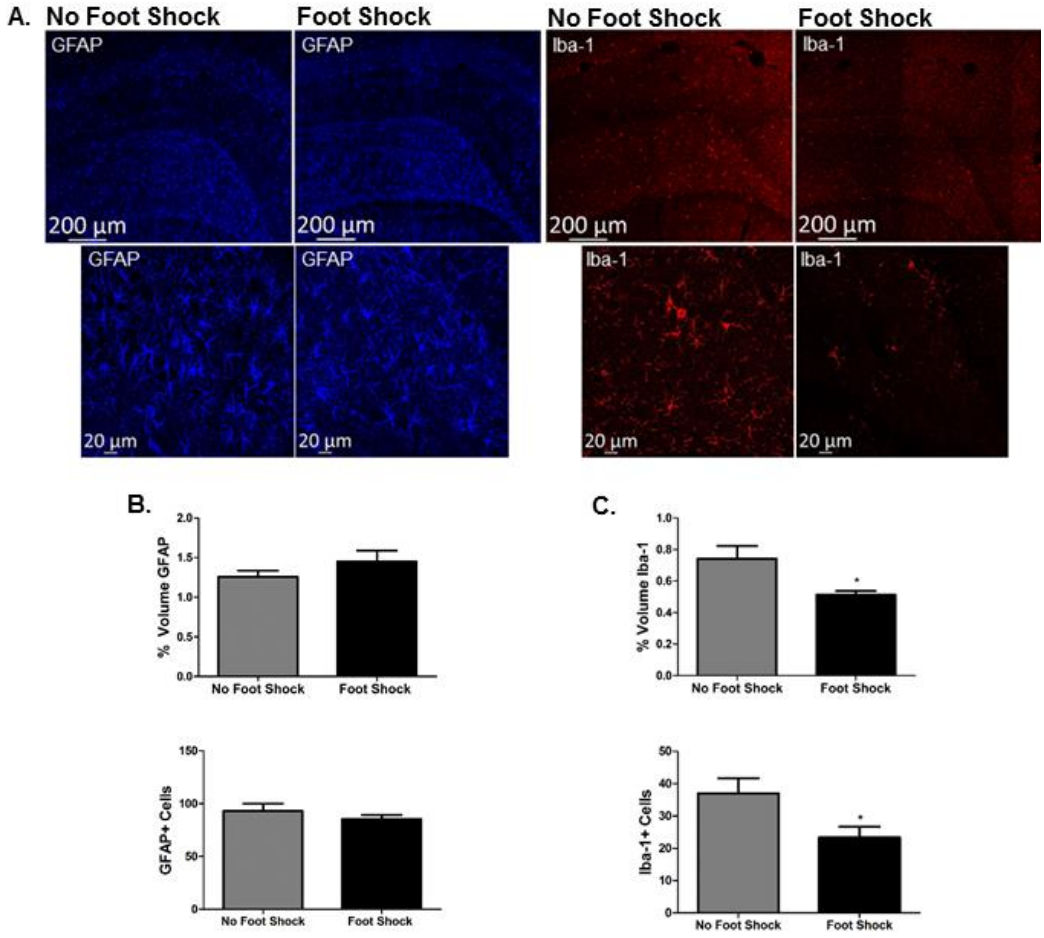

Figure 2.3 Dorsal hippocampal Iba-1 immunoreactivity, but not GFAP immunoreactivity, is attenuated 48 hours after severe stress. (A). Representative images of GFAP and Iba-1 immunoreactivity acquired at 10X (tiled image presented) and 20X are shown from stressed (Foot Shock in Context A) and non-stressed (No Foot Shock in Context A) rats. Images were acquired in the DH, AP -3.36 from bregma. (B) Both Imaris quantification and individual GFAP-positive cell counts indicated there was no effect of stress on GFAP immunoreactivity. (C) In contrast, Imaris quantification and individual Iba-1 positive cell counts revealed that stress exposure significantly attenuated Iba-1 immunoreactivity 48 hours post-stress. * $p < 0.05$.

Experiment 2.2c: Stress-induced hippocampal IL-1β is colocalized primarily with GFAP in both stressed and non-stressed animals

Figures 2.4 and 2.5 show that there was an overwhelming amount of IL-1β colocalized with GFAP, 75% to 79% of the IL-1β signal, and only minimal colocalization with Iba-1 or NeuN, less than 5% of the IL-1β signal. Thus, there was over 15- fold greater colocalization of IL-1β with GFAP compared to the other two cell-type markers in both stressed and non-stressed animals. As such, there was a significant main effect of cell-type analyzed in both the % IL-1β signal colocalized, $F(2, 28) = 2423.859$, $p < 0.001$, and the Pearson's correlation coefficient, $F(2, 28) = 51.166$, $p < 0.001$. Again, regarding both the % IL-1β signal colocalized and the Pearson's correlation coefficient, post hoc comparisons confirmed significantly more colocalization with GFAP than Iba-1, $p < 0.001$, and with GFAP than NeuN, $p < 0.001$. There was no difference between colocalization of IL-1β with Iba-1 and with NeuN, $p > 0.05$.

The cellular distribution of IL-1β was not changed by exposure to severe stress (Figure 2.4). There was no main effect of Context A treatment on either the % IL-1β colocalized with each signal, $F(1, 28) = 1.949$, $p > 0.05$, or the Pearson's correlation coefficient between signals, $F(1, 28) = 1.749$, $p > 0.05$.

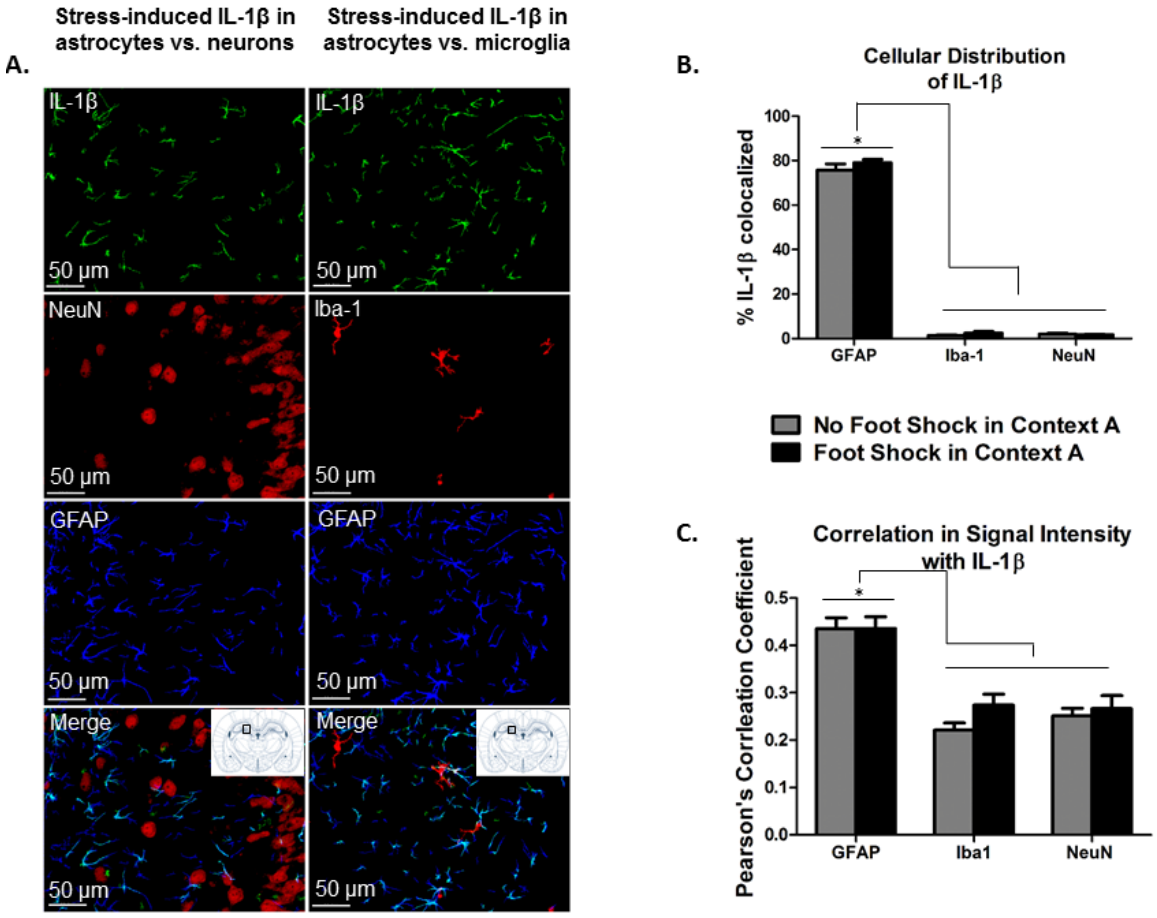

Figure 2.4 IL-1β signal is colocalized with GFAP, and not with Iba-1 or NeuN, in the dorsal hippocampus in stressed and non-stressed animals. (A) Representative images of IL-1β, NeuN, Iba-1, and GFAP immunoreactivity in the dentate gyrus of the DH (AP -3.36 mm from bregma) acquired at 20X are shown. Because we did not detect any differences in colocalization between stressed and non-stressed rats, all images here are taken from animals that received stress exposure. Bitplane Imaris was used for background subtraction to better visualize individual cells presented. (B) Bitplane Imaris software was used to calculate the colocalization of the IL-1β signal with GFAP, Iba-1, and NeuN. Colocalization analyses revealed that the percent of the IL-1β signal colocalized with GFAP was significantly greater than the percent of the IL-1β signal colocalized with either Iba-1 or NeuN. * $p < 0.05$. (C) Similarly, the Pearson's correlation coefficient between the IL-1β signal intensity and the GFAP signal intensity was significantly higher than that for the IL-1β signal and Iba-1 signal or NeuN signal, respectively. * $p < 0.05$.

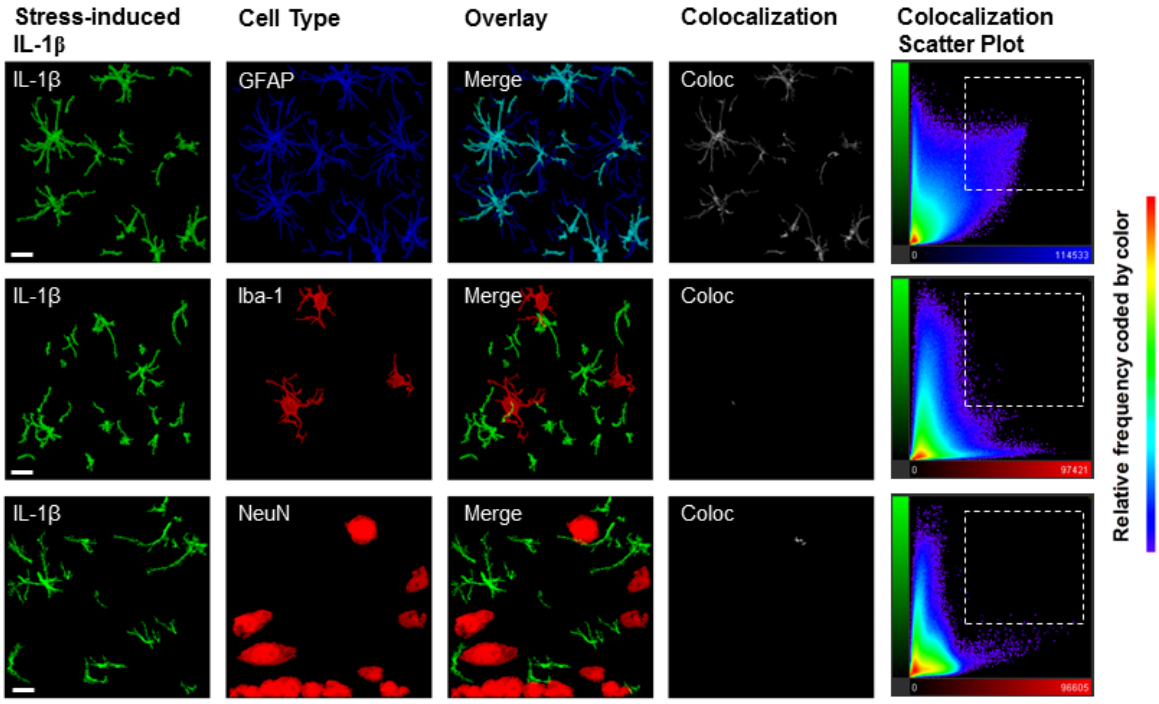

Figure 2.5. IL-1β signal is colocalized with GFAP, and not with Iba-1 or NeuN, in the dorsal hippocampus in stressed and non-stressed animals. Representative images from the DH acquired at 63X (scale bar presented is 10 µm) show colocalization of IL-1β with GFAP, Iba-1, and NeuN. Because we did not detect any differences in colocalization between stressed and non-stressed rats, all images here are taken from animals that received stress exposure. Colocalization panels (white, labeled 'Coloc') show Imaris-generated image of colocalized voxels in each Z stack image presented. Colocalization scatter plots show the signal intensity for each voxel in the Z stack. Specifically, color of each point represents the frequency, the Y axis represents IL-1β signal (Alexa Fluor-488) intensity, and the X axis represents GFAP (Dylight 405), Iba-1 (Alexa Fluor 568), or NeuN signal (Alexa Fluor 568) intensity, respectively. In the top panel, the colocalization scatter plot between IL-1β and GFAP shows a high proportion of voxels that were high in both IL-1β and GFAP signal (selected region), and a high observed correlation, r = 0.3997, demonstrates that for any given voxel, as IL-1 signal increased, GFAP signal was also likely to increase. In contrast, scatter plots for both IL-1β with Iba-1 and IL-1β with NeuN show a high proportion of voxels that were high in only IL-1β or Iba-1 and NeuN signal, respectively (outside of selected region). In addition, there was a lower correlation for the IL-1β and Iba-1 signal, r = 0.1915, and IL-1β and NeuN signal, r = 0.0373, suggesting a much weaker relationship than that with GFAP.

Discussion

In the current chapter, we provide evidence that astrocytes are the cellular source of foot shock-induced hippocampal IL-1β, which plays a critical role in the development of SEFL, an animal model of PTSD. Experiment 2.1 supports our hypothesis that dorsal hippocampal IL-1 signaling is necessary for the development of SEFL in that intra-DH IL-1RA infused 24 and 48 hours following severe stress prevented the expression of SEFL. Further, Experiment 2.2 provides the first evidence that Iba-1 immunoreactivity is reduced 48 hours following foot shock stress and that the IL-1β signal at this critical time point for behavioral consequences of severe stress is almost exclusively colocalized with an astrocyte-specific marker, and not with microglia- or neuron-specific markers.

Our finding that hippocampal astrocytes are the predominant source of stress-induced hippocampal IL-1β is consistent with previously published data suggesting that astrocyte-dependent signaling is important in stress and anxiety-related behavior (Barres 2008; Ben Menachem-Zidon, Avital et al. 2011; Cao, Li et al. 2013; Xia, Zhai et al. 2013; Rial, Lemos et al. 2015). These findings will be discussed further in Chapter 4. However, one limitation of the current findings is that future studies are needed to provide insight into the potential causal link between astrocyte signaling and SEFL. For example, to test whether astrocyte-derived IL-1, specifically, is causally related to SEFL, future studies could examine the development of SEFL using an astrocyte-specific IL-1 knockout strain or test whether pharmacological or genetic astrocyte ablation influences SEFL development. As mentioned in Chapter 1, chemogenetic tools under the control of a GFAP promoter are also commercially available and experiments described in Chapter 4 will contribute to our understanding of the role of astrocyte signaling and fear and anxiety-like behavior using this approach. Thus, while the complete

mechanisms involved in astrocyte regulation of stress and anxiety-related behavior remain unclear, our data and others' reports converge to suggest a critical role for astrocytes in behavioral responses to stress.

Given that microglia-derived cytokines are well-established in models of neurodegenerative disease, for example, Alzheimer's and Parkinson's disease (Sawada, Imamura et al. 2006; Block, Zecca et al. 2007; Rogers, Mastroeni et al. 2007), our observation of a reduction in microglia is somewhat surprising. While our data are in conflict with several reports of stress-induced increases in hippocampal microglia activation or cell count, (Brevet, Kojima et al. 2010; Calcia, Bonsall et al. 2016), we are not the first to observe a decrease in Iba-1 immunoreactivity following stress. Brzozowska and colleagues reported no change in hippocampal microglial cell count but a reduction in microglial cell count in the basolateral amygdala 30 days after stress exposure in another foot shock based rodent model of PTSD (Brzozowska, Smith et al. 2017). Further, Kreisel and colleagues found that multiple markers of microglia, including both Iba-1 and Cd11b mRNA expression and microglia cell count, were decreased in the dentate gyrus following five days of chronic unpredictable stress (CUS) capable of inducing a depressive-like phenotype (Kreisel, Frank et al. 2014). Interestingly, they also showed that after only one day of CUS, these same measures showed an increase in microglia gene expression/ immunoreactivity induced by stress. Thus, severity of stressor and a longer stress exposure or a later time point after the initial stressor may be critical to our observed effect. Nonetheless, the reduction in Iba-1 immunoreactivity observed here further supports the notion that astrocytes, not microglia, are organizing important changes in the DH following severe stress.

We hypothesized that GFAP expression would increase following stress because the IL-1β signal is increased in the hippocampus at this time point following stress, and is highly colocalized with GFAP. While this hypothesis was not confirmed here, there are several potential explanations for our observed lack of effect. First, the amount of GFAP expression in the DH (1-1.5% of the region measured) is more than six times that of IL-1β (0.2-0.3% of the region measured). Thus, an increase in IL-1β in astrocytes can easily occur without a corresponding increase in GFAP. Second, while GFAP is one of the most canonical astrocyte markers relied on in the field, GFAP is a cytoskeletal protein that is only expressed within 15% of a given astrocyte's area and even then, only by a subset of astrocytes (Benediktsson, Schachtele et al. 2005; Rajkowska and Stockmeier 2013). Measures of GFAP have also yielded results that have conflicted with other measures of astrocyte reactivity. Tynan and colleagues examined stress-induced changes in astrocyte activation and showed an increase in S100β, another astrocyte-specific marker, but a decrease in GFAP following the same stressor (Tynan, Beynon et al. 2013). Thus, our measure of GFAP immunoreactivity is an incomplete measure of astrocyte reactivity and experiments described in Chapter 3 take advantage of new technologies to study astrocyte morphology in greater detail.

While the sole focus on IL-1 signaling in the current manuscript is well justified given previous work supporting the importance of IL-1 signaling in the context of behavioral responses to stress (Avital, Goshen et al. 2003; Goshen and Yirmiya 2009; Jones, Lebonville et al. 2015), it is important to note that IL-1β does not act in isolation and several other proinflammatory mediators may play additional vital roles. For example, both interleukin-6 (IL-6) and tumor necrosis factor- α (TNF-α) have been shown to be upregulated following stress (Audet, Mangano et al. 2010; Barnum, Pace et al. 2012). Studies to examine behavioral

implications of stress-induced alterations in additional immune signaling pathways would provide more information regarding the specificity of the IL-1 mechanism or could identify additional mechanisms that play a role.

In summary, the data described herein demonstrate that hippocampal IL-1 drives important neural changes that render animals hypersensitive to fear learning following stress. Further, our data suggest that astrocytes are an important source of hippocampal stress-induced IL-1β. These findings provide additional evidence that IL-1 signaling should be considered a target for the development of novel therapeutics to treat PTSD and suggest one mechanism through which hippocampal astrocytes may influence complex behavior.

Chapter 3

EFFECT OF SEVERE STRESS ON THE MORPHOMETRIC PROPERTIES OF HIPPOCAMPAL ASTROCYTES

Introduction

The goal of Chapter 3 was to conduct a more thorough analysis of severe stress-induced changes in hippocampal astrocyte morphology. Experiments described in Chapter 2 present a potential role for astrocytes in the development of SEFL. Specifically, our data provide evidence that the predominant source of hippocampal stress-induced IL-1β, which we have also shown to be causally related to SEFL, is astrocytes (Figures 2.4 and 2.5). Relatedly, astrocytes not only release IL-1 but also express IL-1 receptors, and IL-1β is thought to be a potent induction signal for astrocyte activation (Giulian, Woodward et al. 1988; Herx and Yong 2001; Proescholdt, Chakravarty et al. 2002; John, Lee et al. 2003). As such, stress-induced IL-1β may, over time, induce further changes in the morphometric properties of astrocytes. While we did not observe a stress-induced change in hippocampal GFAP immunoreactivity, as described in Chapter 2, others have after a variety of stress protocols (Tynan, Beynon et al. 2013; Xia, Zhai et al. 2013; Choi, Ahn et al. 2016; Saur, Baptista et al. 2016) and inconsistencies in our understanding of hippocampal astrocyte function in the context of behavioral responses to stress remain.

Changes in astrocyte morphology are important to investigate because astrocyte morphology and synaptic contact can directly influence astrocyte and neuronal function (Montgomery 1994; Blanco-Suarez, Caldwell et al. 2016; Colombo and Farina 2016). Converging evidence from multiple laboratories confirms that astrocytes can regulate

glutamate homeostasis, synaptic remodeling, secretion of neurotrophic factors, and synaptic strength (Ben Menachem-Zidon, Avital et al. 2011; Scofield and Kalivas 2014; Blanco-Suarez, Caldwell et al. 2016). In the context of our data, if stress induces an increase in the volume, surface area, or synaptic contacts of hippocampal astrocytes, then more IL-1β might reach the synapse.

Current studies that have examined astrocyte morphology following stress have been limited by the reliance on GFAP or S100β immunoassays (Tynan, Beynon et al. 2013; Xia, Zhai et al. 2013; Choi, Ahn et al. 2016; Saur, Baptista et al. 2016). As mentioned in Chapter 2, GFAP constitutes only about 15% of the total volume of an astrocyte and is limited to a subset of astrocytes (Benediktsson, Schachtele et al. 2005; Rajkowska and Stockmeier 2013). Thus, while these studies do provide support to our hypotheses, they do not provide full information about how hippocampal signaling might be influenced by astrocyte changes. For example, how fine processes of glial cells that make synaptic contacts are altered following stress is unclear from immunoassays of GFAP alone (Scofield, Li et al. 2016).

Experiments described in the current Chapter will use the novel approach to examine astrocyte morphology that is described in Chapter 1. Briefly, Dr. Kathryn Reissner and colleagues have optimized a method to isolate and quantify astrocyte volume and synaptic contacts throughout a 3-dimensional reconstruction of an individual cell (Scofield, Li et al. 2016). Their method leads to both reliable and reproducible results, and provides rich detail regarding astrocyte morphology that will provide for more information than previous methods allowed. This method employs a genetically-encoded, membrane-tagged fluorescent marker to allow visualization of the fine peripheral processes of astrocytes (Scofield, Li et al. 2016). High resolution confocal microscopy and Bitplane Imaris analyses can be used to employ intensity

based thresholding to quantify astrocyte volume, surface area, and colocalization with synaptic contacts. Here, we apply this technology in the context of the severe stressor within the SEFL paradigm.

To measure synaptic colocalization, we examined expression of postsynaptic density 95 (PSD95), an integral protein of the postsynaptic density of primarily excitatory synapses which is associated with stabilization of a synaptic contact (Mir, Sen et al. 2014; Berry and Nedivi 2017). While PSD95 is strongly associated with NMDA and AMPA receptors, it is not exclusively present at excitatory synapses but rather is thought to be a marker of a mature synaptic contact (Berry and Nedivi 2017). PSD95 expression in a newly formed spine predicts its survival in cultured pyramidal neurons (Taft and Turrigiano 2014; Berry and Nedivi 2017) and a reduction in PSD95 in pyramidal neurons is strongly associated with spine retraction (Woods, Oh et al. 2011). As such, changes in PSD95 are involved in both hippocampal long term potentiation (LTP) and dendritic spine morphology, both of which can predict learning and memory performance (Ehrlich and Malinow 2004; Mir, Sen et al. 2014; Serita, Fukushima et al. 2017). Given that plasticity and learning involve a degree of spine turnover (Yang, Pan et al. 2009; Hayashi-Takagi, Yagishita et al. 2015; Berry and Nedivi 2017), an examination of PSD95 levels could provide information regarding learning mechanisms involved in both normal fear conditioning or stress-enhanced fear learning. It is also important to note that susceptibility to a depression-like phenotype following either social defeat stress or exposure to chronic unpredictable mild stress and anxiety-like behavior have been associated with a reduction in hippocampal PSD95 (Jianhua, Wei et al. 2017; Kumar and Thakur 2017; Qiao, An et al. 2017). Furthermore, Mir and colleagues recently reported one mechanism through which IL-1β, which we have shown to be upregulated by stress and causally related to SEFL,

can induce a reduction in PSD95 in cortex that is associated with poor performance in the rotarod and Morris water maze tests (Mir, Sen et al. 2014). Collectively, while a hypothesis regarding the specific memory mechanism involved in mild vs. stress-enhanced fear learning would be premature, we hypothesize that the severe stressor in the context of SEFL may be associated with a reduction in PSD95. Thus, measuring the levels of PSD95 in the acquired Z stacks used for analysis of the morphometric properties of astrocytes is both an important control for any implications in terms of astrocyte morphology as well as an interesting experimental question.

Experiments described in the current chapter tested the hypothesis that severe stress exposure in the context of the SEFL paradigm influences the morphometric properties of astrocytes and the amount of astrocyte synaptic contact in the dorsal hippocampus 48 hours later. Regarding PSD95 specifically, we tested the hypothesis that severe stress would decrease dorsal hippocampal PSD95 immunoreactivity 48 hours following severe foot shock stress. Experiment 3.1 was a brief pilot experiment to ensure that the virus we used was expressed in a membrane-dependent manner and was comparable to the viral construct used by Reissner and colleagues (Scofield, Li et al. 2016). In Experiment 3.2, an AAV was used to express a membrane-dependent fluorescent tag exclusively in hippocampal astrocytes and animals were exposed to 15 foot shocks in Context A. Forty-eight hours later, animals were sacrificed such that brain tissue could be processed for fluorescence immunohistochemistry, microscopy, and high resolution image analysis through Bitplane Imaris such that astrocyte volume, surface area, and colocalization with PSD95, as well as PSD95 immunoreactivity, were analyzed.

Methods

Animals

Male Sprague Dawley rats (225-250 g, Charles River Laboratories, Raleigh, NC) were housed individually under a reversed 12 hour light-dark cycle. They were given ad libitum access to food and water and were handled regularly throughout all experiments. All procedures were conducted in accordance with and approval by the UNC Institutional Animal Care and Use Committee.

Experiment 3.1 Verification of AAV5-GFAP-HA-hM3Dq-IRES-mCitrine as a membrane-dependent tag

Viruses

AAV5-GFAP-HA-hM3Dq(Gq)-IRES-mCitrine was obtained directly from the UNC Gene Therapy and Vector Core (Chapel Hill, NC). AAV5-GFAP-Lck-GFP was provided by Dr. Kathryn Reissner. Purified viruses were obtained pre-dialyzed (350mM NaCl, 5% D-sorbitol in phosphate buffered saline), and combined to a single stock containing both viruses prior to surgery.

Surgery and Sacrifice

Animals (N = 6) were anesthetized with a 1.0 mg/kg intraperitoneal injection of 9:1 (vol:vol) ketamine hydrochloride (100mg/ml) mixed with xylazine (100 mg/ml). All animals were infused with AAV5-GFAP-HA-hM3Dq-IRES-mCitrine *and* AAV5-GFAP-Lck-GFP. Injectors (26 Gauge, Plastics One, Roanoke, VA) were directed bilaterally at the dorsal hippocampus (AP -3.4 mm, ML ± 3.1 mm, DV -3.2 mm, 15 degrees, relative to bregma). Combined virus was injected in a total volume of 1.4 µl per hemisphere at a rate of 0.1 µl per

minute. Injectors were left in place for 15 minutes to allow for diffusion of the virus away from the injector site. Three weeks later, all animals were sacrificed via transcardial perfusion. Briefly, rats were deeply anesthetized with a 1 ml intraperitoneal injection of 9:1 (vol:vol) ketamine hydrochloride (100 mg/ml) mixed with xylazine (100 mg/ml). Animals were transcardially perfused with cold 0.1 M phosphate buffer (pH = 7.4) for three minutes at a rate of 15 mls/ minute and then with cold 4% paraformaldehyde in 0.1 M phosphate buffered saline (pH = 7.4) for seven minutes at a rate of 15 mls/ minute. Brains were extracted and post-fixed in 4% paraformaldehyde in 0.1 M phosphate buffered saline for 4–6 hours and then sliced into 100 µm sections on vibratome.

Immunohistochemistry

Immunohistochemical analysis was used to verify that GFAP-hM3Dq was expressed in the same membrane-dependent manner as GFAP-Lck-GFP and to verify that both viruses were expressed in hippocampal astrocytes and that colocalization with PSD95 could be measured. Brain sections were washed three times for 10 minutes in 0.1 M phosphate buffer (PB, pH = 7.4) and incubated in 5% Normal Goat Serum and 0.5% TritonX100 for 60 minutes. Tissue was then incubated in primary antibody overnight at 4°C in 5% Normal Goat Serum, 0.5% TritonX100, and rabbit anti-HA (Cell Signaling, Danvers, MA, Cat # mAb3724, 1:500), mouse anti-GFAP (1:1000, ThermoFisher Scientific, Waltham, MA, Cat # MS-1376P), or mouse anti-PSD95 (1:500, Thermo Fisher Scientific, Waltham, MA, Cat # MA1-045). The following day, tissue was washed three times for 10 minutes in 0.1 M PB and incubated in 5% Normal Goat Serum, 0.5% TritonX100, and secondary antibody for 120 minutes at room temperature. Secondary antibodies conjugated with Alexa-Fluor dyes (Thermo Fisher Scientific, Waltham, MA, 1:1000) were used for visualization. Tissue was then washed three

times for 10 minutes, mounted onto SuperFrost Plus slides (Fisher Scientific, Pittsburgh, PA) and cover slipped using Vectashield hard set mounting medium (Vector Labs, Burlingame, CA). For all antibodies, control experiments verified that our staining for all target antigens was visible and specific using this method.

Confocal microscopy and Bitplane Imaris analysis

A Zeiss LSM800 confocal microscope was used to acquire Z stacks of individual cells in the dorsal hippocampus that were transduced by both GFAP-hM3Dq and GFAP-Lck-GFP. Z stacks were acquired using a 63X oil immersion lens, 1024 x 1024 frame size, frame average of 4, and step size of 0.8 µm. Laser lines that excite at 405nm, 488nm, 561nm were used to visualize GFP, and the Alexa Fluor tags used to label GFAP-hM3Dq, GFAP, and PSD95. Images were deconvolved using Bitplane AutoQuant X3 (10 iterations, (Lee, Wee et al. 2014)) and exported to Bitplane Imaris software (Zurich, Switzerland).

Experiment 3.2: Effect of stress on the morphometric properties of astrocytes.

Virus

AAV5-GFAP-HA-hM3Dq(Gq)-IRES-mCitrine was obtained directly from the UNC Gene Therapy and Vector Core (Chapel Hill, NC). Purified virus was obtained pre-dialyzed (350mM NaCl, 5% D-sorbitol in phosphate buffered saline) and microinjected at 3.7 x 10^{12} particles/ml.

Surgery

Animals (N = 16) were anesthetized with a 1.0 mg/kg intraperitoneal injection of 9:1 (vol:vol) ketamine hydrochloride (100mg/ml) mixed with xylazine (100 mg/ml). All animals

were infused with AAV5-GFAP-HA-hM3Dq-IRES-mCitrine. Injectors (26 Gauge, Plastics One, Roanoke, VA) were directed bilaterally at the dorsal hippocampus (AP -3.4 mm, ML ± 3.1 mm, DV -3.2 mm, 15 degrees, relative to bregma). Virus was injected in a volume of 0.7 µl per hemisphere at a rate of 0.1 µl per minute. Injectors were left in place for 15 minutes to allow for diffusion of the virus away from the injector site. Experimental procedures began three weeks later.

Stress exposure and sacrifice

Animals (N = 16, n = 8) were randomly assigned to either a Foot Shock (in Context A) or No Foot Shock (in Context A) treatment and exposed to only the initial severe stressor of the SEFL paradigm described in Experiment 2.1. Thus, animals assigned to receive foot shocks were exposed to 15 2 mA scrambled foot shocks in Context A, an environment distinct from the home cage, while control animals were exposed to the same context without foot shocks being delivered. Forty-eight hours after removal from Context A, rats were deeply anesthetized with a 1 ml intraperitoneal injection of 9:1 (vol:vol) ketamine hydrochloride (100 mg/ml) mixed with xylazine (100 mg/ml). Animals were transcardially perfused with cold 0.1 M phosphate buffer (pH = 7.4) for three minutes at a rate of 15 mls/minute and then with cold 4% paraformaldehyde in 0.1 M phosphate buffered saline (pH = 7.4) for seven minutes at a rate of 15 mls/minute. Brains were extracted and post-fixed in 4% paraformaldehyde in 0.1 M phosphate buffered saline for 4–6 hours and then sliced into 100 µm sections on vibratome.

Immunohistochemistry

The immunohistochemistry protocol was adjusted from that described for Experiment 3.1 in order to maximize penetration of the antibodies through the 100 µm section. A no

primary control stain was used to analyze nonspecific background and ensure analyzed signal was specific to the antigens. Brain sections were washed three times for 10 minutes in 0.1 M phosphate buffer (PB, pH = 7.4) and incubated in 10% Normal Goat Serum and 2% TritonX100 for 60 minutes. Tissue was then incubated in primary antibody for three nights at 4°C in 10% Normal Goat Serum, 2% TritonX100, and rabbit anti-HA (Cell Signaling, Danvers, MA, Cat # mAb3724, 1:500) and mouse-anti-PSD95 (1:500, Thermo Fisher Scientific, Cat # MA1-045). The following day, tissue was washed three times for 10 minutes in 0.1 M PB and incubated in 10% Normal Goat Serum, 2% TritonX100, and secondary antibody for three nights at 4°C. Secondary antibodies conjugated with Alexa Fluor dyes (Thermo Fisher Scientific, Waltham, MA, 1:1000) were be used for visualization. Tissue was then washed 3 times for 10 minutes, mounted onto SuperFrost Plus slides (Fisher Scientific, Pittsburgh, PA) and cover slipped using Vectashield Hard Set mounting medium (Vector Labs, Burlingame, CA). For all antibodies, control experiments verified that our staining for all target antigens was visible and specific using this method.

Confocal microscopy and Bitplane Imaris analysis

Image Acquisition

A Zeiss LSM800 confocal microscope was used to acquire Z stacks of individual cells in the dorsal hippocampus that were transduced by AAV5-GFAP-HA-hM3Dq-IRES-mCitrine, extended fully through the x, y, and z planes, and were non-overlapping. Acquisition and analyses were completed by an experimental blind to treatment group. While the virus was expressed throughout the dorsal hippocampus, all of the isolated cells acquired were found in CA1 and CA3. Z stacks were acquired using a 63X oil immersion lens, 1024 x 1024 frame size, 12 bit image resolution, frame average of 4, and step size of 0.8 µm. Laser lines that excite

at 405nm, 488nm, 561nm were used to visualize GFP, and the Alexa Fluor tags used to label GFAP-hM3Dq, GFAP, and PSD95. Acquisition parameters including Master Gain, Digital Offset and Laser Power were kept the same throughout all acquisition. Images were deconvolved using Bitplane AutoQuant X3 (10 iterations, (Lee, Wee et al. 2014)) and exported to Bitplane Imaris software (Zurich, Switzerland).

Astrocyte volume, surface area, and colocalization with PSD95

Bitplane Imaris software was used to create a 3-D reconstruction of each isolated astrocyte (10-15 cells per rat). Alexa Fluor 488 was used to visualize GFAP-hM3Dq and Alexa Fluor 594 was used to visualize PSD95. The surfaces tool was used to generate 3-D reconstructions of the astrocyte and both the astrocyte and PSD95 channels were masked to the surface such that intensity based colocalization thresholds were used to quantify the colocalization with PSD95 in each cell in the Colocalization tab. Ten random samples of the absolute intensity of the PSD95 signal through the Z stack were recorded and the mean intensity was used to set the colocalization threshold. A two-dimensional scatter plot was used to visually inspect the accuracy of colocalization thresholds. The region of interest (ROI) was defined as the astrocyte within the Z stack by masking the colocalization data to the surface of the GFAP-hM3Dq channel. For all analyses, astrocyte surface area, astrocyte volume, and % ROI colocalized with PSD95 were recorded. Each image was also visually inspected to ensure that all cells included in the final analysis were non-overlapping, extended fully through the x, y, and z planes, and that the PSD95 signal was at least 6-fold greater than background detected in the no primary antibody control stain in all Z stacks used for colocalization analysis. Any animal from which fewer than four cells meeting these criteria were able to be acquired from

the dorsal hippocampus was dropped from the analysis, and any such decision was made blind to treatment group.

Quantification of hippocampal PSD95 immunoreactivity

PSD95 immunoreactivity in each of the acquired Z stacks was quantified. A no primary antibody control stain revealed that the secondary incubation was associated with a non-specific band of signal towards the edge of the tissue. This portion of the Z stack was cut from the analysis manually by an experimenter blind to treatment group. Ten random samples of the absolute intensity of the PSD95 signal through the Z stack were recorded and the mean intensity was used to set the absolute intensity threshold. Again, care was taken to ensure that the PSD95 signal was at least 6-fold greater than background detected in the no primary antibody control stain in all Z stacks included in the analysis. The ROI was defined as the whole Z stack and the % ROI with voxels above the absolute intensity threshold determined was recorded.

Statistical Analysis

For Experiment 3.2, two tailed unpaired student's t tests were used to test the effect of foot shock on astrocyte volume, surface area, and the %ROI colocalized with PSD95. A one tailed unpaired student's t test was used to test the effect of foot shock on the %volume of PSD95.

Results

Experiment 3.1 AAV5-GFAP-HA-hM3Dq-IRES- -mCitrine is expressed in a membrane-dependent manner

Confocal Z stacks of co-transduced cells that were deconvolved and exported to Btiplane Imaris were visually inspected for colocalization of GFAP- hM3Dq and GFAP-Lck-GFP signals and for colocalization with GFAP and PSD95. GFAP-Lck-GFP (and GFAP-hM3Dq)-positive cells colocalized with GFAP in the dorsal hippocampus, confirming that astrocytes were effectively targeted, and with PSD95, confirming that this method can be used to quantify astrocyte synaptic contacts (Figure 3.1). In hippocampal astrocytes transduced by both GFAP-hM3Dq and GFAP-Lck-GFP, there was clear colocalization such that GFAP-hM3Dq was expressed in the fine, distal processes of astrocytes in a manner identical to GFAP-Lck-GFP (Figure 3.2). Thus, for Experiment 3.2, GFAP-hM3Dq was used to quantify the morphometric properties and synaptic contacts of astrocytes following stress.

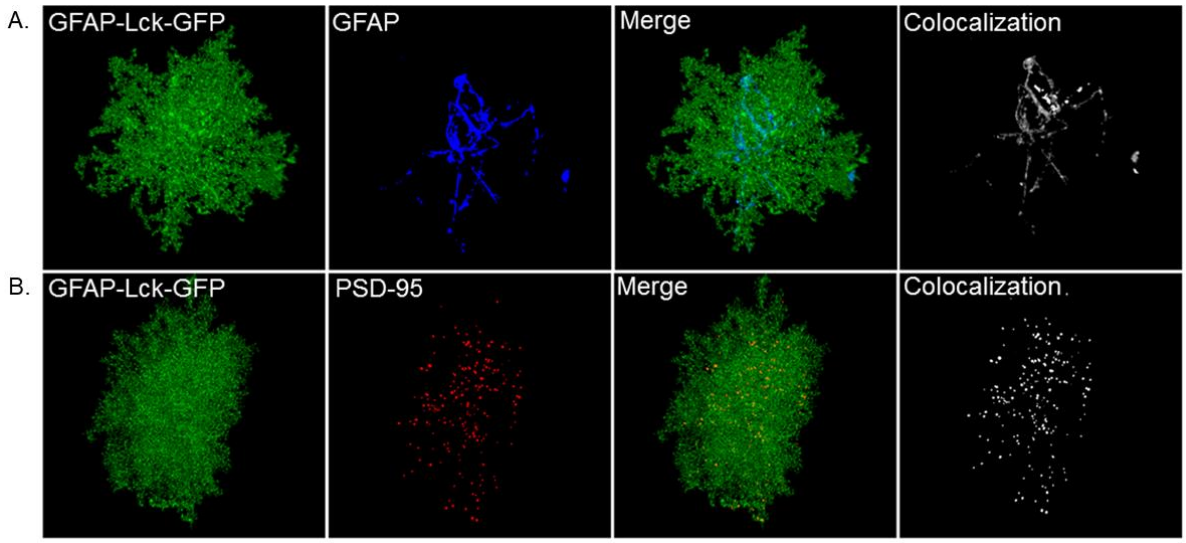

Figure 3.1 GFAP-LcK-GFP is expressed selectively in astrocytes. GFAP-Lck-GFP colocalizes with GFAP, an astrocyte-specific marker (A) and can be visualized with PSD95, a synaptic marker, (B) to quantify astrocyte synaptic contact.

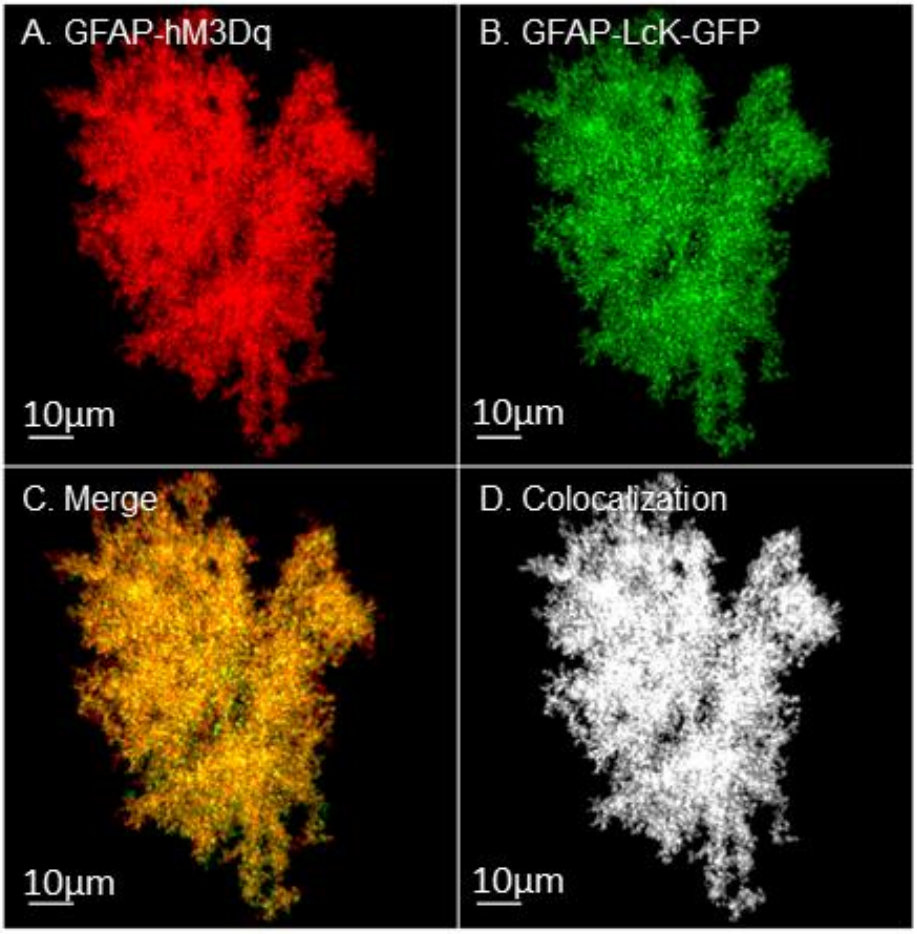

Figure 3.2 GFAP-hM3Dq can be used to examine astrocyte morphology. The glial Gq DREADD construct GFAP-hM3Dq (A) colocalized with GFAP-Lck-GFP (B), suggesting that GFAP-hM3Dq is also expressed in a membrane-dependent manner and can be used for high resolution analyses of the morphometric properties and synaptic colocalization of hippocampal astrocytes. Confocal Z stacks were acquired using a 63X oil immersion lens, deconvolved using AutoQuantX and masked to the astrocyte volume using Bitplane Imaris. The merged image of both signals (C) shows complete colocalization, which is confirmed by an image of Imaris-generated colocalized voxels within the Z stack (D).

Experiment 3.2: Effect of stress on the morphometric properties of astrocytes.

Stress exposure does not alter astrocyte volume, surface area or colocalization with PSD95

There was no effect of foot shock on astrocyte volume, t (11) = 0.8686, $p = 0.8686$, or surface area, t (11) = 0.05384, $p = 0.9580$. There was also no effect of foot shock on the %ROI colocalized with PSD95, t (8) = 1.394, $p = 0.2008$. These data as well as representative images of a 3-D reconstruction of an astrocyte co-labeled with PSD95 from each treatment group are presented in Figure 3.3.

As we have previously published data to suggest that stress-induced IL-1β is most dense in the dentate gyrus of the dorsal hippocampus (Jones, Lebonville et al. 2015), it is important to note that all of the cells that met the criteria for analysis were acquired from CA1 and CA3 (Figure 3.4). Because virus expression was very dense in this region (Figure 3.4), there were no cells that were non-overlapping and extended fully through the x, y, and z planes in this region.

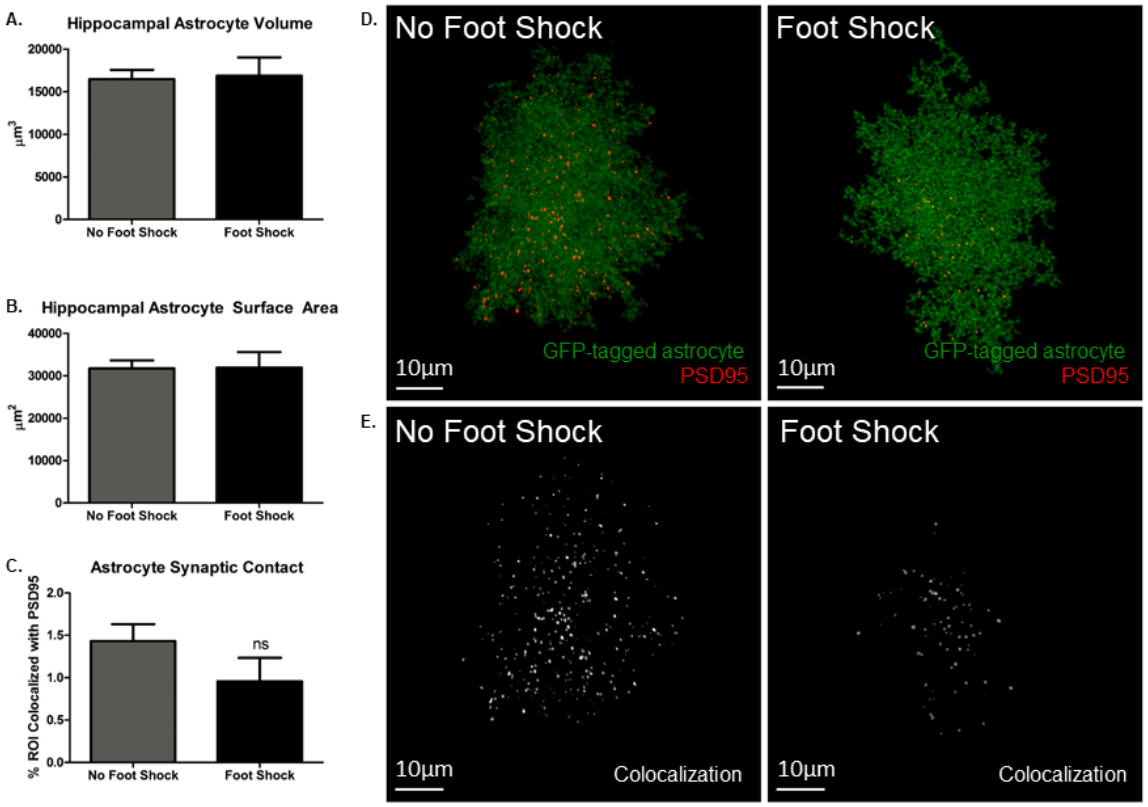

Figure 3.3 Foot shock does not alter the morphometric properties of astrocytes. Bitplane Imaris software was used to calculate the volume (A) and surface area (B) of hippocampal astrocytes 48 hours following severe stress in Context A. There was no effect of foot shock on either volume or surface area. (D) Representative cells that were colabeled with PSD95 from both the stressed (Foot Shock) and non-stressed (No Foot Shock) groups are shown. (C) In addition to volume and surface area analysis, synaptic contact was measured by calculating colocalization of each cell acquired with PSD95 and there was no effect of foot shock on the %ROI colocalized. (E) Imaris-generated images of the colocalized voxels within each Z stack from the representative images are also shown. *ns = not significant, $p > 0.05$.

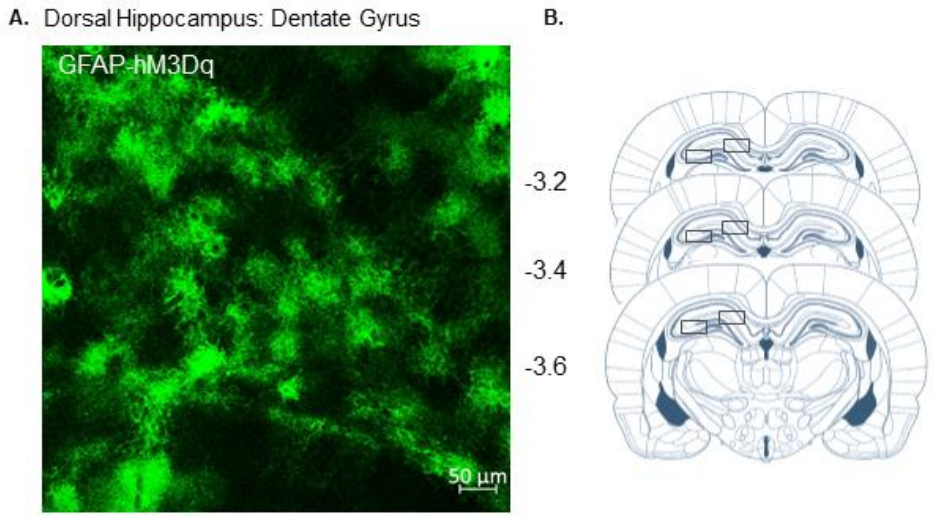

Figure 3.4 Cells included in morphology analyses were predominantly from CA1 and CA3. (A) Dense GFAP-hM3Dq expression in the dentate gyrus of the dorsal hippocampus prevented the acquisition of isolated/ non-overlapping cells. As such, all acquisition occurred in the CA1 and CA3 subregions of the dorsal hippocampus. (A) A representative image acquired at 10X is presented. (B) Outlines represent the approximate areas of CA1 and CA3 were most cells included in the analysis were acquired. Coordinates are relative to Bregma. (Paxinos and Watson, 2007)

Stress exposure attenuates PSD95 Immunoreactivity

As shown in Figure 3.5, foot shock attenuated PSD95 immunoreactivity, t (8) = 1.883, p = 0.482. Thus, the slight mean difference observed suggesting a decrease in astrocyte colocalization with PSD95 in Figure 3.3 is confounded by the fact that foot shock induced a decrease in the PSD95 signal.

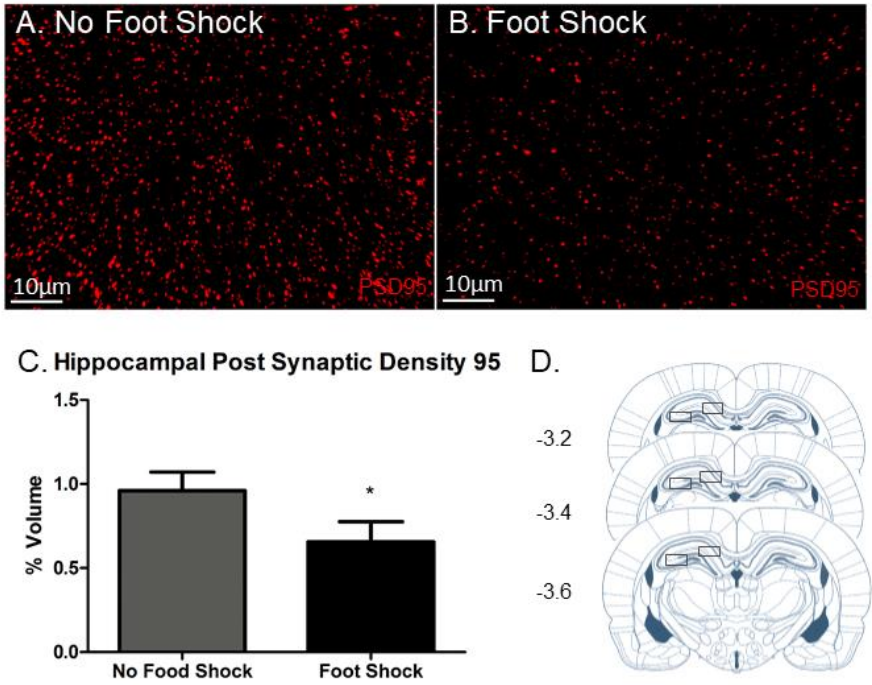

Figure 3.5 Foot shock attenuated PSD95 immunoreactivity. PSD95 was quantified in Z stacks of individual astrocytes acquired using Bitplane Imaris (C). Representative images from non-stressed (A) and stressed (B) rats acquired using a 63X oil immersion lens are shown. Bitplane Imaris was used to subtract background prior to quantification thresholding, and as such, thresholded images are shown. Again, the areas of CA1 and CA3 in the dorsal hippocampus were there images were acquired are presented (D). Coordinates are relative to Bregma. (Paxinos and Watson, 2007)

Discussion

The hypothesis that severe stress induces changes in the morphometric properties of astrocytes 48 hours later was not supported here. There was no change induced by foot shock exposure in Context A in hippocampal astrocyte volume, surface area, or colocalization with PSD95. However, we observed a significant decrease in PSD95 immunoreactivity. The interesting implications of a stress-induced decrease in hippocampal PSD95 are discussed below.

It is important to note that dynamic stress-induced changes in astrocyte morphology may make critical time points for this variable difficult to pinpoint. While important to examine, 48 hours post-stress is not the only time point at which changes in astrocyte morphology might be important to SEFL and may represent a very short time point relative to the initial manipulation. Reissner and colleagues have reported changes in nucleus accumbens astrocyte morphology that were measured following 14-16 days of extinction after self-administration of cocaine (Scofield, Li et al. 2016). A later time point in the SEFL model might allow us to detect changes in the morphometric properties of astrocytes that occur on a slower timeline. For example, examining astrocyte morphology seven days after Context A exposure would give us a measure of astrocyte morphology at the time at which conditioning in Context B would normally take place, and thus the time at which stress-induced changes in plasticity are important for processing future stressors.

The specific learning and memory mechanisms through which a previous stressor can render animals hypersensitive to future fear learning are unknown. We have shown that both IL-1RA (Chapter 2, (Jones, Lebonville et al. 2015)) and morphine (Szczytkowski-Thomson, Lebonville et al. 2013) are sufficient to influence the development of SEFL. However, given

that PSD95 is important for the stabilization of new synaptic contacts, a reduction in PSD95 could be involved in a stress-induced change in dendritic morphology or the rate of spine turnover as another mechanism that is important for this effect (Berry and Nedivi 2017). Interestingly, Qiao and colleagues recently reported that an injection of Brain Derived Neurotrophic Factor (BDNF) rescued chronic mild unpredictable stress-induced deficits in hippocampal dendritic spine density and PSD95 (Qiao, An et al. 2017). Indeed, BDNF function has been implicated in both rodent models of PTSD (Ji, Peng et al. 2017; Lee, Shim et al. 2017) and human PTSD (Rakofsky, Ressler et al. 2012; Green, Corsi-Travali et al. 2013), further supporting the hypothesis that a better understanding of synaptic remodeling in the hippocampus in this context is important. Thus, while the stress-induced reduction in PSD95 should be replicated using multiple methods of measurement and a larger region of tissue sample given that the area we measured was limited to Z stacks of 8-10 cells per rat, our data suggest that attention to synaptic remodeling and spine turnover in the context of SEFL could lead to promising discoveries.

The main advantage of our approach in the current chapter was that the membrane-dependent tag allowed us to visualize and quantify the most distal perisynaptic processes of an astrocyte that position the cell perfectly to interact with synaptic transmission (Blanco-Suarez, Caldwell et al. 2016; Scofield, Li et al. 2016). Thus, despite the fact that we did not detect differences in the morphometric properties of astrocytes 48 hours post-stress, given that a reduction in PSD95 could be associated with spine retraction or the presence of more immature spine s(Berry and Nedivi 2017), neurotrophic factors secreted by astrocytes, such as BDNF or glial cell-derived neurotrophic factor (GDNF) (Hassanpoor, Fallah et al. 2014; Hisaoka-Nakashima, Miyano et al. 2015; Hisaoka-Nakashima, Matsumoto et al. 2017) could still have

a meaningful impact on memory mechanisms in the hippocampus following stress. This hypothesis is discussed further in Chapter 5. As discussed in more detail in Chapter 4, astrocyte-specific manipulations have been shown to be involved in behavioral outcomes following a variety of different stress protocols (Ben Menachem-Zidon, Avital et al. 2011; Xia, Zhai et al. 2013; Levkovitz, Fenchel et al. 2015). Furthermore, our data presented in Chapter 2 strongly suggest that important changes do occur in astrocytes in terms of cytokine expression. The experiments described in Chapter 4 use a second novel approach to further explore hippocampal astrocyte function in the context of SEFL.

Chapter 4

EFFECT OF HIPPOCAMPAL ASTROGLIAL GI SIGNALING ON STRESS-ENHANCED FEAR LEARNING

Introduction

Astroglial signaling is an innovative field of neuroscience that is underrepresented in the current literature. Converging evidence is beginning to suggest an important role for astroglial signaling in a complex behavior (Barres 2008; Rial, Lemos et al. 2015) and several laboratories have suggested that potential treatments that improve behavioral outcomes of PTSD may have acted through glial-dependent mechanisms (Ben Menachem-Zidon, Avital et al. 2011; Xia, Zhai et al. 2013; Levkovitz, Fenchel et al. 2015). Xia and colleagues identified one compound that showed promise to alleviate PTSD-like symptoms following single prolonged stress, Fibroblast growth factor-2 (FGF2), which also prevented stress-induced changes in GFAP expression (Xia, Zhai et al. 2013). Further, Menachem-Zidon and colleagues demonstrated that astrocytes can influence fear learning through an IL-1β – dependent mechanism in that the introduction of neural precursor cells which ultimately differentiated into astrocytes rescued deficits in fear conditioning traditionally observed in an IL-1 receptor knock out line (Ben Menachem-Zidon, Avital et al. 2011). While the complete mechanisms involved in each of these effects remain unclear, they suggest that astroglial signaling is important in PTSD and merits further study. The goal of the experiments described in the current chapter was to examine the development of SEFL following direct manipulation of hippocampal astroglial GPCR signaling.

Chapter 2, as well as our previously published report (Jones, Lebonville et al. 2015), show that hippocampal IL-1β is expressed by hippocampal astrocytes and is causally related to SEFL. Given that IL-1β is both a potent stimulator of astrocytes as well as secreted by astrocytes, directly manipulating astrocytes in the context of enhanced fear learning represents an important area of research. GPCR signaling in astrocytes is a good target for such experiments in that IL-1β expression is known to be regulated by GPCR signaling in the central nervous system. Specifically, second messengers downstream of G_i activation have been linked to the regulation of IL-1β in that Jin and colleagues observed a reduction in LPS-induced IL-1β protein following the application of a PKA inhibitor (Jin, Sato et al. 2014). Furthermore, Nuclear factor kB (NFkB) is a critical component of inflammatory astroglial signaling (Ben Menachem-Zidon, Avital et al. 2011) that regulates IL-1β (Cogswell, Godlevski et al. 1994) and is known to be directly regulated by GPCR signaling (Ye 2001). Lastly, morphine, a systemic treatment known to reduce both SEFL and PTSD (Holbrook, Galarneau et al. 2010; Nixon, Nehmy et al. 2010; Szczytkowski-Thomson, Lebonville et al. 2013; Melcer, Walker et al. 2014) and to attenuate stress-induced IL-1β (Jones, Lebonville et al. 2015), activates G_i-coupled signaling via activation of the μ opioid receptor (Convertino, Samoshkin et al. 2015).

As mentioned in Chapter 1, technological limitations have previously prevented researchers from selectively isolating astrocyte signaling pathways. Recent innovations, such as designer receptors exclusively activated by designer drugs (DREADDs), have overcome this limitation. DREADDs are engineered muscarinic receptors that have no endogenous ligand but can be activated by an otherwise physiologically inert compound, clozapine-N-oxide (CNO) (Zhu and Roth 2014). Dr. Bryan Roth (UNC Chapel Hill) has designed viral constructs for G_i- coupled DREADD receptors under the astrocyte-specific promoter, GFAP.

Impressively, these advances in chemogenetics have allowed researchers to manipulate astroglial GPCR signaling in vivo, and four groups have shown that manipulating astrocytes in the CNS directly influences behavioral outcomes (Agulhon, Boyt et al. 2013; Bull, Freitas et al. 2014; Scofield, Boger et al. 2015; Yang, Qi et al. 2015). Experiments described in the current chapter took advantage of this technology to selectively activate G_i signaling specifically in astrocytes within the dorsal hippocampus in the context of SEFL.

It is important to note that glial-expressing DREADD constructs are still new and, to our knowledge, only one effect has been reported with the AAV8-GFAP-hM4Di-mCherry to date (Yang, Qi et al. 2015). Yang and colleagues reported that hypothalamic astroglial G_i activation enhanced ghrelin-evoked food intake. In the same report, they also showed that hypothalamic astroglial G_q activation attenuated ghrelin-evoked food intake. In an effort to verify both of the glial DREADD constructs the group used, they also reported that CNO administration enhanced GFAP colocalization with cFos, an immediate early gene, only in AAV-GFAP-hM3Dq-mCherry-transduced rats and not in AAV-GFAP-hM4Di-mCherry transduced- rats (Yang, Qi et al. 2015). Thus, while their virus-specific and CNO-specific enhancement of feeding and GFAP colocalization with cFos are supportive of the validity of GFAP-hM4Di, there are no published data reported to directly confirm that CNO activates G_i-coupled signaling when used with this construct.

In an effort to provide support for the validity of this important tool in neuroscience, in a subset of animals in Experiment 4.1, we also used high resolution confocal microscopy to measure the colocalization of the mCherry signal in AAV8-GFAP-hM4Di-mCherry-tranduced hippocampal astrocytes with cyclic adenosine monophosphate (cAMP), a G_i-dependent signaling marker. Of note, given that G_i-coupled signaling is typically inhibitory in nature, it

is possible that a floor effect may confound attempts to verify the hM4Di construct in naïve animals. To account for this, animals selected for this assay were also injected with lipopolysaccharide (LPS, derived from E. coli) to induce a state of central neuroinflammation in which we might be better able to detect CNO-induced changes in G_i-dependent messengers, such as cAMP, in astrocytes (Tarassishin, Suh et al. 2014).

Collectively, the goal of experiments described in the current chapter was to test the hypothesis that hippocampal astroglial G_i signaling is sufficient to attenuate SEFL. Experiment 4.1 used AAV8-GFAP-hM4Di-mCherry to selectively activate astroglial G_i signaling in the hippocampus at 1 mg/kg or 3 mg/kg CNO in SEFL. Experiment 4.2 used fluorescence immunohistochemistry, confocal microscopy, and Bitplane Imaris colocalization analysis to examine cAMP expression in GFAP-hM4Di-mCherry-positive astrocytes following LPS and CNO or Vehicle injection.

Methods

Animals

Male Sprague Dawley rats (225-250 g, Charles River Laboratories, Raleigh, NC) were housed individually under a reversed 12 hour light-dark cycle. They were given ad libitum access to food and water and were handled regularly throughout all experiments. All procedures were conducted in accordance with and approval by the UNC Institutional Animal Care and Use Committee.

Virus

AAV8-GFAP-hM4Di(Gi)-mCherry was obtained directly from the UNC Gene Therapy and Vector Core (Chapel Hill, NC). Purified virus was obtained pre-dialyzed (350mM NaCl, 5% D-sorbitol in phosphate buffered saline) and microinjected at 2.0 x 10^{12} particles/ml.

Surgery

Animals (N = 64, n = 8) were anesthetized with a 1.0 mg/kg intraperitoneal injection of 9:1 (vol:vol) ketamine hydrochloride (100mg/ml) mixed with xylazine (100 mg/ml). All animals were infused with AAV8-GFAP-hM4Di-mCherry. Injectors (26 Gauge, Plastics One, Roanoke, VA) were directed bilaterally at the dorsal hippocampus (AP -3.4 mm, ML ± 3.1 mm, DV -3.2 mm, 15 degrees, relative to bregma). Virus was injected in a volume of 0.7 µl per hemisphere at a rate of 0.1 µl per minute. Injectors were left in place for 15 minutes to allow for diffusion of the virus away from the injector site. Experimental procedures started three weeks later.

Experiment 4.1: Effect of hippocampal astroglial G_i activation on SEFL

Stress-enhanced fear learning

The SEFL procedure used for Experiment 4.1 is identical to that described in Chapter 2. Two cohorts of animals were run, the first tested the effect of 1 mg/kg CNO (N = 32, n = 8) and then second tested the effect of 3 mg/kg CNO (N = 32, n = 8). Briefly, all animals were randomly assigned to a Context A treatment (Foot Shock in Context A or No Foot Shock in Context A) and a drug treatment (CNO or vehicle) and exposed to the SEFL paradigm (Figure 4.1), as has been previously published (Szczytkowski-Thomson, Lebonville et al. 2013; Jones, Lebonville et al. 2015). Rats were injected with CNO (1 mg/kg or 3 mg/kg subcutaneously) or

vehicle immediately, 24, and 48 hours after removal from Context A. Contextual fear to Context B was measured by analyzing freezing behavior at baseline and on test days 1, 2, 7, and 14. Behavior was recorded as described in Chapter 2 and analyzed manually by a rater blind to the treatment group. Similar to Experiment 2.1, there was no significant generalization of fear between contexts in any treatment group (Results of Experiment 4.1), thus any differences observed reflect altered learning to the single shock in Context B.

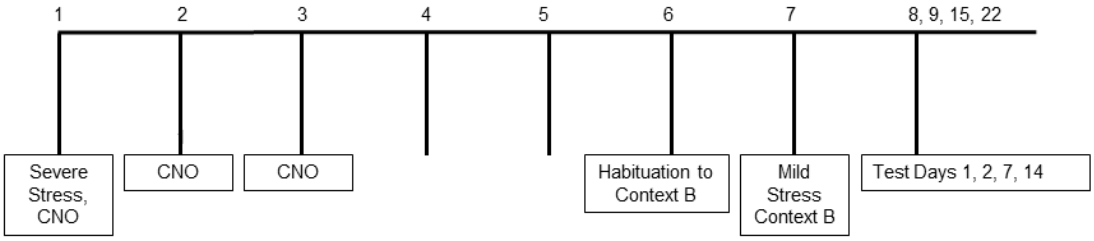

Figure 4.1 Experimental timeline for Experiment 4.1. Rats were infused with AAV8-GFAP-hM4Di-mCherry bilaterally into the dorsal hippocampus, given three weeks to recover, and exposed to the SEFL paradigm. Rats were injected with CNO or vehicle (1 or 3mg/kg) immediately, 24, and 48 hours after Context A exposure.

Drug Administration

CNO was obtained from Sigma (St. Louis, MO) and was reconstituted at 3 mg/ml or 1 mg/ml in sterile saline with 0.5% dimethyl sulfoxide (DMSO). Animals were injected subcutaneously (s.c.) with 1 mg/kg or 3 mg/kg CNO or vehicle (sterile saline with 0.5% DMSO) at the times indicated above.

Sacrifice

All animals were sacrificed via transcardial perfusion. Briefly, rats were deeply anesthetized with a 1 ml intraperitoneal injection of 9:1 (vol:vol) ketamine hydrochloride (100 mg/ml) mixed with xylazine (100 mg/ml). Animals were transcardially perfused with cold 0.1 M phosphate buffer (pH = 7.4) for three minutes at a rate of 15 mls/minute and then with cold 4% paraformaldehyde in 0.1 M phosphate buffered saline (pH = 7.4) for seven minutes at a rate of 15 mls/minute. Brains were extracted and post-fixed in 4% paraformaldehyde in 0.1 M phosphate buffered saline for 4–6 hours, cryoprotected in 30% sucrose in 0.1 M phosphate buffer (pH = 7.4) for at least 48 hours, and sliced into 40 µm sections on freezing microtome. Brains were stored in 0.1 M phosphate buffer with 0.1% sodium azide (pH = 7.4) at 4°C until the time of assay.

Immunohistochemistry

Fluorescence immunohistochemistry was used to ensure that all virus expression was astrocyte- and hippocampus-specific. Brain sections were washed three times for 10 minutes in 0.1 M phosphate buffer (PB, pH = 7.4) and incubated in 5% Normal Goat Serum and 0.5% TritonX100 for 60 minutes. Tissue was then incubated in primary antibody overnight at 4°C in 5% Normal Goat Serum, 0.5% TritonX100, and mouse anti-GFAP (1:1000, ThermoFisher Scientific, Waltham, MA, Cat #MS-1376P), or mouse anti-NeuN (1:1000, Abcam, Cambridge, MA, Cat# Ab207282). The following day, tissue was washed three times for 10 minutes in 0.1 M PB and incubated in 5% Normal Goat Serum, 0.5% TritonX100, and secondary antibody for 120 minutes at room temperature. Secondary antibodies conjugated with Alexa-Fluor dyes (1:1000, Thermo Fisher Scientific, Waltham, MA) were used for visualization. Tissue was then washed three times for 10 minutes, mounted onto SuperFrost Plus slides (Thermo Fisher

Scientific, Waltham, MA) and cover slipped using Vectashield hard set mounting medium (Vector Labs, Burlingame, CA). For all antibodies, control experiments verified that our staining for all target antigens was visible and specific using this method. Slides were stored at 4°C until the time of microscopy. A Zeiss LSM800 confocal microscope was used to ensure that mCherry colocalized with GFAP, and not with NeuN, and thus was specific to astrocytes. Only data from animals with virus expression that was both hippocampus- and astrocyte-specific were included in the final analyses.

Experiment 4.2: Effect of CNO on colocalization of mCherry-positive cells with cAMP

Sacrifice

After the completion of behavioral testing for Experiment 4.1, two rats from the No Foot Shock in Context A/ Vehicle group were randomly selected for a pilot experiment which aimed to verify that CNO activated G_i—coupled signaling in mCherry-positive cells. Both rats selected were injected with Lipopolysaccharide (LPS; derived from E. coli, serotype 055:B5) in order to induce central neuroinflammation and CNO to activate GFAP-hM4Di prior to sacrifice by transcardial perfusion described above. LPS was dissolved in sterile 0.9% saline at 1.0 mg/ml and CNO was dissolved as described above. Three hours and thirty minutes prior to sacrifice, one rat was injected with CNO (3 mg/kg, s.c.) and the other was injected with vehicle. Thirty minutes after CNO or vehicle injection, both rats were injected with 1 mg/kg LPS. Rats were sacrificed via transcardial perfusion three hours after the LPS injection. Experimental timeline is shown in Figure 4.2.

Figure 4.2 Experimental timeline for Experiment 4.2. A subset of animals from Experiment 4.1, that had been bilaterally infused with AAV8-GFAP-hM4Di-mCherry into the dorsal hippocampus, were injected with CNO or vehicle (3 mg/kg, s.c.) and 30 minutes later were injected with LPS (1mg/kg, s.c.). Three hours later, animals were sacrificed by transcardial perfusion and brains were extracted and processed for immunohistochemistry.

Immunohistochemistry

In addition to the immunohistochemistry for virus verification describe above, additional tissue from the animals in Experiment 4.2 was stained for colocalization analysis of mCherry and cAMP. Briefly, sections were washed three times for 10 minutes in 0.1 M phosphate buffer (PB, pH = 7.4) and incubated in 5% Normal Goat Serum and 0.5% TritonX100 for 60 minutes. Tissue was then incubated in primary antibody overnight at 4°C in 5% Normal Goat Serum, 0.5% TritonX100, and mouse anti-cAMP (1:1000, Abcam, Cambridge, MA, Cat # ab24851). The following day, tissue was washed three times for 10 minutes in 0.1 M PB and incubated in 5% Normal Goat Serum, 0.5% TritonX100, and goat anti-mouse Alexa Fluor 488 (1:1000, Thermo Fisher Scientific, Waltham, MA, Cat # A11001) for 60 minutes at room temperature. Tissue was then washed 3 times for 10 minutes, mounted onto SuperFrost Plus slides (Thermo Fisher Scientific, Waltham, MA) and cover slipped using Vectashield hard set mounting medium (Vector Labs, Burlingame, CA). Slides were stored at

-20°C until the time of assay. In addition, as for all other antibodies used, no primary control experiments verified the specificity of the anti-cAMP signal.

Confocal microscopy and Bitplane Imaris colocalization analysis

Image Acquisition

A Zeiss LSM800 confocal microscope was used to acquire Z stacks of individual cells in the dorsal hippocampus that were transduced by AAV8-GFAP-hM4Di-mCherry. Acquisition and analyses were completed by an experimenter blind to treatment group. Z stacks were acquired using a 63X oil immersion lens, 1024 x 1024 frame size, 12 bit image resolution, frame average of 4, and step size of 0.8 µm. Laser lines that excite at 488nm, 561nm were used to visualize Alexa Fluor 488 and the mCherry signal. Acquisition parameters including Master Gain, Digital Offset and Laser Power were kept the same throughout all acquisition. Images were deconvolved using Bitplane AutoQuant X3 (10 iterations, (Lee, Wee et al. 2014)) and exported to Bitplane Imaris software (Zurich, Switzerland).

Colocalization of mCherry and cAMP

Bitplane Imaris software was used to create a 3-D reconstruction of each mCherry-positive astrocyte (20 cells per rat). The surfaces tool was used to set absolute intensity thresholds for both the mCherry and cAMP signals that were used for colocalization analyses in the colocalization tab. A two-dimensional scatter plot was used to visually inspect the accuracy of colocalization thresholds. The region of interest (ROI) was defined as the mCherry reconstruction within the Z stack by masking the colocalization data to the surface of the mCherry channel. As such, the %ROI colocalized represents the percent of voxels within the mCherry reconstruction that were also above the threshold for the cAMP signal. The %ROI

colocalized was recorded. In addition, to avoid a potential confounding floor effect given that we expected CNO to reduce cAMP in mCherry-positive cells, cells from both treatment groups that exhibited less than 10% colocalization were dropped from the analysis. Seven cells from the CNO-treated group and eight cells from the vehicle-treated group were dropped for this reason.

Statistical Analysis

For Experiment 4.1, data from the two experiments (1 mg/kg vs. 3mg/kg CNO) were analyzed independently. For each experiment, a one way ANOVA with treatment group as the between subjects factor was used to analyze baseline freezing data during the three minutes prior to the foot shock during Context B conditioning in order to ensure there were no group differences in freezing to Context B prior to the single shock. A 2 x 2 x 4 repeated measures ANOVA with Context A treatment and drug treatment as between subject factors and test day as a within subjects factor was used to analyze freezing behavior across test days 1, 2, 7 and 14. Significant interactions were examined using Tukey's post-hoc comparisons. Specifically, planned comparisons included: Foot shock in Context A/ Vehicle vs. Foot shock in Context A/ CNO and No Foot shock in Context A/ Vehicle vs. Foot shock in Context A/ Vehicle. For Experiment 4.2, a one tailed student's t test was used to test the effect of drug treatment on the %ROI colocalized.

Results

Experiment 4.1: Hippocampal astroglial G_i activation attenuates SEFL

GFAP-hM4Di was selectively expressed in hippocampal astrocytes and we observed a dose-dependent and CNO-specific effect of CNO on the development of SEFL (Figure 4.3). There was no effect of Context A treatment on baseline freezing in Context B prior to the single shock ineither the cohort that tested the effect of 1 mg/kg CNO, $F(3, 14) = 1.028$, $p = 0.410$, or the cohort that tested the effect of 3 mg/kg $F(3, 16) = 2.034$, $p = 0.150$. Thus, there was no generalization of fear between the two contexts in either experiment. A 2 x 2 x 4 ANOVA revealed a significant main effect of Context A treatment, $F(1, 14) = 7.092$, $p = 0.019$, and significant main effect of test day, $F(3, 14) = 36.221$, $p < 0.001$, for the cohort that tested the effect of 1 mg/kg CNO. However, there was no effect of 1 mg/kg CNO on SEFL in that there was no main effect of drug treatment, $F(1,14) = 0.476$, $p = 0.501$, and no Context A treatment by drug treatment interaction $F(1,14) = 0.613$, $p = 0.447$. Tukey's post hoc tests confirmed that there was significant SEFL in that rats that received Foot Shock in Context A followed by vehicle exhibited enhanced fear to Context B compared to rats that received No Foot Shock in Context A followed by vehicle, $p = 0.011$.

For the cohort that tested the effect of 3 mg/kg CNO, again there was a significant main effect of Context A treatment, $F(1,16) = 16.228$, $p = 0.001$, and a significant main effect of test day, $F(3,16) = 39.277$, $p < 0.001$. Tukey's post hoc comparisons confirmed a significant SEFL effect in that, again, rats that received Foot Shock in Context A followed by vehicle exhibited enhanced fear to Context B compared to rats that received No Foot Shock in Context A followed by vehicle, $p < 0.001$. In addition, there was a significant effect of 3 mg/kg CNO on SEFL in that there was a significant main effect of drug treatment $F(1,16) = 5.213$, p =

0.036. Tukey's post hoc comparisons confirmed that 3 mg/kg CNO significantly attenuated SEFL in that rats that received Foot Shock in Context A followed by CNO exhibited attenuated freezing to Context B compared to rats that received Foot Shock in Context A followed by vehicle, $p = 0.015$.

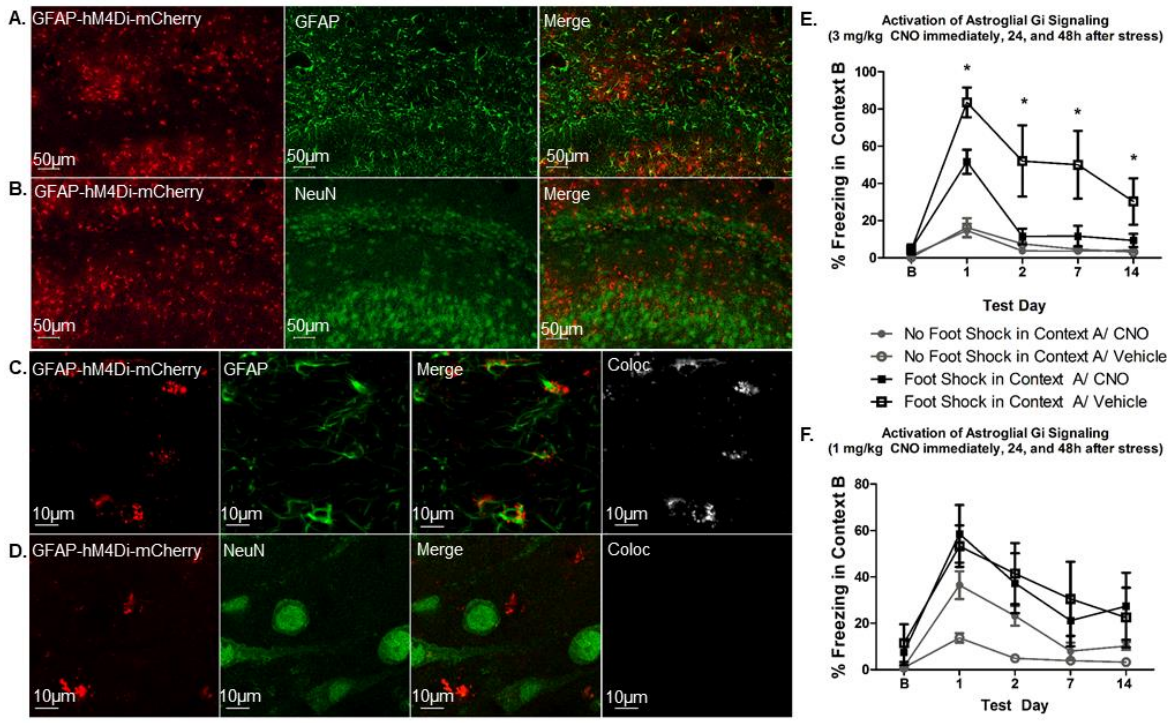

Figure 4.3 Astoglial G_i activation attenuates stress-enhanced fear learning. GFAP-hM4Di-mCherry was expressed selectively in hippocampal astrocytes. Representative images acquired using a 10X and 63X oil immersion lens are shown. GFAP-hM4Di-mCherry colocalized exclusively with hippocampal GFAP/astrocytes (A,C) and did not colocalize with NeuN (B,D). Activation of hippocampal astroglial G_i signaling attenuated stress-enhanced fear learning at 3 mg/kg (E) but not 1 mg/kg (F) CNO. Specifically, enhanced fear learning was observed in that stressed animals who received vehicle exhibited significantly more freezing to Context B than non-stressed animals that received vehicle, $p < 0.01$, for both 1 and 3 mg/kg CNO. Furthermore, CNO attenuated SEFL in that stressed animals that received 3 mg/kg CNO exhibited attenuated freezing to Context B compared to stressed animal that received vehicle, $p < 0.05$. * Foot Shock in Context A/Vehicle vs. Foot Shock in Context A/ CNO, $p < 0.05$.

Experiment 4.2: CNO attenuated colocalization of mCherry-positive cells with cAMP

CNO treatment significantly attenuated cAMP in mCherry-positive hippocampal astrocytes (Figure 4.4). There was a significant effect of CNO on the %ROI colocalized, t (22) = 2.495, p = 0.0103.

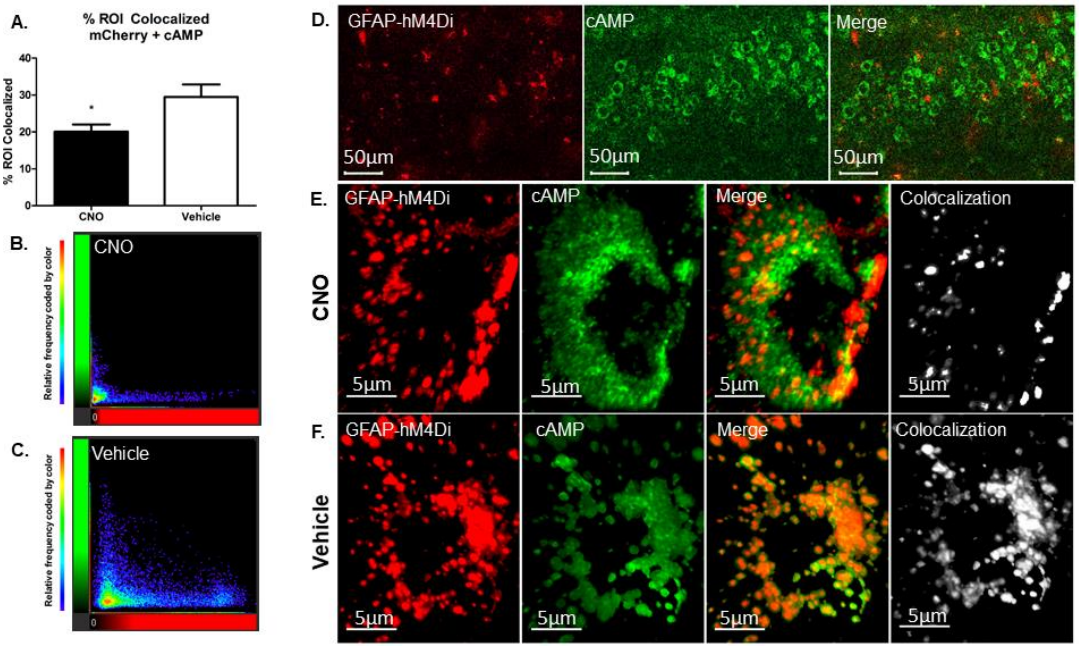

Figure 4.4 CNO attenuates cAMP in GFAP-hM4Di-mCherry -transduced cells. LPS was used as an inflammatory stimulator and hippocampal mCherry positive cells were analyzed for colocalization with cAMP immunoreactivity. Z stacks using a 63x oil immersion lens of 20 cells per group were acquired and analyzed using Bitplane Imaris. The ROI was defined as all voxels within the Z stack that expressed mCherry and the %ROI colocalized for each virus-transduced cell was generated. Three mg/kg CNO significantly attenuated the %ROI colocalized with cAMP (the % of mCherry-positive voxels that were also positive for cAMP) (A). Representative scatter plots show the distribution of voxels in a representative Z stack from each group (B,C). Each point on the scatter plot represents one voxel in the Z stack, the X axis represents the mCherry intensity and the Y axis represents the cAMP (Alexa Fluor 488) intensity. A low magnification example image (acquired at 10X) shows the cAMP and mCherry signals in the dorsal hippocampus. A representative cell from the CNO (E) and Vehicle (F) groups are presented along with the masked cAMP signal (signal above the absolute intensity threshold and within the defined ROI/ mCherry-positive voxels). Bitplane Imaris-generated colocalization panels show the %ROI Colocalized within each Z stack.

Discussion

Here, we found that 3 mg/kg, but not 1 mg/kg, CNO attenuated the development of SEFL in GFAP-hM4Di infused animals. This dose-dependent and CNO-specific effect provides strong evidence that hippocampal astroglial G_i signaling is sufficient to attenuate SEFL. Furthermore, we are the first to show that CNO significantly attenuated cAMP in GFAP-hM4Di-mCherry-positive cells.

The verification of new technologies is critically important to the field of neuroscience. Our data show that CNO influences a G_i-dependent signaling pathway as expected in AAV8-GFAP-hM4Di-mCherry-transduced hippocampal astrocytes. However, these data are limited both by the fact that only two animals were used and the mCherry signal is not expressed throughout the whole astrocyte, making colocalization less precise in that we were limited to only mCherry-positive voxels in any given z stack. Future studies should examine cAMP post-CNO in a larger sample of animals, and should examine other G_i-dependent second messengers, such as Protein Kinase A (PKA), as well.

It is also important to note that these data would be greatly strengthened by an experiment using a control virus for the construct used (AAV8-GFAP-EGFP), as a recent report suggests that CNO may be associated with previously unexpected physiological effects (Roth 2016; Gomez, Bonaventura et al. 2017). However, the 2 x 2 design employed provides control for the expression of virus alone influencing fear learning in that all animals were infused with AAV8-GFAP-hM4Di-mCherry and the lack of effect of CNO on the control freezing behavior (animals that did not receive foot shock in Context A) does provide some support for the specificity of CNO in this model. While we look forward to new data to strengthen the effect either from a control virus experiment or an experiment to test the effect

of hippocampal astroglial G_q signaling (for example, using AAV5-GFAP-HA-hM3Dq-IRES-mCitrine), we are excited about our current findings which provide strong evidence for the involvement of hippocampal astroglial G_i signaling in SEFL.

The current data suggest that astroglial signaling is important in the context of behavioral outcomes following severe stress, but the mechanism through which astroglial G_i signaling influences enhanced fear learning may provide greater insight into potential treatment targets. As has been discussed throughout the current dissertation, one potential mechanism through which hippocampal astroglial G_i activation might act to prevent SEFL is IL-1 signaling. Indeed, as mentioned previously, this hypothesis is supported by several lines of evidence. To directly test whether hippocampal astroglial G_i activation attenuates IL-1β protein and mRNA, both in stressed and naïve animals, and whether coadministration of recombinant IL-1β with CNO rescues the SEFL effect are important follow up experiments to these findings.

Interestingly, another mechanism through which astroglial G_i activation might act in this context can be hypothesized from a recent report which demonstrated that G_i signaling in cultured primary astrocytes was associated with an increase in glial-derived neurotrophic factor (GDNF) and brain-derived neurotrophic factor (BDNF) (Hisaoka-Nakashima, Matsumoto et al. 2017). Their data also suggest that this effect is mediated by the Fibroblast Growth Factor Receptor family (FGFR) as an inhibitor of FGFRs abolished the effect. Further, these data are consistent with an earlier report from the same laboratory which showed that amitriptyline, a tricyclic antidepressant, also increases GDNF through a G_i signaling pathway in astrocytes (Hisaoka-Nakashima, Miyano et al. 2015). It is possible that G_i- driven astroglial release of

GDNF and BDNF are involved in the development of SEFL. This hypothesis is further supported by two lines of evidence.

The first line of evidence to support this hypothesis is that increased BDNF has been shown to be protective both in terms of depressive and anxiety-like phenotypes in rodent models of stress and to be associated with an increase in dendritic spine density in the hippocampus (Lee, Shim et al. 2017; Qiao, An et al. 2017). Given that our data presented in Chapter 3 suggest that the severe stressor in SEFL induces a decrease in hippocampal PSD95 immunoreactivity, an increase in BDNF and GDNF may protect against any stress-induced spine retraction or synaptic remodeling, that a change in PSD95 may be indicative of and, subsequently, protect against any stress-induced changes in memory processing that render animals hypersensitive to future fear learning (Berry and Nedivi 2017). The second line of evidence is that, as mentioned above, Xia and colleagues have shown that Fibroblast growth factor-2, which acts through FGFRs prevented stress-induced changes in GFAP in a model of single prolonged stress, another rodent model of PTSD (Xia, Zhai et al. 2013). Furthermore, amitriptyline, mentioned above, has been considered for and prescribed as a treatment for PTSD with some success (Cavaljuga, Licanin et al. 2003; Hoskins, Pearce et al. 2015) and attenuated a traumatic predator scent stress memory when administered 24 hours after the stressor (Zoladz, Fleshner et al. 2013). Collectively, these findings suggest the hypothesis that astroglial G_i signaling may protect against the development of PTSD-like phenotypes following stress, including the development of SEFL, through a GDNF and/or BDNF increase in the hippocampus. Future experiments should directly test these hypotheses.

In summary, data presented in the current chapter provide strong evidence that astroglial G_i activation is sufficient to attenuate SEFL. The mCherry and cAMP colocalization

data provide strong support for the validity of GFAP-hM4Di, and we expect subsequent studies, including both control virus experiments to verify the specificity of CNO in this model and further experiments to test G_i-dependent second messengers with a larger sample size, to strengthen these data in the future. Nonetheless, the data presented herein suggest that, in addition to IL-1 signaling, astroglial GPCR signaling might represent another potential target for the development of novel therapeutics to treat PTSD.

Chapter 5

GENERAL DISCUSSION

Summary of findings

The experiments presented herein provide important insights into the role of neural immune signaling in the development of a PTSD-like phenotype in stress-enhanced fear learning. Our results suggest that treatments that target neural immune signaling, including two specific signaling pathways, show promise to prevent the development of PTSD following a traumatic experience.

Data presented in Chapter 2 confirm that dorsal hippocampal IL-1 signaling is critical to the development of SEFL in that dorsal hippocampal IL-1RA completely prevented enhanced fear learning following foot shock stress. Further analyses in Chapter 2 uncovered a unique effect on Iba-1 immunoreactivity, and pinpointed astrocytes as the clear predominant source of hippocampal IL-1β in both naïve and stressed rats. Subsequently, Chapter 3 provided a thorough analysis of the morphometric properties of hippocampal astrocytes 48 hours after exposure to the severe stressor in SEFL known to be capable of inducing a PTSD-like phenotype. Interestingly, while we did not detect an effect of stress on astrocyte volume, surface area, or colocalization with PSD95, we did detect a stress-induced reduction in hippocampal PSD95 immunoreactivity. The implications of this finding are discussed in further detail below as they related to potential insights into memory acquisition of traumatic vs. normal memories/experiences. Lastly, data presented in Chapter 4 suggest that

hippocampal astroglial G_i activation alone is sufficient to attenuate enhanced fear learning following foot shock in that CNO dose-dependently attenuated SEFL in AAV8-GFAP-hM4Di-mCherry-infused rats. Importantly, we also quantified colocalization of a G_i-dependent second messenger, cAMP, with virus-transduced cells and our data are the first to validate that CNO attenuates cAMP in AAV8-GFAP-hM4Di-mCherry-transduced cells. The implications of the key findings in Chapters 2 through 4 are integrated and discussed further below.

Implications of the role of IL-1 signaling in SEFL

The first important finding presented in Chapter 2 is that our data confirmed the critical role of hippocampal IL-1 signaling in SEFL (Figure 2.1). Similar to the effect of intracerebroventricular IL-1RA, intra-dorsal hippocampal IL-1RA completely abolished the PTSD-like phenotype. IL-1RA is already approved by the US Food and Drug Association and is marketed for the treatment of rheumatoid arthritis as Anakinra (Tarp, Furst et al. 2017). We argue that our data strongly suggest this drug should be explored as a potential therapeutic to treat human PTSD. An important follow up line of work that will be relevant to the ultimate application of an IL-1-specific treatment for human PTSD is to measure for how long hippocampal IL-1β is elevated following stress. Our early data provide evidence that the stress-induced increase in IL-1β persists for at least 72 hours post stress (Jones, Lebonville et al. 2015), but whether IL-1 is still elevated at the time of Context B conditioning or at later time points throughout testing for contextual fear to Context B and the expression of enhanced fear learning is unknown. Experiments to determine how long central alterations in IL-1 signaling persist are important given that any potential treatment to mitigate or protect against PTSD would be most applicable if it can be administered regardless of the time that has passed since the initial trauma. Of note, as mentioned above, while elevations in peripheral IL-1 do not

necessarily induce and/or reflect central IL-1 levels (Quan and Banks 2007), peripheral IL-1 appears to be chronically upregulated in individuals diagnosed with PTSD (Gill, Saligan et al. 2009; Guo, Liu et al. 2012; Gola, Engler et al. 2013; Lindqvist, Wolkowitz et al. 2014; Passos, Vasconcelos-Moreno et al. 2015; Wang and Young 2016). Thus, the potential use of IL-1RA or Anakinra in this context is well-justified by the data reported in both humans and animals to date.

The mechanism through which IL-1 alters SEFL is another interesting follow up avenue of research. As mentioned above, research to elucidate mechanisms through which memories are acquired and stored is an important line of work. Long term potentiation (LTP) is one phenomenon that has been widely implicated in memory acquisition and learning in this effort (Bliss and Collingridge 1993). While it is not known how hippocampal LTP might directly relate to normal vs. enhanced fear learning, several groups have reported that hippocampal LTP is sensitive to IL-1β signaling. In an initial report, Schneider and colleagues showed that IL-1 signaling was critical to the maintenance, but not the induction of hippocampal LTP (Schneider, Pitossi et al. 1998). However, more recently, converging evidence suggests that there is an inhibitory effect of IL-1β application on hippocampal LTP (Ross, Allan et al. 2003; Prieto and Cotman 2017), with Hoshino and colleagues demonstrating the IL-1β-induced impairment in LTP may be synapse-specific in that IL-1β administration impaired the induction of LTP at some hippocampal synapses but not others (Hoshino, Hasegawa et al. 2017). Consistent with this, BDNF, discussed below and in Chapter 4 as a potential protective mechanism through which astroglial G_i might protect against SEFL, has been shown to facilitate LTP (Pang and Lu 2004; Bekinschtein, Cammarota et al. 2014). Future

studies should examine both how hippocampal LTP relates to normal vs. enhanced fear learning and how the involvement of IL-1 might be involved in the difference between the two.

Implications of the role of astrocytes, and in particular astroglial G_i signaling, in SEFL

The second important implication from the data presented in Chapter 2 is that hippocampal astrocytes have a critical function in SEFL. Colocalization data confirmed that the predominant source of hippocampal IL-1β following the severe stressor is astrocytes. Chapter 4 provided further evidence to support this conclusion in that hippocampal astroglial G_i activation alone was sufficient to attenuate SEFL. It is important to note that while intra-dorsal hippocampal IL-1RA completely abolished SEFL such that Foot Shock in Context A/IL-1RA animals were not different from the No Foot Shock in Context A control animals (Figure 2.1), hippocampal astroglial G_i activation only partially prevented SEFL (Figure 4.3). Thus, follow up studies to determine how hippocampal astroglial G_i activation influences fear learning will provide more information regarding potential treatment targets for the development of novel therapeutics to treat PTSD.

As mentioned above, an important follow up experiment is to test whether the effect of astroglial G_i on SEFL occurs through an IL-1-dependent mechanism. This can easily be achieved by co-administering recombinant IL-1β and CNO following the severe stressor in Context A in SEFL to determine whether supplementing hippocampal IL-1 signaling in combination with CNO activation of astroglial G_i signaling rescues the SEFL effect. Indeed, previous reports do support this hypothesis (Jin, Sato et al. 2014) (Ben Menachem-Zidon, Avital et al. 2011) (Cogswell, Godlevski et al. 1994) (Ye 2001). However, regardless of whether this hypothesis is supported, glial-derived neurotrophic factors represent another

potential mechanism that could be downstream of astroglial GPCR activity in the context of behavioral outcomes following severe stress.

As described above, one astroglial G_i-driven effect is an enhancement in GDNF and BDNF, and this is thought to occur through the activation of FGFRs (Hisaoka-Nakashima, Matsumoto et al. 2017). Consistent with this, both BDNF administration and FGF2 activation directly into the dorsal hippocampus have been shown to be protective against a PTSD-like phenotype (Xia, Zhai et al. 2013; Lee, Shim et al. 2017; Qiao, An et al. 2017). Strikingly, Qiao and colleagues showed that chronic unpredictable mild stress induced a reduction in BDNF, dendritic spine density, and PSD95 levels in the hippocampus and that an exogenous administration of BDNF rescued the stress-induced reduction in spine density and PSD95 and protected against the PTSD-like phenotype (Qiao, An et al. 2017). From these data, we hypothesize that astroglial G_i activation in the hippocampus might attenuate SEFL by enhanced secretion of astroglial-derived neurotrophic factors. Further support for this hypothesis is described in the following section of the current chapter in that, in addition to the evidence reported by Qiao and colleagues, converging evidence suggests that neurotrophic factor secretion can influence dendrite morphology in the hippocampus (McAllister, Katz et al. 1999; Horch and Katz 2002; Chakravarthy, Saiepour et al. 2006; Maynard, Hobbs et al. 2017). Because a stress-induced reduction in PSD95 immunoreactivity, which we presented in Chapter 3 and discuss below, could be a reflection of stress-induced changes dendritic spine dynamics, a potential astroglial G_i-driven secretion of BDNF (or GDNF) that protects against the development of SEFL is consistent with the hypothesis discussed. The implications for interpreting alterations in hippocampal spine dynamics are discussed below.

Lastly, we argue that, given the importance of astrocyte function in this context, although astrocyte morphology and synaptic contacts were not altered 48 hours post-stress, future studies should examine hippocampal astrocyte volume, surface area, and synaptic colocalization at other timepoints within SEFL. Given that most published studies examine astrocyte reactivity on very quick timelines following stress protocols, within 48 hours, this represents a significant gap in the current literature. Arguably the most interesting time point to examine would be the point at which animals are exposed to the subsequent fear challenge in Context B, the time at which hypersensitivity to future fear learning occurs.

Implications of the effect of severe stress on PSD95

While our primary hypothesis tested in Chapter 3 was not supported, we observed a stress-induced reduction in PSD95 immunoreactivity which may have implications related to learning and memory mechanisms in regards to dendritic spine dynamics. As discussed previously, PSD95 is strongly linked with stability or maturation of a given synaptic contact and has been linked to dendritic spine morphology and the survival of a newly formed spine (Ehrlich and Malinow 2004; Ehrlich, Klein et al. 2007; Taft and Turrigiano 2014) (De Roo, Klauser et al. 2008; Berry and Nedivi 2017). Stability of dendritic spines has been observed throughout adulthood in many reports and has even been hypothesized to be a potential location of memory storage, however, recent reports confirm that even into adulthood a degree of plasticity persists and can play a role in learning (Yang, Pan et al. 2009; Lai, Franke et al. 2012; Young, Briggs et al. 2015). Yang and colleagues used in vivo two photon imaging of dendritic spines in the mouse motor and sensory cortices to demonstrate that, regardless of age, motor learning and exposure to novel sensory experiences produce rapid dendritic spine formation and a portion of these persist for at least five months (Yang, Pan et al. 2009).

Interestingly, Lai and colleagues also reported that spine dynamics were altered by fear conditioning (Lai, Franke et al. 2012). Specifically, the group showed that tone-shock pairings were associated with dendritic spine elimination in specific areas of cortex and that the rate of elimination was proportional to the degree of freezing behavior. Furthermore, they showed that extinction training following cued fear conditioning was associated with spine formation, which again correlated with the decrease in the freezing behavior response. Remarkably, they showed that these experience-dependent changes are likely to occur on the same spines (within 2 μm). In summary, the literature suggests that dendritic spines can be rapidly altered throughout learning or the encoding of an experience, and that alterations in PSD95 predict the stability of a given spine and could reflect such learning-dependent changes.

The data presented herein add to the current literature to suggest that stressors capable of inducing PTSD-like phenotypes are associated with region-specific reductions in PSD95 in the hippocampus (Jianhua, Wei et al. 2017; Kumar and Thakur 2017; Qiao, An et al. 2017). As mentioned above, Qiao and colleagues reported a severe stress induced reduction in both PSD95 and dendritic spine density in the hippocampus. Similarly, Hoffman and colleagues observed a reduction in dendritic spine density in the dentate gyrus of the dorsal hippocampus following predator scent stress (Hoffman, Cohen et al. 2016). And Serrano colleagues reported that social defeat stress induces changes in dendritic morphology in the hippocampus, including a reduction in the presence of stubby spines, which were associated with a reduction in the colocalization of PSD95 with the GluA2 subunit of the AMPA receptor (Iniguez, Aubry et al. 2016). These findings converge to suggest that dendritic spine morphology may be altered by severe stressors. However, whether PSD95 tracks dendritic spine dynamics consistently in the context of the hippocampus and severe stress and exactly how such findings relate to

memory acquisition and storage and/or the intensity of the fear memory remains unknown. Future studies should examine whether the severe stressor in SEFL influences hippocampal spine density and spine morphology and, subsequently, whether such changes are related to and/or a component of the neuroplastic change that renders animals hypersensitive to future fear learning.

Of note, while extinction learning has been thought to reflect new learning, as described above, there is evidence to support some degree of erasure of fear memories (Yang, Pan et al. 2009; Lai, Franke et al. 2012). A mechanism that would allow selective erasure of fear memories would be an extremely valuable clinical tool to contribute to efforts to treat PTSD. And in this effort, experiments to better understand spine dynamics in the hippocampus following severe stress may be crucial. Dendritic spine plasticity is regulated by actin polymerization (Young, Briggs et al. 2015) and impressively, selective erasure of methamphetamine-associated memories has been achieved by Miller and colleagues by targeting the actin cytoskeleton (Young, Aceti et al. 2014; Young, Briggs et al. 2015). While our understanding of hippocampal spine dynamics following stress is far from such an endpoint, Miller and colleague's approach may be extremely relevant if a similar mechanism could be identified for selective erasure of severely stressful fear memories.

Role of additional neural immune signaling pathways in behavioral outcomes of severe stress

The last section of future directions related to the experiments reported herein involve distinct brain regions and inflammatory signaling pathways. It is important to note that the hippocampus is just one brain region that is important in the prognosis of PTSD. Several reports have implicated other regions in PTSD development including the prefrontal cortex,

perirhinal cortex, and basolateral amygdala (Lopes da Silva, Witter et al. 1990; Yehuda and LeDoux 2007; Kealy and Commins 2011; Kent and Brown 2012; Perugini, Laing et al. 2012). Examining the morphology of astrocytes and/or inflammation in these areas may provide more information regarding mechanisms that drive the hypersensitivity to fear that is seen in SEFL. Indeed, there are two reports that implicate gliotransmission in the amygdala in fear learning (Ponomarev, Rau et al. 2010; Stehberg, Moraga-Amaro et al. 2012).

In addition, IL-1 does not act in isolation. Several other cytokines, including IL-6, and TNF-α, have been shown to be dysregulated in PTSD (Gill, Saligan et al. 2009; Guo, Liu et al. 2012; Gola, Engler et al. 2013; Lindqvist, Wolkowitz et al. 2014; Passos, Vasconcelos-Moreno et al. 2015; Wang and Young 2016). Further, Levkovitz and colleagues showed that minocycline, a general anti-inflammatory treatment prevented the development of a PTSD-like phenotype following predator scent stress (Levkovitz, Fenchel et al. 2015). Further studies to examine whether the anti-inflammatory protective effect in SEFL is be specific to the IL-1 signaling pathway or whether there are indeed other potential targets would make a significant contribution to this line of work.

Summary of unanswered questions and future directions

The current dissertation confirmed several of our hypotheses regarding the importance of neural immune signaling in SEFL, specifically, hippocampal IL-1 signaling and astroglial signaling. However, many there are many future directions to be pursued to gain a more thorough understanding of this phenomenon. As mentioned previously, both how long stress-induced enhancements in hippocampal IL-1 persist, as well as whether IL-1RA would be effective in attenuating SEFL if administered at later time points relative to the severe stressor in Context A remain unknown. Similarly, the same question is important for whether severe

stress alters astrocyte morphology and whether hippocampal astroglial G_i activation would also be effective at attenuating SEFL at the same later time points relative to Context A. In addition, as mentioned above, experiments to test whether the effect of astroglial G_i activation acts through either an IL-1-dependent or a BDNF- and/or PSD95-related mechanism are important in understanding the mechanism downstream of astroglial G_i activation. Co-administration of CNO and recombinant IL-1β following Context A exposure in GFAP-hM4Di-mCherry-infused rats will provide information as to whether a reduction in IL-1 signaling is required for the effect of hippocampal astroglial G_i activation on SEFL. And experiments to examine whether CNO administration in GFAP-hM4Di-mCherry-infused rats rescues any stress-induced deficits in BNDF or PSD95 in the dorsal hippocampus will provide information regarding this second hypothesized mechanism. If reductions in PSD95 and BDNF or GFDNF are induced by the severe stressor and are rescued by hippocampal astroglial G_i activation, subsequent experiments should test the causal relationship in the context of behavioral consequences of stress.

The current literature on fear memory and anxiety/depressive-like phenotypes and our data presented in the current dissertation converge to support the hypotheses described above regarding potential stress-induced changes in dendritic spine morphology in the hippocampus. We argue that another important future direction will be to, independently of astroglial G_i activity, further describe stress-induced changes in PSD95 or dendrite morphology and test how these are related to either normal or enhanced fear learning following severe stress exposure. Experiments should test how severe stress alters dendrite morphology throughout SEFL, including both the 48 hours post-stress time point as well as later time points throughout the development and expression of SEFL. Subsequently, experiments could test whether

application of BDNF or GDNF rescues these deficits. Further experiments to test how these changes relate to freezing behavior will provide information about the causal relationship between hippocampal dendrite morphology and behavioral consequences of stress.

Lastly, we also reported a stress-induced reduction in hippocampal Iba-1 immunoreactivity in Chapter 2. While microglial are not the focus of the current dissertation, and a reduction of Iba-1 in the hippocampus only strengthens our argument that astrocytes are indeed the key immune/support cell in this region in the context of severe stress, the reduction in microglia should be further explored. We are not the first for report a stress-induced reduction in microglia (Brzozowska, Smith et al. 2017). Furthermore, some evidence suggests that stress-induced changes in microglia are particularly sensitive to severity or duration of the stressor (Kreisel, Frank et al. 2014). Thus, while astrocyte signaling may be more important in the development of SEFL, a through characterization of how stress-induced changes in microglia are related to severity or duration of a stressor may provide insight into the behavioral outcomes following severe vs. more mild stress. It may be that, although reduced by the severe stressor at the critical time point for our effective manipulations to reduce SEFL, microglia are more important in more mild/ adaptive fear learning processes after a less severe fear or stress challenge. Indeed, the differences between memory acquisition of and behavioral consequences of normal vs. enhanced fear learning represent an important question, which will have implications that will contribute to our understanding of PTSD. New technologies to study the role of microglia, including microglia-expressing DREADDs, will be able to contribute to this endeavor (Grace, Strand et al. 2016).

Concluding Remarks

The data presented in the current dissertation demonstrate that hippocampal astrocytes are critically involved in SEFL and identify two signaling pathways that can be targeted to attenuate the development of a PTSD-like phenotype. In addition, we show that the severe stressor in SEFL attenuates hippocampal PSD95, which may reflect important changes in dendritic spine dynamics induced by severe stress that merit further study. Lastly, we show a CNO-specific and dose-specific effect of astroglial G_i activation on the development of SEFL using a glial-expressing DREADD and we are the first to confirm that, in a subset of animals, CNO administration attenuates the colocalization of mCherry with cAMP in AAV8-GFAP-hM4Di-mCherry-transduced cells. Collectively, these data suggest that neural immune signaling is a promising target for the development of novel therapeutics to treat PTSD and provide insight to inform future endeavors to better understand the neurobiological mechanisms driving the acquisition and encoding of fear memories.

REFERENCES

Agulhon, C., K. M. Boyt, et al. (2013). "Modulation of the autonomic nervous system and behaviour by acute glial cell Gq protein-coupled receptor activation in vivo." J Physiol **591**(Pt 22): 5599-5609.

Anagnostaras, S. G., G. D. Gale, et al. (2001). "Hippocampus and contextual fear conditioning: recent controversies and advances." Hippocampus **11**(1): 8-17.

Arakawa, H., P. Blandino, Jr., et al. (2009). "Central infusion of interleukin-1 receptor antagonist blocks the reduction in social behavior produced by prior stressor exposure." Physiol Behav **98**(1-2): 139-146.

Audet, M. C., E. N. Mangano, et al. (2010). "Behavior and pro-inflammatory cytokine variations among submissive and dominant mice engaged in aggressive encounters: moderation by corticosterone reactivity." Front Behav Neurosci **4**.

Avital, A., I. Goshen, et al. (2003). "Impaired interleukin-1 signaling is associated with deficits in hippocampal memory processes and neural plasticity." Hippocampus **13**(7): 826-834.

Banasr, M., G. M. Chowdhury, et al. (2010). "Glial pathology in an animal model of depression: reversal of stress-induced cellular, metabolic and behavioral deficits by the glutamate-modulating drug riluzole." Mol Psychiatry **15**(5): 501-511.

Barnum, C. J., T. W. Pace, et al. (2012). "Psychological stress in adolescent and adult mice increases neuroinflammation and attenuates the response to LPS challenge." J Neuroinflammation **9**: 9.

Barres, B. A. (2008). "The mystery and magic of glia: a perspective on their roles in health and disease." Neuron **60**(3): 430-440.

Bekinschtein, P., M. Cammarota, et al. (2014). "BDNF and memory processing." Neuropharmacology **76 Pt C**: 677-683.

Ben Menachem-Zidon, O., A. Avital, et al. (2011). "Astrocytes support hippocampal-dependent memory and long-term potentiation via interleukin-1 signaling." Brain Behav Immun **25**(5): 1008-1016.

Benediktsson, A. M., S. J. Schachtele, et al. (2005). "Ballistic labeling and dynamic imaging of astrocytes in organotypic hippocampal slice cultures." J Neurosci Methods **141**(1): 41-53.

Bernardinelli, Y., J. Randall, et al. (2014). "Activity-dependent structural plasticity of perisynaptic astrocytic domains promotes excitatory synapse stability." Curr Biol **24**(15): 1679-1688.

Berry, K. P. and E. Nedivi (2017). "Spine Dynamics: Are They All the Same?" Neuron **96**(1): 43-55.

Blanco-Suarez, E., A. L. Caldwell, et al. (2016). "Role of astrocyte-synapse interactions in CNS disorders." J Physiol.

Blandino, P., Jr., C. J. Barnum, et al. (2009). "Gene expression changes in the hypothalamus provide evidence for regionally-selective changes in IL-1 and microglial markers after acute stress." Brain Behav Immun **23**(7): 958-968.

Bliss, T. V. and G. L. Collingridge (1993). "A synaptic model of memory: long-term potentiation in the hippocampus." Nature **361**(6407): 31-39.

Block, M. L., L. Zecca, et al. (2007). "Microglia-mediated neurotoxicity: uncovering the molecular mechanisms." Nat Rev Neurosci **8**(1): 57-69.

Blouin, A. M., S. E. Sillivan, et al. (2016). "The potential of epigenetics in stress-enhanced fear learning models of PTSD." Learn Mem **23**(10): 576-586.

Bowler, R. M., H. Han, et al. (2010). "Gender differences in probable posttraumatic stress disorder among police responders to the 2001 World Trade Center terrorist attack." Am J Ind Med **53**(12): 1186-1196.

Brevet, M., H. Kojima, et al. (2010). "Chronic foot-shock stress potentiates the influx of bone marrow-derived microglia into hippocampus." J Neurosci Res **88**(9): 1890-1897.

Brzozowska, N. I., K. L. Smith, et al. (2017). "Genetic deletion of P-glycoprotein alters stress responsivity and increases depression-like behavior, social withdrawal and microglial activation in the hippocampus of female mice." Brain Behav Immun.

Bubb, E. J., L. Kinnavane, et al. (2017). "Hippocampal - diencephalic - cingulate networks for memory and emotion: An anatomical guide." Brain Neurosci Adv **1**(1).

Bull, C., K. C. Freitas, et al. (2014). "Rat Nucleus Accumbens Core Astrocytes Modulate Reward and the Motivation to Self-Administer Ethanol after Abstinence." Neuropsychopharmacology.

Byrne, S. P., J. H. Krystal, et al. (2017). "Correlates of Nonimprovement to Pharmacotherapy for Chronic, Antidepressant-Resistant, Military Service-Related Posttraumatic Stress Disorder: Insights From the Veterans Affairs Cooperative Study No. 504." J Clin Psychopharmacol.

Calcia, M. A., D. R. Bonsall, et al. (2016). "Stress and neuroinflammation: a systematic review of the effects of stress on microglia and the implications for mental illness." Psychopharmacology (Berl) **233**(9): 1637-1650.

Cao, X., L. P. Li, et al. (2013). "Astrocyte-derived ATP modulates depressive-like behaviors." Nat Med **19**(6): 773-777.

Cavaljuga, S., I. Licanin, et al. (2003). "Therapeutic effects of two antidepressant agents in the treatment of posttraumatic stress disorder (PTSD)." Bosn J Basic Med Sci **3**(2): 12-16.

Chakravarthy, S., M. H. Saiepour, et al. (2006). "Postsynaptic TrkB signaling has distinct roles in spine maintenance in adult visual cortex and hippocampus." Proc Natl Acad Sci U S A **103**(4): 1071-1076.

Chao, L. L., K. Yaffe, et al. (2014). "Hippocampal volume is inversely related to PTSD duration." Psychiatry Res **222**(3): 119-123.

Choi, M., S. Ahn, et al. (2016). "Hippocampus-based contextual memory alters the morphological characteristics of astrocytes in the dentate gyrus." Mol Brain **9**(1): 72.

Cogswell, J. P., M. M. Godlevski, et al. (1994). "NF-kappa B regulates IL-1 beta transcription through a consensus NF-kappa B binding site and a nonconsensus CRE-like site." J Immunol **153**(2): 712-723.

Cohen, H., N. Kozlovsky, et al. (2012). "Animal model for PTSD: from clinical concept to translational research." Neuropharmacology **62**(2): 715-724.

Cohen, M., T. Meir, et al. (2011). "Cytokine levels as potential biomarkers for predicting the development of posttraumatic stress symptoms in casualties of accidents." Int J Psychiatry Med **42**(2): 117-131.

Colombo, E. and C. Farina (2016). "Astrocytes: Key Regulators of Neuroinflammation." Trends Immunol.

Convertino, M., A. Samoshkin, et al. (2015). "mu-Opioid receptor 6-transmembrane isoform: A potential therapeutic target for new effective opioids." Prog Neuropsychopharmacol Biol Psychiatry **62**: 61-67.

Czeh, B., J. I. Muller-Keuker, et al. (2007). "Chronic social stress inhibits cell proliferation in the adult medial prefrontal cortex: hemispheric asymmetry and reversal by fluoxetine treatment." Neuropsychopharmacology **32**(7): 1490-1503.

Dabbs, C., E. Y. Watkins, et al. (2014). "Opiate-related dependence/abuse and PTSD exposure among the active-component U.S. military, 2001 to 2008." Mil Med **179**(8): 885-890.

Dantzer, R. (2009). "Cytokine, sickness behavior, and depression." Immunol Allergy Clin North Am **29**(2): 247-264.

De Jongh, A., P. A. Resick, et al. (2016). "Critical Analysis of the Current Treatment Guidelines for Complex Ptsd in Adults." Depress Anxiety **33**(5): 359-369.

De Roo, M., P. Klauser, et al. (2008). "Activity-dependent PSD formation and stabilization of newly formed spines in hippocampal slice cultures." Cereb Cortex **18**(1): 151-161.

Ehrlich, I., M. Klein, et al. (2007). "PSD-95 is required for activity-driven synapse stabilization." Proc Natl Acad Sci U S A **104**(10): 4176-4181.

Ehrlich, I. and R. Malinow (2004). "Postsynaptic density 95 controls AMPA receptor incorporation during long-term potentiation and experience-driven synaptic plasticity." J Neurosci **24**(4): 916-927.

Fareed, A., P. Eilender, et al. (2013). "Comorbid posttraumatic stress disorder and opiate addiction: a literature review." J Addict Dis **32**(2): 168-179.

Flannery, S. and A. G. Bowie (2010). "The interleukin-1 receptor-associated kinases: Critical regulators of innate immune signalling." Biochemical Pharmacology **80**(12): 1981-1991.

Frank, M. G., M. V. Baratta, et al. (2007). "Microglia serve as a neuroimmune substrate for stress-induced potentiation of CNS pro-inflammatory cytokine responses." Brain Behav Immun **21**(1): 47-59.

Giachero, M., G. D. Calfa, et al. (2015). "Hippocampal dendritic spines remodeling and fear memory are modulated by GABAergic signaling within the basolateral amygdala complex." Hippocampus **25**(5): 545-555.

Gill, J. M., L. Saligan, et al. (2009). "PTSD is associated with an excess of inflammatory immune activities." Perspect Psychiatr Care **45**(4): 262-277.

Giulian, D., J. Woodward, et al. (1988). "Interleukin-1 injected into mammalian brain stimulates astrogliosis and neovascularization." J Neurosci **8**(7): 2485-2490.

Gola, H., H. Engler, et al. (2013). "Posttraumatic stress disorder is associated with an enhanced spontaneous production of pro-inflammatory cytokines by peripheral blood mononuclear cells." BMC Psychiatry **13**: 40.

Gomez, J. L., J. Bonaventura, et al. (2017). "Chemogenetics revealed: DREADD occupancy and activation via converted clozapine." Science **357**(6350): 503-507.

Goshen, I., T. Kreisel, et al. (2007). "A dual role for interleukin-1 in hippocampal-dependent memory processes." Psychoneuroendocrinology **32**(8-10): 1106-1115.

Goshen, I. and R. Yirmiya (2009). "Interleukin-1 (IL-1): a central regulator of stress responses." Front Neuroendocrinol **30**(1): 30-45.

Grace, P. M., K. A. Strand, et al. (2016). "Morphine paradoxically prolongs neuropathic pain in rats by amplifying spinal NLRP3 inflammasome activation." Proc Natl Acad Sci U S A **113**(24): E3441-3450.

Green, C. R., S. Corsi-Travali, et al. (2013). "The Role of BDNF-TrkB Signaling in the Pathogenesis of PTSD." J Depress Anxiety **2013**(S4).

Guasch, R. M., A. M. Blanco, et al. (2007). "RhoE participates in the stimulation of the inflammatory response induced by ethanol in astrocytes." Exp Cell Res **313**(17): 3779-3788.

Guo, M., T. Liu, et al. (2012). "Study on serum cytokine levels in posttraumatic stress disorder patients." Asian Pac J Trop Med **5**(4): 323-325.

Hassanpoor, H., A. Fallah, et al. (2014). "Mechanisms of hippocampal astrocytes mediation of spatial memory and theta rhythm by gliotransmitters and growth factors." Cell Biol Int **38**(12): 1355-1366.

Hayashi-Takagi, A., S. Yagishita, et al. (2015). "Labelling and optical erasure of synaptic memory traces in the motor cortex." Nature **525**(7569): 333-338.

Hayes, J. P., S. Hayes, et al. (2017). "Automated measurement of hippocampal subfields in PTSD: Evidence for smaller dentate gyrus volume." J Psychiatr Res **95**: 247-252.

Herx, L. M. and V. W. Yong (2001). "Interleukin-1 beta is required for the early evolution of reactive astrogliosis following CNS lesion." J Neuropathol Exp Neurol **60**(10): 961-971.

Hisaoka-Nakashima, K., C. Matsumoto, et al. (2017). "Pharmacological Activation Gi/o Protein Increases Glial Cell Line-Derived Neurotrophic Factor Production through Fibroblast Growth Factor Receptor and Extracellular Signal-Regulated Kinase Pathway in Primary Cultured Rat Cortical Astrocytes." Biol Pharm Bull **40**(10): 1759-1766.

Hisaoka-Nakashima, K., K. Miyano, et al. (2015). "Tricyclic Antidepressant Amitriptyline-induced Glial Cell Line-derived Neurotrophic Factor Production Involves Pertussis Toxin-sensitive Galphai/o Activation in Astroglial Cells." J Biol Chem **290**(22): 13678-13691.

Hoffman, J. R., H. Cohen, et al. (2016). "Exercise Maintains Dendritic Complexity in an Animal Model of Posttraumatic Stress Disorder." Med Sci Sports Exerc **48**(12): 2487-2494.

Hoge, C. W., C. A. Castro, et al. (2004). "Combat duty in Iraq and Afghanistan, mental health problems, and barriers to care." N Engl J Med **351**(1): 13-22.

Holbrook, T. L., M. R. Galarneau, et al. (2010). "Morphine use after combat injury in Iraq and post-traumatic stress disorder." N Engl J Med **362**(2): 110-117.

Horch, H. W. and L. C. Katz (2002). "BDNF release from single cells elicits local dendritic growth in nearby neurons." Nat Neurosci **5**(11): 1177-1184.

Hoshino, K., K. Hasegawa, et al. (2017). "Synapse-specific effects of IL-1beta on long-term potentiation in the mouse hippocampus." Biomed Res **38**(3): 183-188.

Hoskins, M., J. Pearce, et al. (2015). "Pharmacotherapy for post-traumatic stress disorder: systematic review and meta-analysis." Br J Psychiatry **206**(2): 93-100.

Huang, Y., D. E. Smith, et al. (2011). "Neuron-specific effects of interleukin-1beta are mediated by a novel isoform of the IL-1 receptor accessory protein." J Neurosci **31**(49): 18048-18059.

Hutchinson, M. R. and L. R. Watkins (2014). "Why is neuroimmunopharmacology crucial for the future of addiction research?" Neuropharmacology **76 Pt B**: 218-227.

Iniguez, S. D., A. Aubry, et al. (2016). "Social defeat stress induces depression-like behavior and alters spine morphology in the hippocampus of adolescent male C57BL/6 mice." Neurobiol Stress **5**: 54-64.

Iwata, M., Y. Shirayama, et al. (2011). "Hippocampal astrocytes are necessary for antidepressant treatment of learned helplessness rats." Hippocampus **21**(8): 877-884.

Izquierdo, I., C. R. Furini, et al. (2016). "Fear Memory." Physiol Rev **96**(2): 695-750.

Ji, L. L., J. B. Peng, et al. (2017). "Sigma-1 receptor activation ameliorates anxiety-like behavior through NR2A-CREB-BDNF signaling pathway in a rat model submitted to single-prolonged stress." Mol Med Rep **16**(4): 4987-4993.

Jianhua, F., W. Wei, et al. (2017). "Chronic social defeat stress leads to changes of behaviour and memory-associated proteins of young mice." Behav Brain Res **316**: 136-144.

Jin, Y., K. Sato, et al. (2014). "Inhibition of interleukin-1beta production by extracellular acidification through the TDAG8/cAMP pathway in mouse microglia." J Neurochem **129**(4): 683-695.

John, G. R., S. C. Lee, et al. (2003). "Cytokines: powerful regulators of glial cell activation." Neuroscientist **9**(1): 10-22.

Jones, M. E., C. L. Lebonville, et al. (2015). "The role of brain interleukin-1 in stress-enhanced fear learning." Neuropsychopharmacology **40**(5): 1289-1296.

Jones, M. E., C. L. Lebonville, et al. (2017). "Hippocampal interleukin-1 mediates stress-enhanced fear learning: A potential role for astrocyte-derived interleukin-1beta." Brain Behav Immun.

Kealy, J. and S. Commins (2011). "The rat perirhinal cortex: A review of anatomy, physiology, plasticity, and function." Prog Neurobiol **93**(4): 522-548.

Kent, B. A. and T. H. Brown (2012). "Dual functions of perirhinal cortex in fear conditioning." Hippocampus **22**(10): 2068-2079.

Koo, J. W. and R. S. Duman (2009). "Interleukin-1 receptor null mutant mice show decreased anxiety-like behavior and enhanced fear memory." Neurosci Lett **456**(1): 39-43.

Kozlovsky, N., M. A. Matar, et al. (2009). "The role of the galaninergic system in modulating stress-related responses in an animal model of posttraumatic stress disorder." Biol Psychiatry **65**(5): 383-391.

Kozlovsky, N., J. Zohar, et al. (2012). "Microinfusion of a corticotrophin-releasing hormone receptor 1 antisense oligodeoxynucleotide into the dorsal hippocampus attenuates stress responses at specific times after stress exposure." J Neuroendocrinol **24**(3): 489-503.

Kreisel, T., M. G. Frank, et al. (2014). "Dynamic microglial alterations underlie stress-induced depressive-like behavior and suppressed neurogenesis." Mol Psychiatry **19**(6): 699-709.

Kumar, D. and M. K. Thakur (2017). "Anxiety like behavior due to perinatal exposure to Bisphenol-A is associated with decrease in excitatory to inhibitory synaptic density of male mouse brain." Toxicology **378**: 107-113.

Kwon, M. S., Y. J. Seo, et al. (2008). "The repeated immobilization stress increases IL-1beta immunoreactivities in only neuron, but not astrocyte or microglia in hippocampal CA1 region, striatum and paraventricular nucleus." Neurosci Lett **430**(3): 258-263.

Lai, C. S., T. F. Franke, et al. (2012). "Opposite effects of fear conditioning and extinction on dendritic spine remodelling." Nature **483**(7387): 87-91.

Lawson, L. J., V. H. Perry, et al. (1990). "Heterogeneity in the distribution and morphology of microglia in the normal adult mouse brain." Neuroscience **39**(1): 151-170.

Lee, B., I. Shim, et al. (2017). "Effect of oleuropein on cognitive deficits and changes in hippocampal brain-derived neurotrophic factor and cytokine expression in a rat model of post-traumatic stress disorder." J Nat Med.

Lee, J. S., T. L. Wee, et al. (2014). "Calibration of wide-field deconvolution microscopy for quantitative fluorescence imaging." J Biomol Tech **25**(1): 31-40.

Levkovitz, Y., D. Fenchel, et al. (2015). "Early post-stressor intervention with minocycline, a second-generation tetracycline, attenuates post-traumatic stress response in an animal model of PTSD." Eur Neuropsychopharmacol **25**(1): 124-132.

Lindqvist, D., O. M. Wolkowitz, et al. (2014). "Proinflammatory milieu in combat-related PTSD is independent of depression and early life stress." Brain Behav Immun **42**: 81-88.

Lopes da Silva, F. H., M. P. Witter, et al. (1990). "Anatomic organization and physiology of the limbic cortex." Physiol Rev **70**(2): 453-511.

Maren, S., S. G. Anagnostaras, et al. (1998). "The startled seahorse: is the hippocampus necessary for contextual fear conditioning?" Trends Cogn Sci **2**(2): 39-42.

Maynard, K. R., J. W. Hobbs, et al. (2017). "Bdnf mRNA splice variants differentially impact CA1 and CA3 dendrite complexity and spine morphology in the hippocampus." Brain Struct Funct.

McAllister, A. K., L. C. Katz, et al. (1999). "Neurotrophins and synaptic plasticity." Annu Rev Neurosci **22**: 295-318.

Melcer, T., J. Walker, et al. (2014). "Glasgow Coma Scores, early opioids, and posttraumatic stress disorder among combat amputees." J Trauma Stress **27**(2): 152-159.

Mendiola, A. S. and A. E. Cardona (2017). "The IL-1beta phenomena in neuroinflammatory diseases." J Neural Transm (Vienna).

Minghetti, L., M. A. Ajmone-Cat, et al. (2005). "Microglial activation in chronic neurodegenerative diseases: roles of apoptotic neurons and chronic stimulation." Brain Res Brain Res Rev **48**(2): 251-256.

Mir, S., T. Sen, et al. (2014). "Cytokine-induced GAPDH sulfhydration affects PSD95 degradation and memory." Mol Cell **56**(6): 786-795.

Montgomery, D. L. (1994). "Astrocytes: form, functions, and roles in disease." Vet Pathol **31**(2): 145-167.

Nelson, M. D. and A. M. Tumpap (2017). "Posttraumatic stress disorder symptom severity is associated with left hippocampal volume reduction: a meta-analytic study." CNS Spectr **22**(4): 363-372.

Niciu, M. J., I. D. Henter, et al. (2014). "Glial abnormalities in substance use disorders and depression: does shared glutamatergic dysfunction contribute to comorbidity?" World J Biol Psychiatry **15**(1): 2-16.

Nixon, R. D., T. J. Nehmy, et al. (2010). "Predictors of posttraumatic stress in children following injury: The influence of appraisals, heart rate, and morphine use." Behav Res Ther **48**(8): 810-815.

O'Doherty, D. C., K. M. Chitty, et al. (2015). "A systematic review and meta-analysis of magnetic resonance imaging measurement of structural volumes in posttraumatic stress disorder." Psychiatry Res **232**(1): 1-33.

O'Neill, L. A. (2006). "Targeting signal transduction as a strategy to treat inflammatory diseases." Nat Rev Drug Discov **5**(7): 549-563.

Pang, P. T. and B. Lu (2004). "Regulation of late-phase LTP and long-term memory in normal and aging hippocampus: role of secreted proteins tPA and BDNF." Ageing Res Rev **3**(4): 407-430.

Passos, I. C., M. P. Vasconcelos-Moreno, et al. (2015). "Inflammatory markers in post-traumatic stress disorder: a systematic review, meta-analysis, and meta-regression." Lancet Psychiatry **2**(11): 1002-1012.

Perry, V. H., D. A. Hume, et al. (1985). "Immunohistochemical localization of macrophages and microglia in the adult and developing mouse brain." Neuroscience **15**(2): 313-326.

Perugini, A., M. Laing, et al. (2012). "Synaptic plasticity from amygdala to perirhinal cortex: a possible mechanism for emotional enhancement of visual recognition memory?" Eur J Neurosci **36**(4): 2421-2427.

Phillips, R. G. and J. E. LeDoux (1992). "Differential contribution of amygdala and hippocampus to cued and contextual fear conditioning." Behav Neurosci **106**(2): 274-285.

Ponomarev, I., V. Rau, et al. (2010). "Amygdala transcriptome and cellular mechanisms underlying stress-enhanced fear learning in a rat model of posttraumatic stress disorder." Neuropsychopharmacology **35**(6): 1402-1411.

Prieto, G. A. and C. W. Cotman (2017). "Cytokines and cytokine networks target neurons to modulate long-term potentiation." Cytokine Growth Factor Rev **34**: 27-33.

Proescholdt, M. G., S. Chakravarty, et al. (2002). "Intracerebroventricular but not intravenous interleukin-1beta induces widespread vascular-mediated leukocyte infiltration and immune signal mRNA expression followed by brain-wide glial activation." Neuroscience **112**(3): 731-749.

Qiao, H., S. C. An, et al. (2017). "Role of proBDNF and BDNF in dendritic spine plasticity and depressive-like behaviors induced by an animal model of depression." Brain Res **1663**: 29-37.

Quan, N. and W. A. Banks (2007). "Brain-immune communication pathways." Brain Behav Immun **21**(6): 727-735.

Rajkowska, G. and C. A. Stockmeier (2013). "Astrocyte pathology in major depressive disorder: insights from human postmortem brain tissue." Curr Drug Targets **14**(11): 1225-1236.

Rakofsky, J. J., K. J. Ressler, et al. (2012). "BDNF function as a potential mediator of bipolar disorder and post-traumatic stress disorder comorbidity." Mol Psychiatry **17**(1): 22-35.

Rau, V., J. P. DeCola, et al. (2005). "Stress-induced enhancement of fear learning: an animal model of posttraumatic stress disorder." Neurosci Biobehav Rev **29**(8): 1207-1223.

Rial, D., C. Lemos, et al. (2015). "Depression as a Glial-Based Synaptic Dysfunction." Front Cell Neurosci **9**: 521.

Ringwood, L. and L. Li (2008). "The involvement of the interleukin-1 receptor-associated kinases (IRAKs) in cellular signaling networks controlling inflammation." Cytokine **42**(1): 1-7.

Rogers, J., D. Mastroeni, et al. (2007). "Neuroinflammation in Alzheimer's disease and Parkinson's disease: are microglia pathogenic in either disorder?" Int Rev Neurobiol **82**: 235-246.

Rosas-Vidal, L. E., F. H. Do-Monte, et al. (2014). "Hippocampal--prefrontal BDNF and memory for fear extinction." Neuropsychopharmacology **39**(9): 2161-2169.

Ross, F. M., S. M. Allan, et al. (2003). "A dual role for interleukin-1 in LTP in mouse hippocampal slices." J Neuroimmunol **144**(1-2): 61-67.

Roth, B. L. (2016). "DREADDs for Neuroscientists." Neuron **89**(4): 683-694.

Rubin, M., E. Shvil, et al. (2016). "Greater hippocampal volume is associated with PTSD treatment response." Psychiatry Res **252**: 36-39.

Saur, L., P. P. Baptista, et al. (2016). "Experimental Post-traumatic Stress Disorder Decreases Astrocyte Density and Changes Astrocytic Polarity in the CA1 Hippocampus of Male Rats." Neurochem Res **41**(4): 892-904.

Sawada, M., K. Imamura, et al. (2006). "Role of cytokines in inflammatory process in Parkinson's disease." J Neural Transm Suppl(70): 373-381.

Schneider, H., F. Pitossi, et al. (1998). "A neuromodulatory role of interleukin-1beta in the hippocampus." Proc Natl Acad Sci U S A **95**(13): 7778-7783.

Scofield, M. D., H. A. Boger, et al. (2015). "Gq-DREADD Selectively Initiates Glial Glutamate Release and Inhibits Cue-induced Cocaine Seeking." Biol Psychiatry **78**(7): 441-451.

Scofield, M. D. and P. W. Kalivas (2014). "Astrocytic dysfunction and addiction: consequences of impaired glutamate homeostasis." Neuroscientist **20**(6): 610-622.

Scofield, M. D., H. Li, et al. (2016). "Cocaine Self-Administration and Extinction Leads to Reduced Glial Fibrillary Acidic Protein Expression and Morphometric Features of Astrocytes in the Nucleus Accumbens Core." Biol Psychiatry **80**(3): 207-215.

Serita, T., H. Fukushima, et al. (2017). "Constitutive activation of CREB in mice enhances temporal association learning and increases hippocampal CA1 neuronal spine density and complexity." Sci Rep **7**: 42528.

Silverman, M. N., M. G. Macdougall, et al. (2007). "Endogenous glucocorticoids protect against TNF-alpha-induced increases in anxiety-like behavior in virally infected mice." Mol Psychiatry **12**(4): 408-417.

Srinivasan, D., J. H. Yen, et al. (2004). "Cell type-specific interleukin-1beta signaling in the CNS." J Neurosci **24**(29): 6482-6488.

Stehberg, J., R. Moraga-Amaro, et al. (2012). "Release of gliotransmitters through astroglial connexin 43 hemichannels is necessary for fear memory consolidation in the basolateral amygdala." FASEB J **26**(9): 3649-3657.

Stepanichev, M., N. N. Dygalo, et al. (2014). "Rodent models of depression: neurotrophic and neuroinflammatory biomarkers." Biomed Res Int **2014**: 932757.

Sugama, S., M. Fujita, et al. (2007). "Stress induced morphological microglial activation in the rodent brain: involvement of interleukin-18." Neuroscience **146**(3): 1388-1399.

Sugama, S., T. Takenouchi, et al. (2011). "Immunological responses of astroglia in the rat brain under acute stress: interleukin 1 beta co-localized in astroglia." Neuroscience **192**: 429-437.

Swiergiel, A. H. and A. J. Dunn (2007). "Effects of interleukin-1beta and lipopolysaccharide on behavior of mice in the elevated plus-maze and open field tests." Pharmacol Biochem Behav **86**(4): 651-659.

Szczytkowski-Thomson, J. L., C. L. Lebonville, et al. (2013). "Morphine prevents the development of stress-enhanced fear learning." Pharmacol Biochem Behav **103**(3): 672-677.

Taft, C. E. and G. G. Turrigiano (2014). "PSD-95 promotes the stabilization of young synaptic contacts." Philos Trans R Soc Lond B Biol Sci **369**(1633): 20130134.

Tarassishin, L., H. S. Suh, et al. (2014). "LPS and IL-1 differentially activate mouse and human astrocytes: role of CD14." Glia **62**(6): 999-1013.

Tarp, S., D. E. Furst, et al. (2017). "Defining the optimal biological monotherapy in rheumatoid arthritis: A systematic review and meta-analysis of randomised trials." Semin Arthritis Rheum **46**(6): 699-708.

Thomas, J. L., J. E. Wilk, et al. (2010). "Prevalence of mental health problems and functional impairment among active component and National Guard soldiers 3 and 12 months following combat in Iraq." Arch Gen Psychiatry **67**(6): 614-623.

Tynan, R. J., S. B. Beynon, et al. (2013). "Chronic stress-induced disruption of the astrocyte network is driven by structural atrophy and not loss of astrocytes." Acta Neuropathol **126**(1): 75-91.

Wang, Z. and M. R. Young (2016). "PTSD, a Disorder with an Immunological Component." Front Immunol **7**: 219.

Woods, G. F., W. C. Oh, et al. (2011). "Loss of PSD-95 enrichment is not a prerequisite for spine retraction." J Neurosci **31**(34): 12129-12138.

Woodward, S. H., D. G. Kaloupek, et al. (2006). "Hippocampal volume, PTSD, and alcoholism in combat veterans." Am J Psychiatry **163**(4): 674-681.

Xia, L., M. Zhai, et al. (2013). "FGF2 blocks PTSD symptoms via an astrocyte-based mechanism." Behav Brain Res **256**: 472-480.

Yabuuchi, K., M. Minami, et al. (1994). "Localization of Type-I Interleukin-1 Receptor Messenger-Rna in the Rat-Brain." Molecular Brain Research **27**(1): 27-36.

Yamamoto, S., S. Morinobu, et al. (2009). "Single Prolonged Stress: Toward an Animal Model of Posttraumatic Stress Disorder." Depression and Anxiety **26**(12): 1110-1117.

Yang, G., F. Pan, et al. (2009). "Stably maintained dendritic spines are associated with lifelong memories." Nature **462**(7275): 920-924.

Yang, L., Y. Qi, et al. (2015). "Astrocytes control food intake by inhibiting AGRP neuron activity via adenosine A1 receptors." Cell Rep **11**(5): 798-807.

Ye, R. D. (2001). "Regulation of nuclear factor kappaB activation by G-protein-coupled receptors." J Leukoc Biol **70**(6): 839-848.

Yehuda, R. and J. LeDoux (2007). "Response variation following trauma: a translational neuroscience approach to understanding PTSD." Neuron **56**(1): 19-32.

Young, E. J., M. Aceti, et al. (2014). "Selective, retrieval-independent disruption of methamphetamine-associated memory by actin depolymerization." Biol Psychiatry **75**(2): 96-104.

Young, E. J., S. B. Briggs, et al. (2015). "The Actin Cytoskeleton as a Therapeutic Target for the Prevention of Relapse to Methamphetamine Use." CNS Neurol Disord Drug Targets **14**(6): 731-737.

Zhang, R., Z. Peng, et al. (2014). "Gastrodin ameliorates depressive-like behaviors and up-regulates the expression of BDNF in the hippocampus and hippocampal-derived astrocyte of rats." Neurochem Res **39**(1): 172-179.

Zhang, R., L. Sun, et al. (2010). "Acute p38-mediated inhibition of NMDA-induced outward currents in hippocampal CA1 neurons by interleukin-1beta." Neurobiol Dis **38**(1): 68-77.

Zhu, H. and B. L. Roth (2014). "DREADD: A Chemogenetic GPCR Signaling Platform." Int J Neuropsychopharmacol **18**(1).

Zoladz, P. R., M. Fleshner, et al. (2013). "Differential effectiveness of tianeptine, clonidine and amitriptyline in blocking traumatic memory expression, anxiety and hypertension in an animal model of PTSD." Prog Neuropsychopharmacol Biol Psychiatry **44**: 1-16.